Selective Small Molecule Targeting of Anti-Apoptotic MCL-1

(Article begins on next page)

Dissertation advisor: Dr. Loren Walensky, M.D., Ph.D.   Nicole Alyssa Cohen

Selective Small Molecule Targeting of Anti-Apoptotic MCL-1

BCL-2 family proteins are key regulators of the mitochondrial apoptotic pathway in health and disease. Anti-apoptotic members such as BCL-2, BCL-X_L, and MCL-1 have been implicated in the initiation, progression, and chemoresistance of human cancer. Small molecules and peptides have successfully targeted the anti-apoptotic BCL-2/BCL-X_L groove that binds and sequesters pro-apoptotic BH3 death helices. Such compounds induce tumor cell apoptosis and are being advanced in clinical trials as promising next-generation cancer therapeutics. Notably, selective antagonists such as ABT-737 are highly effective at inducing apoptosis in BCL-2/BCL-X_L-dependent cancers but are rendered inactive by overexpression of MCL-1, a formidable chemoresistance protein that lies outside the molecule's binding spectrum. By screening a library of stabilized alpha-helices of BCL-2 domains (SAHBs), we previously discovered that the MCL-1 BH3 helix is itself a potent and exclusive MCL-1 inhibitor. Here, we deployed this chemically-constrained peptidic inhibitor of MCL-1, MCL-1 SAHB, in a competitive binding screen to identify selective small molecule inhibitors of MCL-1. Rigorous *in vitro* binding and functional assays were used to validate the compounds and their mechanisms of action, and most notably, MCL-1 inhibitor molecule 1 (MIM1) displayed exquisite selectivity in these assays. NMR analysis documented that MIM1 engages the canonical BH3-binding pocket of MCL-1. Importantly, MIM1 selectively triggers caspase 3/7 activation and apoptosis of a cancer cell line that is dependent on induced overexpression of MCL-1 but showed no activity in the isogenic cell line that is driven instead by overexpressed BCL-X_L. Thus, a selective stapled peptide inhibitor of MCL-1 was successfully applied to identify a high fidelity small molecule inhibitor of MCL-1 that exhibits anti-cancer activity in the specific context of MCL-1 dependence.

Table of Contents

List of Figures and Tables

ideas and learned how to write and speak like a scientist. I am especially grateful for Loren's support over the past year when I broke the news that I was going to become a high school science teacher after graduate school. He never questioned my choice and helped me achieve my goal of graduating. His leadership in running the lab is something that I will always try to emulate. Thank you for creating an environment that I could not imagine not being a part of.

Without my friends and family, I would not be where I am today. I'd like to thank my parents for supporting me in everything that I do. They always pushed me to do better, and my drive to succeed was instilled from a young age. Those values that I admire so much came from their parents, so I would like to thank all of my grandparents for tirelessly supporting me, bragging to their friends about their granddaughter at Harvard, and proudly reading my papers, nodding and pretending to understand what I do. To all my other family members and friends – thank you for everything. My best friend and fiancé James is the final person I would like to thank; his love and support mean the world to me, and he has stood by me from near-breakdowns around my qualifying exam all the way to the stressful dissertation preparation period. Thank you from the bottom of my heart.

For my grandfather, Robert Cohen.

Chapter 1

Introduction

The BCL-2 Family Regulates Cellular Apoptosis

Introduction to apoptosis

Apoptosis, a type of programmed cell death, is critical for both normal development and the preservation of cellular homeostasis[1]. Deregulation of apoptotic pathways often results in disease; for example, inhibition of apoptosis leads to cell accumulation in various types of cancer, while excessive cell death is evident in neurodegenerative disorders[2]. The morphological cellular hallmarks of apoptosis include cell shrinkage, chromatin condensation, DNA cleavage, and blebbing of the plasma membrane[3]. From early studies in *C. elegans*[4] to the complex human models known today, caspases (cysteine-aspartic proteases) have been shown to be essential for the progression of apoptosis[5]. Caspases are most often expressed as inactive zymogens and are proteolytically activated upon apoptotic pathway induction, either acting as initiators that respond to upstream signals or effectors that execute these death signals[6]. Ultimately, the cell is fragmented into apoptotic bodies, which are engulfed by macrophages, preventing an inflammatory cellular response[7].

Apoptotic pathways can be subdivided into two classes based on the death-inducing signal involved: the extrinsic pathway and the intrinsic pathway. The extrinsic apoptotic pathway, or the death-receptor pathway, is propagated by transmembrane receptors that are bound by their extracellular ligands, such as Fas ligand (FasL) or tumor necrosis factor-related apoptosis inducing ligand (TRAIL). FasL binds to the transmembrane Fas (also called CD95 or Apo1) receptor, while TRAIL binds death receptors 4 and 5 (DR 4/5)[8]. In either case, ligand binding induces a conformational change in the receptor complex, leading to assembly of the death-inducing signaling complex (DISC)[9]. Adaptor proteins, such as Fas-associated protein with

death domain (FADD), then bind to the death domain of the receptor, recruiting pro-caspase 8 to the complex[5]. Caspase-8's auto-proteolytic activation can then proceed through one of two pathways. In type I cells, large amounts of active caspase-8 directly cleave additional downstream caspases, including caspase-3 and caspase-7 among others, which cleave and activate cytosolic pro-death substrates[10]. In type II cells, caspase-8 cleaves the cytosolic BCL-2 family BH3-only protein BID, amplifying the death signal by linking the extrinsic and intrinsic apoptotic pathways[6].

The intrinsic apoptotic pathway, or the mitochondrial apoptotic pathway, is induced by intracellular death signals that converge at the mitochondria. This process is highly regulated, primarily by interactions between the BCL-2 family pro-death and pro-survival proteins[11]. Pro-apoptotic stimuli, such as radiation[12], DNA damage[13], or growth factor withdrawal[14], lead to mitochondrial outer membrane permeabilization, inhibiting the respiratory chain and releasing cytochrome c and other apoptogenic fators[15]. Cytochrome c then combines with the adaptor protein apoptotic protease activating factor-1 (APAF-1) and pro-caspase-9 to form the apoptosome, which proteolytically cleaves and activates caspase-9[16,17]. Similar to the extrinsic pathway, caspase-9 then sequentially activates caspase-3 and caspase-7, triggering the downstream caspase cascade and irreversibly initiating apoptosis.

Introduction to the BCL-2 family

BCL-2 family proteins are critical regulators of the intrinsic pathway of apoptosis[1]. The discovery of BCL-2 at the t(14;18) chromosomal breakpoint in follicular lymphoma led to a landmark paradigm shift that linked disease pathogenesis to deregulation of the proteins that regulate the apoptotic balance[18-20]. All BCL-2 family proteins possess BCL-2 homology (BH)

domains, with the most conserved BH3 death domain being contained by all members of the family (**Figure 1.1**). Based on structure and function, the BCL-2 family is subdivided into three classes: the multidomain pro-apoptotic, the "BH3-only" pro-apoptotic, and the multidomain anti-apoptotic proteins[21].

The pro-apoptotic proteins are classified as either multidomain members or BH3-only proteins[22]. The multidomain pro-apoptotic proteins BAX and BAK contain BH1-3 domains and are responsible for oligomerizing in the outer mitochondrial membrane, inducing mitochondrial outer membrane permabilization, releasing apoptogenic factors, and initiating the caspase cascade[23]. BAX and BAK are essential for mitochondrial outer membrane permeabilization and apoptosis induction, as cells lacking these proteins fail to undergo apoptosis following cellular insult by a range of stimuli[24]. The BH3-only proteins, such as BID, BIM, BAD, and NOXA, transmit afferent death signals to the core apoptotic machinery by interacting with either anti- or both pro- and anti-apoptotic multidomain proteins. The multidomain anti-apoptotic proteins MCL-1, BCL-2, BCL-X$_L$, BCL-w, and BFL-1/A1 contain up to four BH domains, and their expression promotes cellular survival[25].

Structurally, the BH3 death domain is an amphipathic alpha-helical motif conserved among all family members and mediates the critical protein interactions regulating apoptosis[26]. Anti-apoptotic BCL-2 members counteract apoptosis by sequestering the BH3 domains of both BH3-only and multidomain pro-apoptotic proteins. Specifically, the pro-apoptotic BH3 domain binds a hydrophobic groove formed by helices 2, 3, 4, 5, and 8 (also termed the BH1-3 regions) of the anti-apoptotic proteins; this groove contains a region of hydrophobic residues that is highly conserved among BCL-2 family anti-apoptotic proteins[12]. Complex formation is mediated by both hydrophobic and charged interactions between the pro-apoptotic BH3 domain and anti-
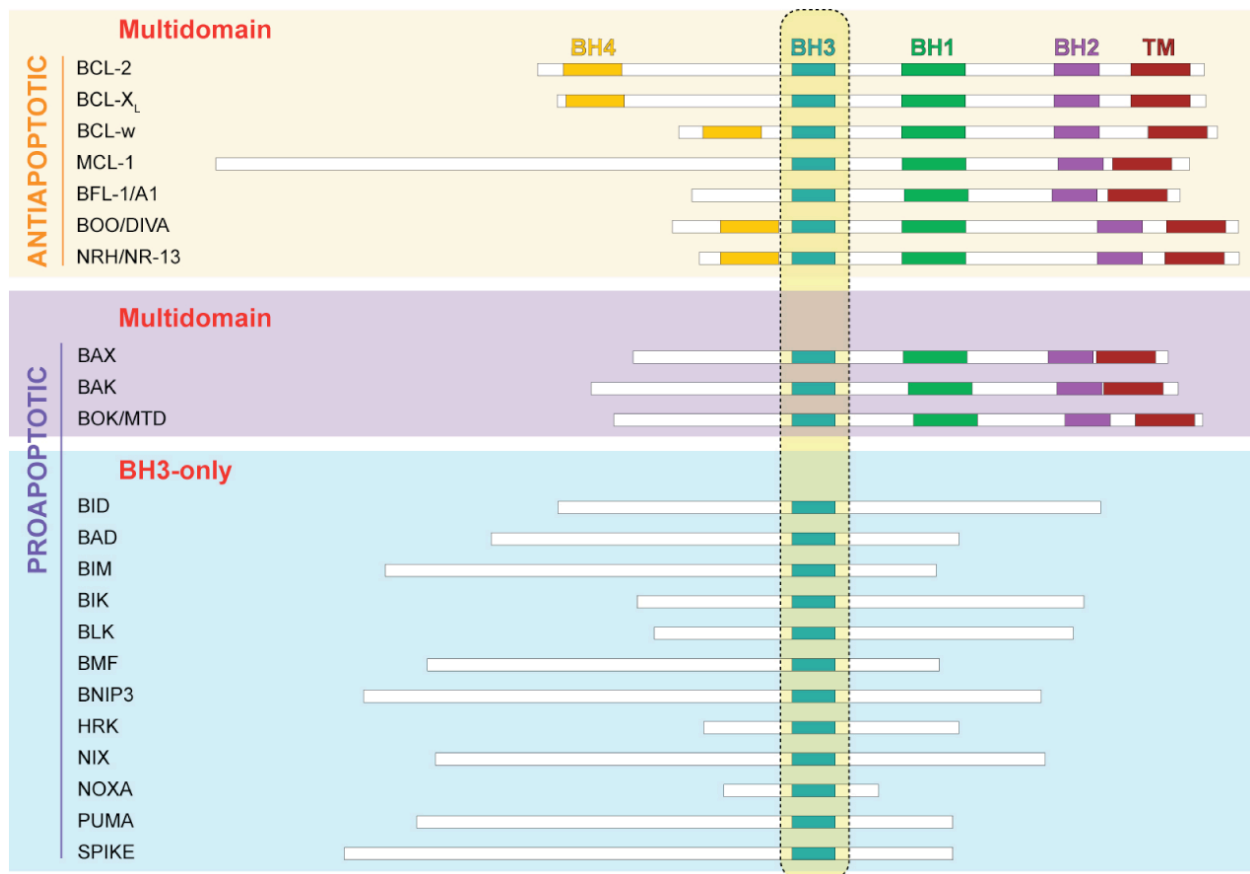
Figure 1.1. *BH3 domain conservation among BCL-2 family proteins.* Multidomain anti-apoptotic proteins contain BH1-4 domains (with the exception of MCL-1), forming a hydrophobic groove capable of sequestering the BH3 helices of pro-death proteins. The pro-apoptotic multidomain proteins contain BH1-3 domains, which form a similar hydrophobic groove whose function is less well understand but may involve BH3-only α-helical binding during the BAK/BAX activation process or participate in homo-oligomerization interactions once triggered from an allosteric site, as has been identified for BAX. BH3-only proteins exclusively contain the BH3 domain, which is essential for pro-apoptotic function.

apoptotic binding site[27-29], as shown by the first solution structure of BAK BH3 bound to BCL-X_L[29] (**Figure 1.2**).

BH3-only pro-apoptotic proteins exhibit differential binding profiles for anti-apoptotic proteins. For example, NOXA selectively binds MCL-1 and BFL-1/A1, BAD selectively binds BCL-2, BCL-X_L, and BCL-w, and BID, BIM, and PUMA bind all anti-apoptotic proteins with varying affinities[30] (**Figure 1.3**). BAX and BAK are also bound with differential selectivities, with MCL-1 and BFL-1/A1 preferentially binding BAK, and the anti-apoptotic BCL-2 predominantly blocking BAX[31-33]. These differences in binding profiles arise due to slight structural differences within the BH3 grooves and/or the BH3 helix itself. Structural studies have revealed slight differences in the MCL-1 and BCL-X_L grooves, for example, upon binding BIM BH3; mutational analysis revealed that position 4 within MCL-1's binding site is more open and solvent exposed, thus being tolerant of BH3 mutations (e.g., reducing amino acid size from phenylalanine within BIM BH3)[34]. The difference in BH3 binding profiles of MCL-1 and BFL-1/A1 compared to BCL-2, BCL-X_L, and BCL-w confers distinct anti-apoptotic functions with important physiologic implications[30].

The mechanisms by which the anti-apoptotic blockade is overcome and how BAX and BAK are activated remains an area of intensive study[35]. The direct activation model divides the BH3-only proteins into sensitizers (e.g., BAD and NOXA) that only bind anti-apoptotic proteins and activators (e.g., BID and BIM) that interact directly with both the multidomain anti- and pro-apoptotic proteins. The direct binding of the activator BH3 domains to BAX and BAK results in their oligomerization within the mitochondrial outer membrane, pore formation, and the subsequent release of cytochrome *c* and other apoptogenic factors[36,37]. In contrast, binding of the sensitizer BH3 domain to anti-apoptotic proteins results in the displacement of activator BH3-
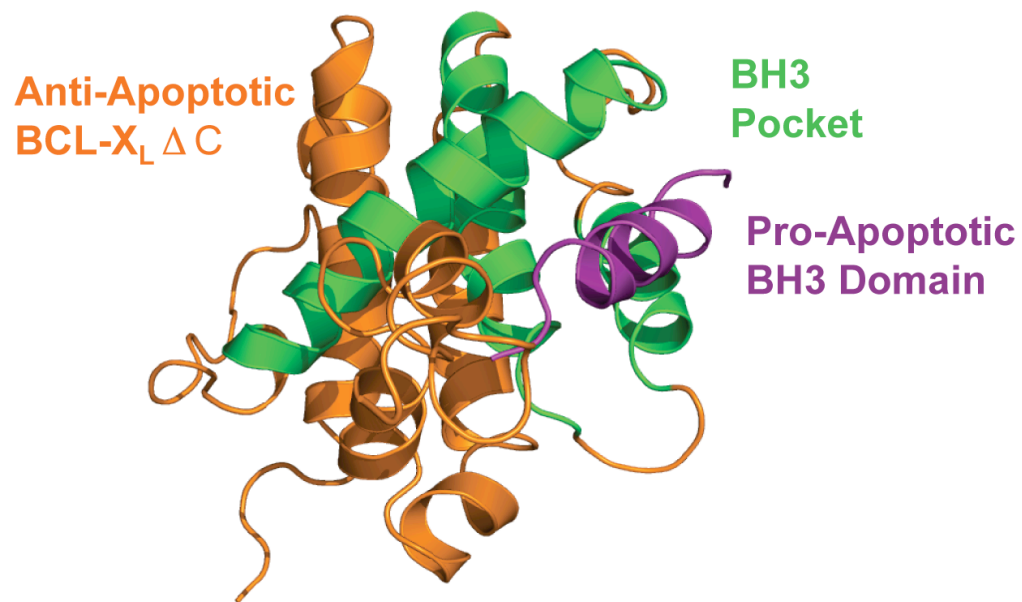
Figure 1.2. *NMR solution structure of anti-apoptotic BCL-X$_L$ bound to BAK BH3.* This solution structure[29] was the first visualization of the anti-apoptotic BH3-binding pocket, which is composed of helices 2-5, 8 (green); BAK BH3 (purple) binds to the surface pocket, resulting in functional sequestration of the BH3 death domain and consequent suppression of apoptosis.
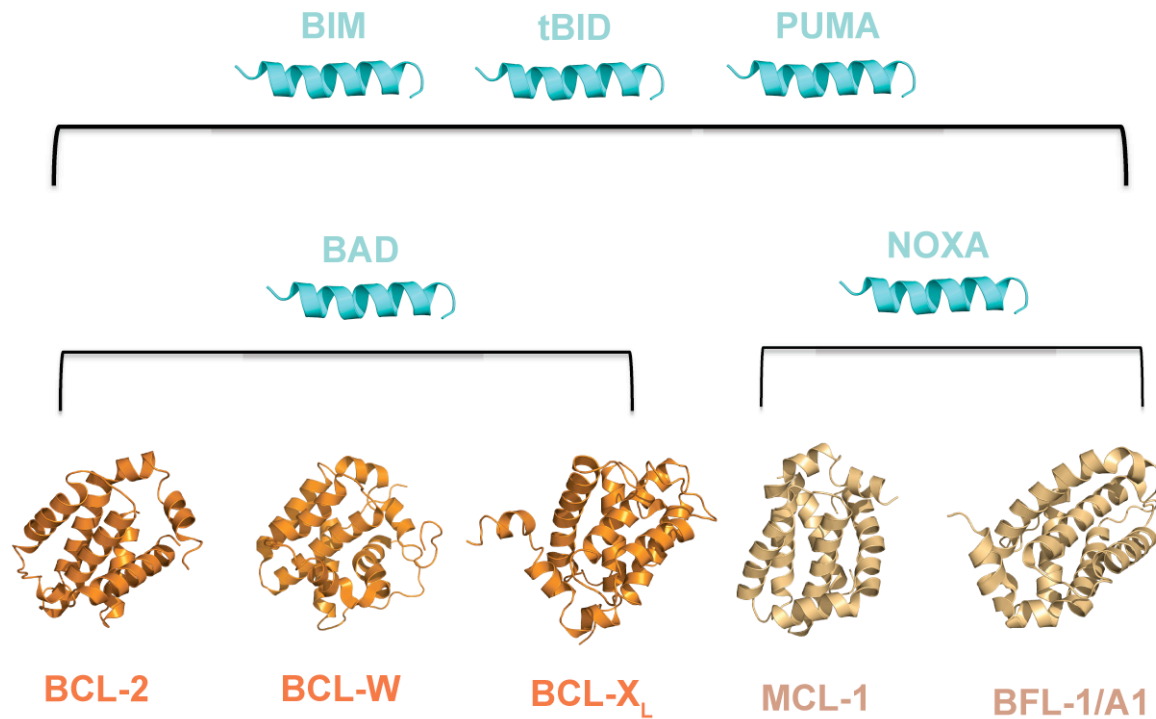
Figure 1.3. *The BH3-only proteins selectively bind discrete anti-apoptotic protein subclasses.* The BH3-only signaling proteins BIM, BID, and PUMA bind all five anti-apoptotic proteins with similar affinities. However, BAD specifically binds to the BCL-2/BCL-w/BCL-X$_L$ subclass of anti-apoptotic proteins, whereas NOXA only binds to MCL-1 and BFL-1/A1. The peptides' natural affinities for these proteins reveal important differences in anti-apoptotic BH3 pocket structure, which distinguishes their binding partners and functions.

only proteins that can subsequently directly activate BAX and BAK[38-40]. The indirect activation model suggests that all BH3-only proteins bind anti-apoptotic proteins exclusively, leading to the disruption of constitutive, heterodimeric, and inhibitory interactions with BAX and BAK, and allowing auto-oligomerization to proceed[41,30]. These models are not mutually exclusive; in both models, anti-apoptotic proteins likely act by binding and directly inhibiting both the multidomain pro-apoptotic proteins BAX and BAK and a subset of the BH3-only proteins.

Anti-apoptotic MCL-1

Mcl-1 was originally discovered as a *Bcl-2* homology gene that is transcribed upon differentiation induction of a human myeloid leukemia cell line[42]. MCL-1 predominantly localizes to the mitochondria, but lower quantities have been observed in the cytoplasm, endoplasmic reticulum, and nucleus[43]. The anti-apoptotic role of MCL-1 was revealed by a marked delay in stress-induced cell death upon MCL-1 expression in Chinese hamster ovary and hematopoietic cells[44]. Overexpression of MCL-1 in transgenic mice promotes immortalization of hematopoietic cells, while loss of MCL-1 results in peri-implantation embryonic lethality[45]. MCL-1 also plays a key role in the survival of hematopoietic stem cells and the development and maintenance of B and T lymphocytes[46,47]. MCL-1 has important distinctions from its anti-apoptotic counterparts, including its larger size, the presence of 3 rather than 4 BH domains, and a long N-terminal extension. Another distinguishing feature is that MCL-1 has a short half-life, with protein levels tightly regulated by proteasomal degradation, phosphorylation, and transcriptional regulation, including the production of multiple alternative spliceforms[48-55]. The heightened regulation of MCL-1 compared to other anti-apoptotic proteins suggests that MCL-1 activities may be finely tuned to accommodate discrete cellular activities[56].

The BCL-2 family and cancer pathogenesis

Cancer cells often hijack the apoptotic machinery to promote cellular survival in the face of therapeutic intervention. Several examples of this include downregulation of pro-apoptotic proteins, deregulation of microRNAs (miRNAs), disruption of upstream signaling pathways, and/or upregulation of anti-apoptotic proteins. Death-promoting apoptotic proteins, such as BAX, can be deleted or mutated in cancer. For example, frameshift mutations in *Bax* have been found in specific cases of colon cancer[57], and the loss of BAX expression in a mouse breast cancer model leads to accelerated mammary tumor formation[57]. Additionally, the BH3-only pro-apoptotic BIM was found to be necessary for apoptosis induction in thymocytes[58]. Recently, a common *Bim* deletion polymorphism was found to mediate resistance to kinase inhibitors in chronic myelogenous leukemia and non-small cell lung cancer[59].

Downregulation of specific pro-apoptotic proteins by increased miRNA expression is an analogous pathway that drives cancer cells toward survival. A number of miRNAs target the pro-death BH3-only BIM; for example, miR-32 acts as an oncogene that contributes to prostate cancer chemotherapy resistance[60], while elevated expression of miR-19/92 via amplification of the coding regions in lymphocytes leads to lymphoma development in patients and lymphoproliferative disease in mice[61]. BH3-only PUMA is targeted by miR-221/222, inducing cellular survival in glioblastoma cells[62,63]. Finally, the pro-apoptotic executioner BAK is targeted by miR-125b, and this miRNA has been found to be upregulated in both taxol-resistant breast cancer[64] and prostate cancer[65].

Additionally, deregulation of upstream apoptotic signaling pathways can provide the driving force behind cancer cell survival through modulation of the BCL-2 family. p53, a common tumor suppressor whose loss of function mutations often promote carcinogenesis or

10

chemotherapeutic resistance, exerts its pro-apoptotic function through a number of pathways.

One such example is the upregulation of BH3-only PUMA and NOXA as a result of DNA

damage through p53 activation[66-68]. Therefore, mutations in p53 resulting in its repression will

also lower the expression levels of PUMA and NOXA, leading to increased cell survival. A

second example of upstream targeting affecting apoptotic proteins is through modulation of the

MAP kinase (MAPK) pathways, regulating anti-apoptotic protein levels. Inhibition of p38 was

shown to increase p53 functionality, leading to downregulation of both MCL-1 and BCL-X$_L$[69].

Therefore, mutations causing increased function of p38 would lead to increased levels of MCL-1

and BCL-X$_L$, promoting cell survival.

Upregulation of the BCL-2 anti-apoptotic family of proteins, which can occur through a

number of different mechanisms, is a major strategy cancer cells utilize to evade cell death and

promote chemoresistance[70,71]. BCL-2 family anti-apoptotic overexpression is present in a

number of hematologic malignancies such as multiple myeloma, chronic lymphocytic leukemia,

acute lymphocytic leukemia, and acute myelogenous leukemia[71]. Increased levels of BCL-2 and

BCL-X$_L$ have been associated with more aggressive cancer phenotypes and increased drug and

radiation resistance in both hematologic malignancies and solid tumors[72]. miR-143 has been

found to be downregulated in osteosarcoma cell lines and primary tumor samples, and apoptosis

can be induced by restoring miRNA expression, thus reducing BCL-2 levels[73].

Important differences in anti-apoptotic BCL-2 family protein expression occur among

cancer cell types; whereas BCL-2 and BCL-X$_L$ overexpression are more prominent in small cell

lung cancer, MCL-1 overexpression has been linked to the pathogenesis of a variety of refractory

cancers, including multiple myeloma[74,75], acute myelogenous leukemia[76], melanoma[77], and poor

prognosis breast cancer[78]. BCL-2-overexpressing transgenic mice exhibit a high occurrence of T

cell lymphomas[79], and Eµ myc/BCL-2 mice show a much greater incidence of B cell tumors in comparison to Eµ myc mice[80]. Similarly, transgenic mice overexpressing MCL-1 resulted in high levels of immortalized hematopoetic cells and lymphomas[81,82]. Increased MCL-1 levels are also frequently present in relapsed and refractory acute myelogenous and acute lymphocytic leukemias and can be used as a prognostic marker[83]. Recently, cancer cells containing amplifications in MCL-1 have been shown to be dependent on MCL-1[40,84]. miR-29b targets MCL-1 mRNA and is downregulated in malignant cells, which correlates with increased MCL-1 expression[85]. Similarly, mIR-101, which also targets MCL-1, is downregulated in hepatocellular carcinoma[86]. Importantly, *Mcl-1* was found to be one of the "top ten" most amplified genomic regions in human cancers[84]. Targeting MCL-1 in MCL-1-overexpressing cancers with anti-sense oligonucleotides, shRNA, or non-specific MCL-1 modulators has been effective in promoting apoptosis, singly or in combination with other agents[56,87,88]. Because the BCL-2 family plays critical roles in cancer pathogenesis, the development of targeted inhibitors of anti-apoptotic proteins has become a pressing pharmacologic goal for combating refractory malignancies[72].

Summary

Apoptosis, or programmed cell death, is important in both development and disease. The BCL-2 family of proteins regulates the mitochondrial apoptotic pathway through interactions among pro-apoptotic BH3 domains and anti-apoptotic BH3 binding grooves. Disease states arise upon deregulation of the BCL-2 family of proteins, where cell death is either promoted or evaded; one of the most common tactic cancer cells utilize to promote survival is anti-apoptotic protein overexpression. Specifically, MCL-1 overexpression has been shown to be a major

chemoresistance factor in a number of human cancers, and for this reason, MCL-1 targeting is a

pharmacologic priority in the quest to reactivate cell death for therapeutic benefit in cancer.

Targeting Protein Interactions within the BCL-2 Family

The BCL-2 family anti-apoptotic proteins are viable therapeutic targets in cancer

Because BCL-2 family anti-apoptotic proteins are often overexpressed in refractory or relapsed cancers, targeting these proteins either at the gene or the protein level is an important therapeutic strategy that has been validated by a series of experimental successes. The first strategy utilized anti-sense oligonucleotides to target the first six codons of BCL-2 mRNA, resulting in mRNA degradation and a decrease in protein translation[89]. In cancer cells that overexpress BCL-2, this molecular "hit" should reset the cell's rheostat from survival to death in the face of therapeutic intervention. This was indeed the case, as oblimersen sodium (G3139, Genasense) downregulated BCL-2 protein levels and led to apoptosis induction in t(14;18)-expressing lymphoma cells[89]. In a human melanoma mouse xenograft model, G3139 led to sensitization with cyclophosphamide[90], although on-mechanism responses were elusive (or ambiguous) *in vivo*[91] . Similar anti-sense strategies have been used to target BCL-X$_L$ in epithelial cells in response to DNA damage[92] and MCL-1 in human multiple myeloma[92] or a human melanoma xenograft in severe combined immunodeficient (SCID) mice[92]. Further proof-of-concept studies show that downregulation of MCL-1 through siRNA overcomes ABT-737 resistance in small cell lung cancer cell lines, triggering cell death.[93]

In addition to direct anti-sense targeting of the anti-apoptotic proteins, upstream targeting of signaling pathways that leads to decreased anti-apoptotic protein expression has also been explored. Sorafenib is a small molecule inhibitor of multiple kinases in the MAPK signaling pathway[94], and its administration promotes rapid downregulation of MCL-1 levels through indirect and non-targeted translational inhibition, thus contributing to apoptosis induction in

chronic lymphocytic leukemia cells[95]. Another example of upstream targeting of the BCL-2

family involves the galectin-3 antagonist, GCS-100, which was found to overcome bortezomib-

mediated resistance in melanoma cells[96]. Further mechanistic studies revealed that this

compound exerted its apoptotic effect in part by downregulating MCL-1 and BCL-X_L, which is

accompanied by an increase in NOXA expression[97]. Additionally, cell cycle proteins were

deregulated, and although the exact connection between these three pathways (apoptotic, cell

cycle, and carbohydrate binding via galectin-3) is incompletely understood, the ultimate result

was that BCL-2-family modulation sensitized cancer cells to apoptosis. These approaches and

results confirm that the BCL-2 family anti-apoptotic proteins are high-priority targets in cancer

due to their essential roles in preserving pathologic cell survival.

The relevance of targeting anti-apoptotic proteins in cancer has been clearly

demonstrated by the successes of the described therapeutic strategies. However, off-target effects

and poor pharmacokinetic properties are major drawbacks, preventing the clinical utility of anti-

sense oligonucleotides, for example. Because BCL-2 family proteins perform functions

independent of their BH3 domain interactions, eliminating the protein entirely, including its non-

apoptotic functions, may be detrimental to normal cells. Furthermore, inhibitors targeting

upstream pathways that lead to apoptotic modulation also produce off-target effects owing to

their effects on downstream pathways other than intrinsic apoptotic signaling. For this reason,

selective disruption of pro-apoptotic BH3 domain sequestration by targeting the anti-apoptotic

proteins' canonical and conserved BH3 grooves has become a priority in the developmental

cancer therapeutics field.

Targeting protein-protein interactions

Typical contact surfaces within a protein-protein interaction are often very large (1,500-3,000 Å), as compared to standard small molecule-protein contact surfaces (300-1,000 Å)[98]. Moreover, most protein surfaces are flat, without defined grooves, making small molecule targeting of protein-protein interactions difficult. Despite the large size of protein contact surfaces, mutational studies such as alanine scanning have demonstrated that the free energy of binding is typically dictated by specific "hot-spots" within the binding site[99,100]. Based on the hot-spot hypothesis, small molecule targeting of protein-protein interactions would theoretically be feasible if the critical subportion of the binding interface could be appropriately targeted. Suitability for small molecule targeting is typically dictated by a well-defined deep pocket within the binding site where a small molecule can bind effectively. A select group of protein-protein interactions are amenable for high throughout small molecule drug development[101], and the BCL-2 family falls into this class because they contain well-defined, conserved binding pockets that are deeper than most protein interfaces. Additionally, the structures of all anti-apoptotic proteins are known. This structural knowledge allows for the design and optimization of inhibitors to increase binding potency and selectivity.

Targeting protein-protein interaction sites is typically difficult when both interaction partners are large, soluble proteins[102]. While this may be the case for some BCL-2 family interactions (e.g., MCL-1/BAK), these protein interactions can be simplified; for example, the pro-apoptotic BH3 domain of the pro-death proteins, which binds to the anti-apoptotic protein's BH3 groove, has been successfully substituted for full-length soluble proteins in *in vitro* assays[38]. Whereas peptidic targeting of these protein interfaces would allow for the disruption of large surface areas, native peptides often display unfavorable pharmacokinetic properties due to

rapid degradation *in vivo* and cell impermeability. Therefore, small molecules have traditionally been the modality of choice for drug development, with the development of screens to target a soluble protein/α-helical interaction a feasible starting point for BCL-2 family drug discovery.

Lipinski's Rule of Five highlights important physiochemical properties necessary for favorable pharmacokinetics and potential oral bioavailability of small molecule drugs. According to Lipinski's Rule, a drug-like compound must possess a molecular weight of less than 500 Da, contain less than five hydrogen bond donors, contain less than ten hydrogen bond acceptors, and have an octanol-water partition coefficient of less than five[103]. Typical compounds that follow these rules are enzyme inhibitors (e.g. GPCRs, ion channels), which bind to a small portion within a protein active site. However, small molecules that inhibit protein-protein interactions often must be much larger than 500 Da in order to engage sufficient surface area for effective targeting. Currently, only 51% of FDA-approved drugs on the market are orally bioavailable and follow Lipinski's rule of five[104], highlighting an increase in small molecule diversity and the need to inhibit more difficult and non-traditional targets, such as protein-protein interactions. This shift of small molecule properties is referred to as the "rule of four," with compounds that successfully target these interactions possessing higher molecular weights (> 400 Da), higher hydrophobicity (octanol water coefficient > 4), more rings within their structures (> 4), and more hydrogen bond acceptors (> 4) than common drugs obeying Lipinski's Rule[105].

Because protein-protein interactions have become increasingly recognized as critical to modulating cellular processes in homeostasis and disease, the search for small molecule inhibitors of these interactions has jumped to the forefront of academic and pharmaceutical research efforts. Recently, a number of effective small molecule inhibitors of protein interactions have been discovered, such as Nutlin-3 that targets the p53-MDM2 interaction. MDM2 is the

ubiquitin E3 ligase that binds p53 and is responsible for targeting it for proteasomal degradation[106]. Small molecule Nutlins disrupt the interaction between p53 and MDM2 by directly binding to MDM2, restoring p53's pro-death function in cancer cells[106]. Another example involves disruption of the Inhibitor of Apoptosis (IAP)/caspase interaction in cancer cells. The IAPs (including XIAP, cIAP-1 and cIAP-2) bind caspases, restraining their apoptotic activity, and are commonly overexpressed in cancer[107]. The second mitochondria-derived activator of caspases (Smac) peptide becomes activated during apoptosis induction, binding the IAPs and leading to release and activation of the caspases[108]. Therefore, discovering Smac mimetics that would bind IAP and displace caspases emerged as an important goal in the cell death field. The first small molecule Smac mimetic was discovered to disrupt both XIAP/Smac and XIAP/caspase-9 interactions *in vitro*, binding XIAP in glioblastoma cells and potentiating TRAIL and TNFα-mediated cell death[109]. These examples highlight the utility of targeting protein-protein interactions for therapeutic application in cancer.

Stapled peptides are unique tools to manipulate apoptosis

Since the conserved alpha-helical BH3 domain mediates interactions among BCL-2 family members, peptides containing these sequences have been used to dissect apoptotic signaling[38]. However, native BH3 peptides lack secondary structure, display high proteolytic degradation, and exhibit low cell permeability[110]. To overcome these issues, Verdine and coworkers developed hydrocarbon "stapling" to reinforce the structure of a natural alpha helix[111]. In this approach, non-natural amino acids containing olefinic side chains are substituted at the $i,(i+4)$ positions and are subsequently tethered by ruthenium-catalyzed ring closing

methathesis[112] (**Figure 1.4**). Stapled peptides show improved pharmacologic properties and have been used to initiate apoptosis in cancer cells both *in vitro* and *in vivo*[110,113,114].

Walensky *et al.* demonstrated for the first time the therapeutic utility of stapled peptides for targeting the BCL-2 family of proteins. First, BID SAHB (for stabilized alpha helix of BCL-2 domain) displayed favorable *in vitro* and *in vivo* properties, including increased helicity, protease resistance, and increased cellular uptake as compared to the native non-stapled BID BH3 peptide[110]. Cellular uptake was blocked by the addition of sodium azide and deoxyglucose, which inhibit active forms of uptake such as endocytosis. Furthermore, BID SAHB bound its BCL-2 family targets, such as BCL-X_L, with ten-fold greater affinity then its unstapled counterpart. Importantly, BID SAHB induced apoptosis in leukemia cells at low micromolar concentrations and led to tumor suppression in a mouse model of human leukemia, sparing normal cells from toxic side-effects over the one week treatment course[110].

In addition to targeting apoptotic proteins, stapled peptides have been used as novel discovery tools to uncover mechanistic details underlying pro-apoptotic protein activation and subsequent apoptosis induction. In addition to binding anti-apoptotic targets, BID SAHB was also shown to directly bind pro-apoptotic BAX, leading to functional BAX activation in liposomal and cytochrome *c* release assays[113]. Gavathiotis *et al.* utilized BIM SAHB to discover a previously uncharacterized allosteric binding site on pro-apoptotic BAX; here, the stapled peptide was shown to directly bind to and activate BAX at a novel interaction surface on the opposite side of the protein from the canonical BH3-binding groove[115]. Furthermore, BIM SAHB was utilized to determine BAX's structural reorganization upon activation[116]. Similar to BIM SAHB, BAX SAHB was also found to bind BAX at the novel interaction site, suggesting a role for BAX BH3 in self-propagating BAX activation once triggered by BH3-only proteins
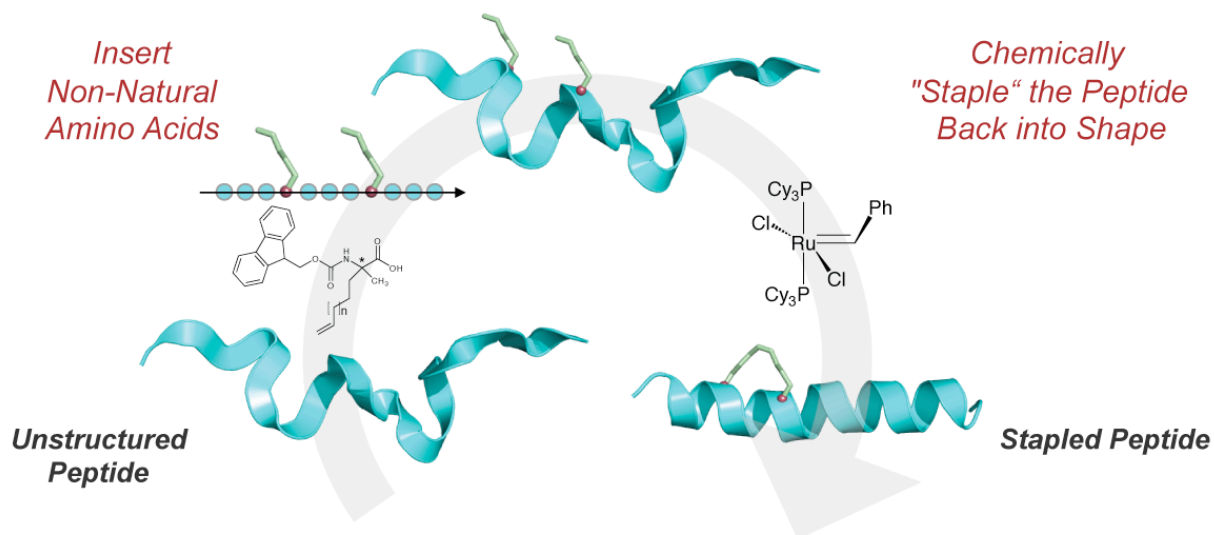
Figure 1.4. *Chemical stapling restores helical structure to peptide sequences.* Unstructured peptide sequences are synthesized with non-natural olefinic-side chain-containing amino acids inserted into the sequence. The peptide is then chemically stapled via a ruthenium-catalyzed ring-closing metathesis, resulting in a rigid and stabilized stapled peptide that retains its helical structure.

during apoptosis induction[116].

While BID SAHB acts as a pan-apoptotic protein binder, the discovery of MCL-1 SAHB, which is an MCL-1 specific inhibitor, highlighted the utility of stapled peptides as selective targeting agents. Here, a panel of stapled peptides corresponding to the BH3 domains of all BCL-2 family members were synthesized and biochemically characterized for their ability to bind anti-apoptotic BCL-2 family proteins. Ironically, the BH3 helix of MCL-1 itself was the only specific MCL-1-targeting peptide[117]. The most potent stapled peptide, MCL-1 SAHB$_D$, bound MCL-1 with low nanomolar affinity, and a co-crystal structure with recombinant MCL-1 suggested important specificity and binding determinants, which were confirmed by peptide mutagenesis. In cells, MCL-1 SAHB binds MCL-1, as shown by chemical cross-linking, and dissociates important physiologic interactions, such as MCL-1/BAK, thus sensitizing OPM2 and Jurkat cells to death-receptor-mediated apoptosis[117].

While stapled peptides have effectively targeted BCL-2 family interactions *in vitro*, in cells, and in preclinical models, efforts to advance these novel agents to clinical trials are currently underway, with their potential impact on expanding the arsenal of therapies for human disease currently unknown. However, their large size and exquisite natural selectivity allows for potent and selective targeting of protein interactions in cells, whereas isolating small molecules to disrupt such large surface areas has been challenging[118]. Nonetheless, small molecules have historically dominated the drug collections available for clinical use. Indeed, stapled peptides that specifically bind MCL-1 may likewise serve as ideal tools for discovering new MCL-1-targeting small molecules that can be applied to probe MCL-1 biology and target MCL-1 *in vivo* for therapeutic purposes.

Small molecule modulators of BCL-2 family interactions

The importance of BCL-2 family members in promoting tumorigenesis has stimulated numerous efforts to develop small molecules that regulate the apoptotic pathway. In particular, investigators have searched for small molecules that mimic BH3 death domains and bind the hydrophobic pocket of anti-apoptotic BCL-2 family members, thus releasing the endogenous pro-apoptotic family members and stimulating apoptosis[118]. Some of the first small molecules targeting the BCL-2 family were discovered using high-throughput screening approaches, including virtual (e.g., HA14-1)[119], cell-based (e.g., antimycin A)[120], and competitive binding assays (e.g., BH3Is)[121]. However, optimizing specificity, binding affinity, and *in vivo* activity has remained a formidable challenge.

The development of the BH3 mimetic ABT-737 represented the first major breakthrough in small molecule targeting of a discrete subset of BCL-2 proteins. This compound was found to bind anti-apoptotic family members BCL-2, BCL-X_L, and BCL-w and was discovered using an "SAR by NMR" strategy that effectively mimicked the BAD BH3 peptide's binding to the BH3-binding site of anti-apoptotic BCL-X_L[122]. Specifically, an NMR-based screening approach was used to link low affinity small molecules that bound to specific sites of the BH3 groove, yielding higher affinity compounds. By binding to the BH3 pocket of a subset of anti-apoptotic proteins[122], ABT-737 disrupts key physiologic interactions, such as BCL-2/BAX *in vivo*[123]. Furthermore, ABT-737 induces apoptosis in cancer cells and regression of solid tumors and hematologic malignances[122,123]. An orally bioavailable version of ABT-737, ABT-263, is currently undergoing clinical evaluation. Interestingly, the compound displays an on-target side effect of rapid platelet clearance, due to induction of platelet senescence by blocking BCL-X_L[124]. Thus, the development of a more precise BCL-2 inhibitor, for example, would serve to avoid

thrombocytopenia and its attendant risks in a patient population that is typically compromised by bone marrow suppression.

Because ABT-737 only targets BCL-2-like anti-apoptotics (BCL-2, BCL-X$_L$, and BCL-w), MCL-1 and BFL-1/A1 overexpression have emerged as clinically relevant resistance mechanisms that can only be addressed by developing neutralizing inhibitors of these proteins as well[93,125-127] (**Figure 1.5**). The small molecule obatoclax (GX15-070) was found to bind MCL-1 in addition to the anti-apoptotic proteins targeted by ABT-737[128]. By also targeting MCL-1, obatoclax is believed to overcome the MCL-1-mediated resistance to apoptosis observed for ABT-737, the extrinsic death receptor ligand TRAIL, and the proteasome inhibitor Bortezomib[128,129]. Although features of obatoclax's mechanism of action remain unclear, this molecule demonstrates a preliminary proof-of-concept that diminishing MCL-1 activity by targeting its BH3 groove can lead to sensitization of cancer cells to apoptosis[128]. For this reason, the pursuit of selective small molecules that target MCL-1 is receiving much attention despite previous challenges.

Summary

Targeting protein-protein interactions using small molecules is difficult due to large protein surface areas and ill-defined binding pockets; however, BCL-2 family anti-apoptotic proteins possess a deep binding pocket amenable to small molecule targeting, as displayed by recent successes in compound/pocket binding. Biological peptides possess natural binding potency and selectivity, but their *in vivo* properties - namely protease susceptibility and lack of cell penetrance - make them ill-suited for therapeutic targeting. For this reason, peptide stapling has been utilized to stabilize alpha-helical structures and target protein-protein interactions;

Figure 1.5. *Therapeutic rationale for targeting MCL-1*. (A) When BCL-2 and BCL-X$_L$ are overexpressed in cancer cells, they bind and sequester BAX and BAK, leading to cellular survival. (B) Upon treatment with a BCL-2/BCL-X$_L$ specific inhibitor, these interactions are disrupted, and apoptosis proceeds. (C) However, if MCL-1 is overexpressed in addition to BCL-2 and BCL-X$_L$, even upon selective treatment with ABT-737 (which does not bind MCL-1), the cells will survive due to the inhibitory BH3 pockets of MCL-1, which can bind and sequester pro-apoptotic proteins. (D) Dual overexpression of both subclasses of anti-apoptotic proteins requires combination treatment with MCL-1-selective and BCL-2/X$_L$-selective agents. If MCL-1 is the only anti-apoptotic apoptotic protein overexpressed, specific MCL-1 targeting is expected to be sufficient to tip the balance in the direction of apoptosis in a cancer cell.

Figure 1.5 (continued)

A BCL-2/BCL-X$_L$
   overexpression

B

ABT-737

BCL-2   BAX/BAK

BCL-2   BAX/BAK

Mitochondrion

Activated
BAX/BAK

SURVIVAL

APOPTOSIS
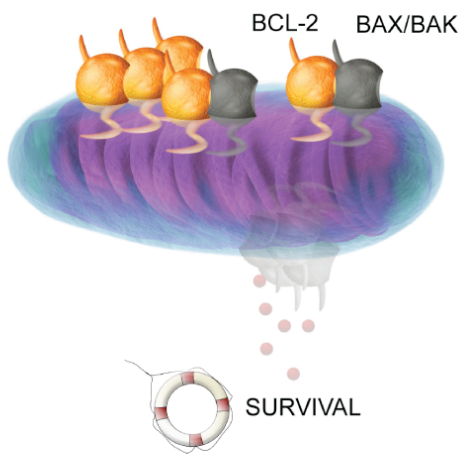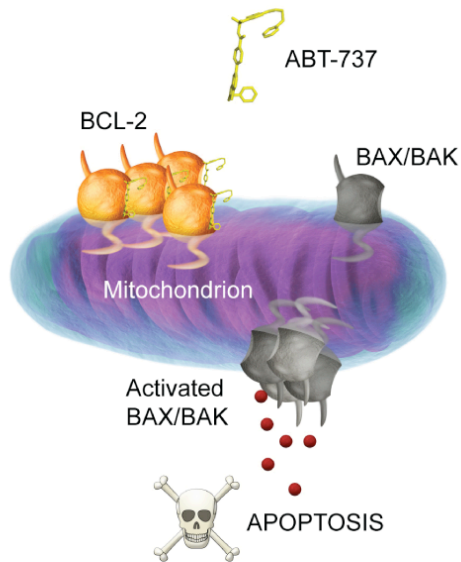
C BCL-2/BCL-X$_L$
   overexpression
   +
   MCL-1
   overexpression

ABT-737

D

ABT-737   MCL-1
           Inhibitor

MCL-1   MCL-1

SURVIVAL

APOPTOSIS
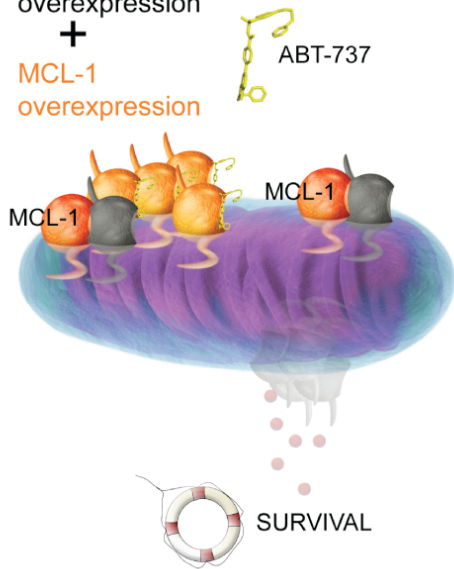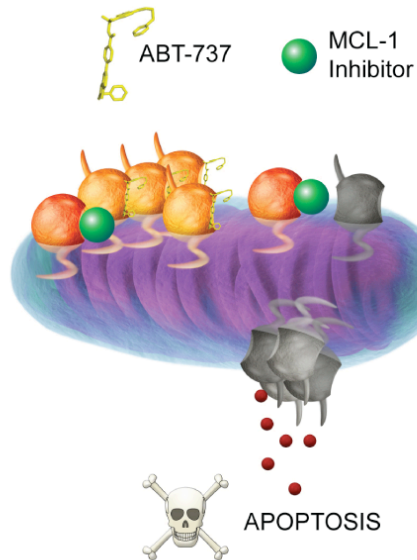
proof-of-concept studies have shown favorable *in vivo* peptide properties and selective disruption of protein interactions in cells. Stapled peptides have successfully targeted BCL-2 family interactions by mimicking and displacing natural BH3 interactors. Due to the anti-apoptotic surface groove's well-defined and relatively deep binding pocket, small molecules have also been discovered that disrupt anti-apoptotic/pro-apoptotic BH3 domain interactions. The most successful small molecule candidate to date is ABT-737/ABT-263, which binds BCL-2, BCL-X_L, and BCL-w; however, MCL-1 overexpression renders this compound ineffective in MCL-1-dependent cancers. For this reason, selective targeting of MCL-1 remains a high priority and an unmet clinical need. The discovery of a stapled MCL-1 BH3 helix as a potent and selective MCL-1 inhibitor and potential prototype therapeutic also provides a new opportunity to mine chemical space for novel anti-MCL-1 molecules based on their capacity to disrupt this unique stapled peptide/MCL-1 interaction.

References

1.   Danial, N.N. BCL-2 Family Proteins: Critical Checkpoints of Apoptotic Cell Death. *Clin. Cancer Res.* **13**, 7254-7263 (2007).

2.   Thompson, C.B. Apoptosis in the pathogenesis and treatment of disease. *Science* **267**, 1456-62 (1995).

3.   Kerr, J.F., Wylie, A.H. & Currie, A.R. Apoptosis: A basic biological phenomenon with wide-ranging inssues in tissue kinetics. *Br J Cancer* **26**, 239-57 (1972).

4.   Yuan, J., Shaham, S., Ledoux, S., Ellis, H.M. & Horvitz, H.R. The C. elegans cell death gene ced-3 encodes a protein similar to mammalian interleukin-1b-converting enzyme. *Cell* **75**, 54`-552 (1993).

5.   Thornberry, N.A. & Lazebnik, Y. Caspases: Enemies within. *Science* **281**, 1312-1316 (1998).

6.   Schug, Z.T., Gonzalvez, F., Houtkooper, R.H. & Gottlieb, E. BID is cleaved by caspase-8 within a native complex on the mitochondrial membrane. *Cell Death and Differentiation* **18**, 538-548 (2011).

7.   Ren, Y. & Savill, J. Apoptosis: the importance of being eaten. *Cell Death and Differentiation* **5**(1998).

8.   Ashkenazi, A. & Dixit, V.M. Death receptors; signaling and modulation. *Science* **281**, 1305-8 (1998).

9.   Muzio, M. et al. FLICE, a novel FADD-homologous ICE/CED-3-like protease, is recruited to the CD95 (Fas/APO-1) death-inducing signaling complex. *Cell* **85**, 817-27 (1996).

10.   Scaffidi, C. et al. Differential modulation of apoptosis sensitivity in CD95 type I and type II cells. *J Biol. Chem.* **274**, 22532-22538 (1999).

11.   Tait, S.W.G. & Green, D.R. Mitochondria and cell death: outer membrane permeabilization and beyond. *Nature Rev. Mol. Cell Biol.* **11**, 621 (2010).

12.   Oda, E. et al. Noxa, a BH3-only member of the BCL-2 family and candidate mediator of p53 induced apoptosis. *Science* **288**, 1053-1058 (2000).

13.   Cuconati, A., Muhkerjee, C., Perez, D. & White, E. DNA damage response and MCL-1 destruction inititate apoptosis in adenovirus-infected cells. *Genes and Development* **17**, 2922-2932 (2003).

14.   Puthalakath, H. et al. ER stress triggers apoptosis by activating BH3-only protein BIM. *Cell* **129**, 1337-1349 (2007).

15.   Chipuk, J.E., Bouchier-Hayes, L. & Green, D.R. Mitochondrial outer membrane permabilization during apoptosis: the innocent bystander scenario. *Cell Death and Differentiation* **13**, 1396-1402 (2006).

16.   Zou, H., Li, Y., Liu, X. & Wang, X. An APAF-1 cytochrome c multimeric complex is a functiona apoptosome that activates procaspase-9. *J Biol. Chem.* **274**, 11549-11556 (1999).

17.   Li, P. et al. Cytochrome c and dATP-dependent formation of Apaf-1/caspase-9 complex initiates an apoptotic protease cascade. *Cell* **91**, 479-489 (1997).

18.   Tsujimoto, Y., Finger, L.R., Yunis, J., Nowell, P.C. & Croce, C.M. Cloning of the chromosome breakpoint of neoplastic B cells with the t(14;18) chromosome translocation. *Science* **226**, 1097-1099 (1984).

19.   Tsujimoto, Y., Cossman, J., Jaffe, E. & Croce, C.M. Involvement of the bcl-2 Gene in Human Follicular Lymphoma. *Science* **228**, 1440-1443 (1985).

20.   Vaux, D.L., Cory, S. & Adams, J.M. Bcl-2 gene promotes haemopoietic cell survival and cooperates with c-myc to immortalize pre-B cells. *Nature* **335**, 440-442 (1988).

21.   Cory, S., Huang, D.C.S. & Adams, J.M. The Bcl-2 family: roles in cell survival and oncogenesis. *Oncogene* **22**, 8590-8607 (2003).

22.   Willis, S.N. & Adams, J.M. Life in the balance: how BH3-only proteins induce apoptosis. *Curr. Op. Cell Biol.* **17**, 617-625 (2005).

23.   Korsmeyer, S.J. et al. Pro-apoptotic cascade activates BID, which oligomerizes BAK or BAX into pores that result in the release of cytochrome c. *Cell Death and Differentiation* **7**, 1166-1173 (2000).

24.   Wei, M.C. et al. Proapoptotic BAX and BAK: A requisite gateway to mitochondrial disfunction and death. *Science* **292**, 727-730 (2001).

25.   Danial, N.N. & Korsmeyer, S.J. Cell Death: Critical Control Points. *Cell* **116**, 205-216 (2004).

26.   Walensky, L.D. BCL-2 in the crosshairs: tipping the balance of life and death. *Cell Death Diff.* **33**, 1339-1350 (2006).

27.   Muchmore, S.W. et al. X-ray and NMR structure of human Bcl-xL, an inhibitor of programmed cell death. *Nature* **381**, 335-341 (1996).

28.   Yin, X.M., Oltvai, Z.N. & Korsmeyer, S.J. BH1 and BH2 domains of Bcl-2 are required for inhibition of apoptosis and heterodimerization with Bax. *Nature* **369**, 321-323 (1994).

29.   Sattler, M. et al. Structure of Bcl-xL-Bak peptide complex: Recoginition between regulators of apoptosis. *Science* **275**, 983-986 (1997).

30.	Chen, L. et al. Differential targeting of prosurvival Bcl-2 proteins by their BH3-only ligands allows complementary apoptotic function. *Mol. Cell* **17**, 393-204 (2006).

31.	Willis, S.N. et al. Proapoptotic Bak is sequestered by Mcl-1 and Bcl-xL, but not Bcl-2, until displaced by BH3-only proteins. *Genes Dev.* (2005).

32.	Zhai, D., Jin, C., Huang, Z., Satterthwait, A.C. & Reed, J.C. Differential Regulation of Bax and Bak by Anti-apoptotic Bcl-2 Family Proteins Bcl-B and Mcl-1. *J. Biol. Chem.* **283**, 9580-9586 (2008).

33.	Simmons, M.J. et al. Bfl-1/A1 functions, similar to Mcl-1, as a selective tBid and Bak antagonist. *Oncogene* **27**, 1421-1428 (2008).

34.	Dutta, S. et al. Determinants of BH3 binding specificity for MCL-1 vs. BCL-XL. *J Mol Biol* **398(5)**, 747-762 (2010).

35.	Fletcher, J.I. & Huang, D.C.S. Controlling the cell death mediators: Bax and Bak. *Cell Cycle* **7**, 39-44 (2008).

36.	Dewson, G. et al. To trigger apoptosis, Bak exposes its BH3 domain and homodimerizes via BH3:groove interactions. *Mol. Cell* **30**, 369-380 (2008).

37.	Annis, M.G. et al. Bax forms multi-spanning momoners that oligomerize to permeabilize membranes during apoptosis. *EMBO J* **24**, 2096-2103 (2005).

38.	Letai, A. et al. Distinct BH3 domains either sensitize or activate mitochondrial apoptosis, serving as prototype cancer therapeutics. *Cancer Cell* **2**, 183-192 (2002).

39.	Kuwana, T. et al. BH3 domains of BH3-only proteins differentially regulate Bax-mediated mitochondrial membrane permeabilization both directly and indirectly. *Mol. Cell* **17**, 525-535 (2005).

40.	Merino, D. et al. The role of BH3-only protein Bim extends beyond inhibiting Bcl-2-like prosurvival proteins. *J. Cell Biol.* **186**, 355-362 (2009).

41.	Willis, S.N. et al. Apoptosis initiated when BH3 ligands engage multiple BCL-2 homologs, not Bax or Bak. *Science* **315**, 856-859 (2007).

42.	Kozopas, K.M., Yang, T., Buchan, H.L., Zhou, P. & Craig, R.W. MCL1, a gene expressed in programmed myeloid cell differentiation, has sequence similarity to BCL2. *PNAS* **90**, 3516-3520 (1993).

43.	Yang, H., Kozopas, K.M. & Craig, R.W. The Intracellular Distribution and Pattern of Expression of Mcl-1 Overlap with, but are not Identical to, those of BCL-2. *J. Cell Biol.* **128**, 1173-1184 (1995).

44.   Zhou, P., Qian, L., Kozopas, K.M. & Craig, R.W. Mcl-1, a Bcl-2 family member, delays the death of hematopoetic cells under a variety of apoptosis-inducing conditions. *Blood* **89**, 630-643 (1997).

45.   Rinkenberger, J.L., Horning, S., Klocke, B., Roth, K.A. & Korsmeyer, S.J. Mcl-1 deficiency results in peri-implantation embryonic lethality. *Genes Dev.* **14**, 23-27 (2000).

46.   Opferman, J.T. et al. Obligate Role of Anti-Apoptotic MCL-1 in the Survival of Hematopoetic Stem Cells. *Science* **307**, 1101-1104 (2005).

47.   Opferman, J.T. et al. Development and maintenance of B and T lymphocytes requires anti-apoptotic MCL-1. *Nature* **426**, 671-676 (2003).

48.   Bae, J., Leo, C.P., Hsu, S.Y. & Hsueh, A.J.W. MCL-1s, a Splicing Variant of the Antiapoptotic BCL-2 Family Member MCL-1, Encodes a Proapoptotic Protein Possessing Only the BH3 Domain. *J Biol. Chem.* **275**, 25255-25261 (2000).

49.   Bingle, C.D. et al. Exon skipping in MCL-1 Results in a BCL-2 Homology Domain 3 Only Gene Product that Promotes Cell Death. *J Biol. Chem.* **29**, 22136-22164 (2000).

50.   Germain, M. & Duronio, V. The N Terminus of the Anti-apoptotic BCL-2 Homologue MCL-1 Regulates its Localization and Function. *J Biol. Chem.* **282**, 32233-32242 (2007).

51.   Herrant, M. et al. Cleavage of Mcl-1 by caspases impaired its ability to counteract Bim-induced apoptosis. *Oncogene* **23**, 7863-7873 (2004).

52.   Kobayashi, S. et al. Serine 64 Phosphorylation Enhances the Antiapoptotic Function of MCL-1. *J Biol. Chem.* **282**, 18407-18417 (2007).

53.   Opferman, J.T. Unraveling MCL-1 degradation. *Cell Death Diff.* **13**, 1260-1262 (2006).

54.   Zhong, Q., Gao, W., Du, F. & Wang, X. Mule/ARF-BP1, a BH3 -only E3 Ubiquitin Ligase, Catalyzes the Polyubiquitination of Mcl-1 and Regulates Apoptosis. *Cell* **121**, 1085-1095 (2005).

55.   Schwickart, M. et al. Deubiquiinase USP9X stabilizes MCL1 and promotes tumour cell survival. *Nature* **463**, 103-107 (2010).

56.   Akgul, C. Mcl-1 is a potential therapeutic target in multiple types of cancer. *Cell. Molec. Life Sci.* **66**, 1326-1336 (2009).

57.   Rampino, N. et al. Somatic frameshift mutations in the BAX gene in colon cancers of the microsatellite mutator phenotype. *Science* **275**, 967-969 (1997).

58.   Bouillet, P. et al. BH3-only Bcl-2 family member BIM is required for apoptosis of autoreactive thymocytes. *Nature* **415**, 922-926 (2002).

59. Ng, K.P. et al. A common BIM deletion polymorphism mediates intrinsic resistance and inferior response to tyrosine kinase inhbitors in cancer. *Nature Medicine* **18**, 521-528 (2012).

60. Ambs, S. et al. Genomic profiling of microRNA and messenger RNA reveals deregulated microRNA expression in prostate cancer. *Cancer Research* **68**, 6162-6170 (2008).

61. Xiao, C. et al. Lymphoproliferative disease and autoimmunity in mice with increased miR-17-92 expression in lymphocytes. *Nature Immunology* **9**, 405-414 (2008).

62. Chen, L. et al. Downregulation of miR-221/222 sensitizes glioma cells to temozolomide by regulating apoptosis independently of p53 status. *Oncology Reports* **27**, 854-860 (2012).

63. Zhang, C.Z. et al. MiR-221 and miR-222 target PUMA to induce cell survival in glioblastoma. *Mol Cancer* **9**, 229 (2010).

64. Zhou, M. et al. MicroRNA-125b confers the resistance of breast cancer cells to paclitaxel through suppression of pro-apoptotic Bcl-2 antagonist killer 1 (Bak1) expression. *J Biol. Chem.* **285**, 21496-21507 (2012).

65. Shi, X.B. et al. An androgen-regulated miRNA suppresses Bak1 expression and induces androgen-independent growth of prostate cancer cells. *Proc Natl Acad Sci* **104**, 19983-19988 (2007).

66. Yu, J., Zhang, L.C., Hwang, P.M., Kinzler, K.W. & Vogelstein, B. PUMA induces the rapid apoptosis of colorectal cancer cells. *Mol Cell* **7**, 673-682 (2001).

67. Nakano, K. & Vousden, K.H. PUMA, a novel proapoptotic gene, is induced by p53. *Mol Cell* **7**, 683-694 (2001).

68. Oda, E. et al. Noxa, a BH3-only member of the BCL-2 family and candidate mediatior of p53-induced apoptosis. *Science* **288**, 1053-1058 (2000).

69. Navas, T.A. et al. Inhibition of p38alpha MAPK enhances proteasome inhibitor-induced apoptosis of myeloma cells by modulating Hsp27, Bcl-X(L), Mcl-1 and p53 levels in vitro and inhibits tumor growth in vivo. *Leukemia* **20**, 1017-1027 (2006).

70. Hanada, M., Delia, D., Aiello, A., Stadtmauer, E. & Reed, J.C. Bcl-2 gene hypomethylation and high-level expression in B-cell chronic lymphocytic leukemia. *Blood* **82**, 4279-4284 (1993).

71. Kitada, S., Pederson, I.M., Schimmer, A. & Reed, J.C. Dysregulation of apoptosis genes in hematopoietic malignancies. *Oncogene* **21**, 3459-3474 (2002).

72. Kang, M.H. & Reynolds, C.P. BCL-2 inhibitors: targeting mitochondrial apoptotic pathways in cancer therapy. *Clin. Cancer Res.* **15**, 1126-1132 (2009).

73.   Zhang, H. et al. microRNA-143, down-regulated in osteosarcoma, promotes apoptosis and suppresses tumorigenicity by targeting Bcl-2. *Oncology Reports* **24**, 1363-1369 (2010).

74.   Derenne, S. et al. Antisense strategy shows that Mcl-1 rather than Bcl-2 or Bcl-x(L) is an essential survival protein of human myeloma cells. *Blood* **100**, 194-9 (2002).

75.   Zhang, B., Gojo, I. & Fenton, R.G. Myeloid cell factor-1 is a critical survival factor for multiple myeloma. *Blood* **99**, 1885-93 (2002).

76.   Konopleva, M. et al. Mechanisms of apoptosis sensitivity and resistance to the BH3 mimetic ABT-737 in acute myeloid leukemia. *Cancer Cell* **10**, 375-88 (2006).

77.   Boisvert-Adamo, K., Longmate, W., Abel, E.V. & Aplin, A.E. Mcl-1 is required for melanoma cell resistance to anoikis. *Mol Cancer Res* **7**, 549-56 (2009).

78.   Ding, Q. et al. Myeloid Cell Leukemia-1 Inversely Correlates with Glycogen Synthase Kinase-3{beta} Activity and Associates with Poor Prognosis in Human Breast Cancer. *Cancer Res* **67**, 4564-71 (2007).

79.   McDonnell, T.J. et al. Bcl-2 immunoglobulin transgenic mice demonstrate extended B cell survival and follicular lymphoproliferation. *Cell* **57**, 79-88 (1989).

80.   Strasser, A., harris, A.W., Bath, M.L. & Cory, S. Novel primitive lymphoid tumors induced in transgenic mice by cooperation between myc and bcl-2. *Nature* **348**, 331-333 (1990).

81.   Zhou, P. et al. MCL1 transgenic mice exhibit a high incidence of B-cell lymphoma manifested as a spectrum of histologic subtypes. *Blood* **97**, 3902-3909 (2001).

82.   Zhou, P. et al. Mcl-1 in transgenic mice promotes survival in a spectrum of hematopoetic cell types and immortalization in the myeloid lineage. *Blood* **92**, 3226-3239 (1998).

83.   Kauffman, S.H. et al. Elevated expression of the apoptotic regulator Mcl-1 at the time of leukemic relapse. *Blood* **91**, 991-1000 (1998).

84.   Beroukhim R, Mermel CH, Porter D, Wei G & Raychaudhuri S, D.J., Barretina J, Boehm JS, Dobson J, Urashima M, Mc Henry KT, Pinchback RM, Ligon AH, Cho YJ, Haery L, Greulich H, Reich M, Winckler W, Lawrence MS, Weir BA, Tanaka KE, Chiang DY, Bass AJ, Loo A, Hoffman C, Prensner J, Liefeld T, Gao Q, Yecies D, Signoretti S, Maher E, Kaye FJ, Sasaki H, Tepper JE, Fletcher JA, Tabernero J, Baselga J, Tsao MS, Demichelis F, Rubin MA, Janne PA, Daly MJ, Nucera C, Levine RL, Ebert BL, Gabriel S, Rustgi AK, Antonescu CR, Ladanyi M, Letai A, Garraway LA, Loda M, Beer DG, True LD, Okamoto A, Pomeroy SL, Singer S, Golub TR, Lander ES, Getz G, Sellers WR, Meyerson M. The landscape of somatic copy-number alteration across human cancers. *Nature* **18**, 899-905 (2010).

85.   Mott, J.L., Kobayashi, S., Bronk, S.F. & Gores, S.D. mir-29 regulates Mcl-1 protein expression and apoptosis. *Oncogene* **26**, 6133-6140 (2007).

86.   Su, H. et al. MicroRNA-101, down-regulated in hepatocellular carcinoma, promotes apoptosis and suppresses tumorigenicity. *Cancer Research* **69**, 1135-1142 (2009).

87.   Derenne, S. et al. Antisense strategy shows that Mcl-1 rather than Bcl-2 or Bcl-xL is an essential survival protein of human myeloma cells. *Blood* **100**, 194-199 (2002).

88.   Seighart, W. et al. MCL-1 overexpression in hepatocellular carcinoma: a potential target for antisense therapy. *J. Hepatol.* **44**, 151-157 (2006).

89.   Cotter, F.E., Waters, J. & Cunningham, D. Human BCL-2 antisense therapy for lymphomas. *Biochimica et Biphysica Acta* **1489**, 97-106 (1999).

90.   Jansen, B. et al. Bcl-2 antisense therapy chemosensitizes human malnoma in SCID mice. *Naure Medicine* **4**, 232-234 (1998).

91.   Moulder, S.L. et al. Phase I/II Study of G3139 (Bcl-2 antisense oligonucleotide) in combination with doxorubicin and docetaxel in breast cancer. *Clinical Cancer Research* **14**, 7909 (2008).

92.   Derenne, S. et al. Antisense strategy shows that MCL-1 rather than BCL-2 or BCL-XL is an essential survival protein in human myeloma cells. *Blood* **100**, 194-199 (2002).

93.   Lin, X. et al. "Seed" analysis of off-target siRNAs reveals an essential role of MCL-1 in resistance to the small-molecule Bcl-2/Bcl-xL inhibitor ABT-737. *Oncogene* **26**, 3972-3979 (2007).

94.   Wilhelm, S. et al. BAY 43-9006 exhibits broad spectrum oral antitumor activity and targets the RAF/MEK/ERK pathway and receptor tyrosine kinases involved in tumor progression and angiogenesis. *Cancer Res.* **64**, 7099-7109 (2004).

95.   Fectaeu, J.F. et al. Sorafenib-induced apoptosis of chronic lymphocytic leukemia cells is associated with downregulation of RAF and myeloid cell leukemia sequence 1 (Mcl-1). *Mol Med* **18**, 19-28 (2012).

96.   Chauhan, D. et al. A novel carbohydrate-based therapeutic GCS-100 overcomes bortezomib resistance and enhances dexamethasone-induced apoptosis in multiple myeloma cells. *Cancer Res.* **65**, 8350-8358 (2005).

97.   Streetly, M.J. et al. GCS-100, a novel galectin-3 antagonist, modulates MCL-1, NOXA, and cell cycle to induce myeloma cell death. *Blood* **115**, 3939-3948 (2010).

98.   Wells, J.A. & McClendon, C.L. Reaching for high-hanging fruit in drug discovery at protein-protein interfaces. *Nature* **450**(2007).

99. Moreira, I.S., Fernandes, P.A. & Ramos, M.J. Hot-spot mimicry - a review of the protein-protein interface determinant amino acid residues. *Proteins* **68**(2007).

100. Bogan, A.A. & Thorn, K.S. Anatomy of hot spots in protein interfaces. *J Mol Biol* **280**, 1-9 (1998).

101. Fry, D.C. & Vassilev, L.T. Targeting protein-protein interactions for cancer therapy. *J Mol Med* **83**, 955-963 (2005).

102. Cochran, A.G. Antagonists of protein-protein interactions. *Chem Biol* **7**, R85-R94 (2000).

103. Lipinski, C.A., Lombardo, F., Dominy, B.W. & Feeney, P.J. Experimental and computational approaches to estimate solubility and permeability in drug discovery and development settings. *Adv Drug Deliv Rev* **46**, 3-26 (2001).

104. Zhang, M.Q. & Wilkinson, B. Drug discovery beyond the 'rule-of-five'. *Curr Op Biotech* **18**, 478-488 (2007).

105. Morelli, X., Bourgeus, R. & Roche, P. Chemical and structural lessons from recent successes in protein-protein interaction inhibition. *Curr Op Chem Biol* **15**, 475-481 (2011).

106. Kubbutat, M.H., Jones, S.N. & Vousden, K.H. Regulation of p53 stability by Mdm2. *Nature* **387**, 299-303 (1997).

107. Fulda, S. & Vucic, D. Targeting IAP proteins for therapeutic intervention in cancer. *Nature Rev. Drug Disc.* **11**, 109-124 (2012).

108. Du, C., Fang, M., Li, Y., Li, L. & Wang, X. Smac, a mitochondrial protein that promotes cytochrome-c dependent caspase activation by eliminating IAP inhibition. *Cell* **102**, 33-42 (2000).

109. Li, L. et al. A small molecule Smac mimic potentiates TRAIL and TNFA-mediated cell death. *Science* **305**, 1471-1474 (2004).

110. Walensky, L.D. et al. Activation of apoptosis in vivo by a hydrocarbon stapled BH3 helix. *Science* **305**, 1466-1470 (2004).

111. Schafmeister, C.E., Po, J. & Verdine, G.L. An All-hydrocarbon cross-linking system for enhancing the helicity and metabolic stability of peptides. *JACS* **122**, 5891-5892 (2000).

112. Blackwell, H.E. & Grubbs, R.H. Highly efficient synthesis of covalently crosslinked peptide helices by ring closing metathesis. *Agnew Chem Int Edit* **37**, 3281-3284 (1998).

113. Walensky, L.D. et al. A stapled BID BH3 helix directly binds and activates BAX. *Mol. Cell* **24**, 199-210 (2006).

114.   Bernal, F., Tyler, A.F., Korsmeyer, S.J., Walensky, L.D. & Verdine, G.L. Reactivation of the p53 tumor suppressor pathway by a stapled p53 peptide. *JACS* **129**, 2456-2457 (2007).

115.   Gavathiotis, E. et al. BAX activation is initiated at a novel interaction site. *Nature* **455**, 1076-81 (2008).

116.   Gavathiotis, E., Reyna, D.E., Davis, M.L., Bird, G.H. & Walensky, L.D. BH3-triggered structural reorganization drives the activation of proapoptotic BAX. *Mol Cell* **40**, 481-492 (2010).

117.   Stewart, M.L., Fire, E., Keating, A.E. & Walensky, L.D. The MCL-1 BH3 helix is an exclusive MCL-1 inhibitor and apoptosis sensitizer. *Nature Chem Biol* **6**, 595-601 (2010).

118.   Berg, T. Small-molecule inhibitors of protein-protein interactions. *Curr. Op. Drug Disc. Dev.* **11**, 666-674 (2008).

119.   Wang, J.L. et al. Structure based discovery of an organic compound that binds BCL-2 protein and induces apoptosis of tumor cella. *PNAS* **97**, 7124-7129 (2000).

120.   Tzung, S.P. et al. Antimycin A mimics a cell-death-inducing BCL-2 homology domain 3. *Nature Cell Biol.* **3**, 183-191 (2001).

121.   Degeretev, A. et al. Identification of small molecule inhibitors of interaction between the BH3 domain and BCL-X$_L$. *Nature Cell Biol.* **3**, 173-182 (2001).

122.   Oltersdorf, T. et al. An inhbitor of Bcl-2 family proteins induces regression of solid tumours. *Nature* **435**, 677-681 (2005).

123.   Konopleva, M. et al. Mechanisms of apoptosis sensitity and resistance to the BH3 mimetic ABT-737 in acute myeloid leukemia. *Cancer Cell* **10**, 375-388 (2006).

124.   Tse, C. et al. ABT-263: A Potent and Orally Bioavialable Bcl-2 Family Inhibitor. *Cancer Res.* **68**, 3421-3428 (2008).

125.   Hauck, P., Chao, B.H., Litz, J. & Krystal, G.W. Alterations in the NOXA/MCL-1 axis determine sensitivity of small cell lung cancer to the BH3 mimetic ABT-737. *Mol. Cancer Ther.* **8**, 883-892 (2009).

126.   Vogler, M. et al. Concurrent up-regulation of Bcl-xL and BCL2A1 induces approximately 1000-fold resistance to ABT-737 in chronic lymphocytic leukemia. *Blood* **113**, 4403-4413 (2009).

127.   van Delft, M.F. et al. The BH3 mimetic ABT-737 targets selective Bcl-2 proteins and efficiently induces apoptosis via Bak/Bax if Mcl-1 is neutralized. *Cancer Cell* **10**, 389-399 (2006).

128.   Nguyen, M. et al. Small molecule obatoclax (GX15-070) antagonizes MCL-1 and overcomes MCL-1-mediated resistance to apoptosis. *PNAS* **104**, 19512-19517 (2007).

129.   Huang, S., Okumura, K. & Sinicrope, F.A. BH3 Mimetic Obatoclax Enhances TRAIL-mediated Apoptosis in Human Pancreatic Cancer Cells. *Clin. Cancer Res.* **15**, 150-159 (2009).

Chapter 2

Utilization of MCL-1 SAHB to Discover Small Molecules That Specifically Bind MCL-1

Abstract

Stewart *et al.* recently generated a library of stabilized alpha helices of BCL-2 domains (SAHBs) and discovered that the BH3 helix of MCL-1 was itself the most potent and selective natural BH3 inhibitor of MCL-1[1]. Whereas the unmodified MCL-1 BH3 peptide was predominantly unstructured and showed little MCL-1 binding activity, we sought to determine if the structurally-fortified and MCL-1-selective stapled peptide could be deployed in a competitive binding screen to in turn identify a selective small molecule antagonist for reactivating apoptosis in MCL-1-dependent cancer. Top compound hits found in the high-throughput screen proceeded through a series of secondary assays to analyze their potency and specificity. The development and application of high affinity/high selectivity stapled peptides for competitive screening was therefore utilized as an effective and generalizable strategy for small molecule drug discovery.

Introduction

The discovery of BCL-2 at the t(14;18) chromosomal breakpoint in follicular lymphoma led to the novel paradigm that malignant transformation can be driven by proteins that regulate the balance between cellular survival and death[2-4], specifically through upregulation of anti-apoptotic proteins. The anti-apoptotic BCL-2 proteins MCL-1, BCL-2, BCL-X_L, BCL-w, and BFL-1/A1 counteract apoptosis by sequestering the BH3 domains of both BH3-only and multidomain pro-apoptotic proteins. Specifically, the pro-apoptotic BH3 domain binds a groove formed by helices α2 (BH3) and portions of α3, α4, α5 (BH1) and α8 (BH2) of the anti-apoptotic proteins; this pocket contains a region of hydrophobic residues that is highly conserved among BCL-2 family anti-apoptotic proteins[5]. Because the BCL-2 family plays critical roles in cancer pathogenesis, the development of targeted inhibitors of anti-apoptotic proteins has become a pressing pharmacologic goal for combating refractory malignancies[6].

The physiologic role of BCL-2 family protein overexpression in promoting tumorigenesis has stimulated numerous efforts to develop small molecules and peptides to reactivate the apoptotic pathway through anti-apoptotic protein blockade. A series of small molecule screens and structure-based methodologies were initially applied to target BCL-2, yielding an eclectic array of small molecules and peptides with various degrees of biochemical, cellular, and *in vivo* activity[7-16]. Specifically, small molecule screens are important tools used to identify lead compounds that mimic BH3 death domains for anti-apoptotic targeting, allowing for displacement of pro-apoptotic family members and promoting apoptosis induction[17]. Previous high-throughput screening strategies have led to the successful discovery of small molecules that disrupt an anti-apoptotic protein interaction with its alpha-helical binding partner. For example, early screening platforms were optimized to discover small molecules that disrupt the BCL-

X_L/BAK BH3[18] or BCL-X_L/BAD BH3[19] interaction via competitive fluorescence polarization (FP) assays, with the prior screen uncovering the BH3I class of small molecules that were shown to inhibit the BCL-X_L/BAK interaction in cells, thus inducing apoptosis[18]. More recently, a high-throughput screen was performed that identified small molecules capable of disrupting the BFL-1/A1/BID BH3 interaction through a similar competitive FP assay[20]. These examples highlight the utility of high-throughput biochemical screening to identify prototype molecular modulators of BCL-2 family proteins. The application of MCL-1 SAHB as an MCL-1-selective agent provides a unique screening tool for discovering MCL-1-selective small molecules.

The breakthrough molecule ABT-263 is an orally bioavailable and selective BCL-2/BCL-X_L inhibitor, which is advancing through the clinical trials process, manifesting both safety and preliminary efficacy in BCL-2-dependent cancers[21-24]. Broad experimentation with the ABT-263 molecule and its progenitor ABT-737 revealed that expression of anti-apoptotic proteins lying outside their binding spectra caused resistance[25-28], compelling the development of alternative or complementary agents that would either harbor broader anti-apoptotic targeting capacity or inherent selectivity for anti-apoptotics like MCL-1 that evade ABT-263/737 antagonism.

The small molecule obatoclax[10] and the peptidic stabilized alpha-helices of BCL-2 domains (SAHBs) modeled after the BID and BIM BH3 domains[29-31] are examples of novel agents that more broadly target the BCL-2 family anti-apoptotic proteins. Given the emergence of MCL-1 as a "top ten" pathologic factor across the diversity of human cancers[32], elucidating the blueprint for selective MCL-1 inhibition has also become a major focus of academic and pharmaceutical researchers. MCL-1 SAHB, the recently discovered selective stapled peptide that targets MCL-1, sensitized OPM2 and Jurkat cancer cells to death receptor-induced apoptosis[1], highlighting the importance of targeting MCL-1 to dismantle its pro-survival role in cancer cells.

For this reason, the quest for exquisitely selective small molecules to target MCL-1 is receiving tremendous attention despite the inherent challenges of generating small molecules that can distinguish among homologous BH3-binding surfaces.

Results

Discovery of MCL-1-selective small molecules by a high-throughput screen utilizing the MCL-1/MCL-1 SAHB interaction

The previous discovery of MCL-1 SAHBs, or hydrocarbon-stapled MCL-1 BH3 α-helices, by Stewart *et al.* prompted their utilization in a high-throughput biochemical screen for small molecules that disrupt the *in vitro* interaction with MCL-1ΔNΔC. MCL-1 SAHBs were previously shown to selectively target MCL-1 in biochemical, structural, and functional analyses, thus sensitizing cancer cells to death-receptor-induced, caspase-dependent apoptosis[1]. Here, we deployed MCL-1 SAHB$_A$ (**Table 2.1**) as a high fidelity screening tool to determine if its potency and specificity-of-action could be harnessed for small molecule discovery. A high-throughput competitive FP screening assay (Z-factor[33], 0.62) was developed based on the direct binding interaction between FITC-MCL-1 SAHB$_A$ and MCL-1ΔNΔC (EC$_{50}$, 14 nM) (**Figure 2.1A-C**). This system was validated for screening with the positive control peptide BID SAHB$_A$, a known MCL-1 binder, and the negative control peptide BCL-2 SAHB$_A$, which does not interact with MCL-1. A compilation of 71,296 commercial small molecules was screened for the capacity to displace FITC-MCL-1 SAHB$_A$ from recombinant MCL-1ΔNΔC (aa 172-327) (**Figure 2.2**). To enrich for MCL-1-selective compounds by detecting binding activity for the BCL-X$_L$ subclass of anti-apoptotic proteins, the libraries were also counter-screened using a competitive FP assay (Z-factor, 0.71) developed based on the direct and selective interaction between FITC-BAD BH3 and BCL-X$_L$$\Delta$C (EC$_{50}$, 26 nM)[19,34] (**Figure 2.1D-F**). This system was validated for counter-screening with the positive control peptide BAD SAHB$_A$, a known BCL-X$_L$ binder, and the negative control peptide MCL-1 SAHB$_A$, which does not interact with BCL-X$_L$. Small molecules with an apparent preference for MCL-1ΔNΔC (208 compounds, 0.3% hit rate),

Table 2.1. *BH3 peptide compositions used in the high-throughput screen and subsequent assays.*

Peptide	Sequence	N-terminus	MW	M/3
MCL-1 SAHB$_A$	KALETLRXVGDXVQRNHETAF	FITC-βAla-	2893	965.5
MCL-1 SAHB$_D$	KALETLRRVGDGVXRNHXTAF	Acetyl-βAla-	2502	835.0
MCL-1 SAHB$_D$	KALETLRRVGDGVXRNHXTAF	FITC-βAla-	2850	950.8
BAD SAHB$_A$	NLWAAQRYGRELRXBSDXFVDSFKK	Acetyl-	3090	1030.9
BID SAHB$_A$	DIIRNIARHLAXVGDXBDRSI	Acetyl-	2438	813.7
BCL-2 SAHB$_A$	VVHLTLRXAGDXFSRRY	Acetyl-	2082	694.4

Figure 2.1. *Development of a stapled peptide-based high-throughput competitive screening assay for identifying MCL-1-selective small molecules.* (A-C) A high-throughput competitive FP binding assay was developed based on the direct binding interaction between FITC-MCL-1 SAHB*A* and MCL-1ΔNΔC (EC$_{50}$, 14 nM), and validated for screening using a positive control for complete displacement (BID SAHB*A*) and a negative control for no displacement (BCL-2 SAHB*A*), yielding an assay Z-factor of 0.62. (D-F) To enrich for MCL-1-selective small molecules, a counter-screen was developed based on the direct binding interaction between FITC-BAD BH3 and BCL-X$_L$ΔC (EC$_{50}$, 26 nM), and validated for screening using a positive control for complete displacement (BAD SAHB*A*) and a negative control for no displacement (MCL-1 SAHB*A*), yielding an assay Z-factor of 0.71.

Figure 2.2. *Workflow toward identification of small molecules that selectively bind anti-apoptotic MCL-1*. 71,296 compounds were initially screened for their selective MCL-1 binding capability in combination with a BCL-X$_L$ counter-screen. The putative small molecule hits (208) were re-examined in a confirmatory repeat screen, leading to 130 positive hits. FITC-BID BH3 was utilized as the ligand for specificity testing, and the 64 most potent and selective compounds were purchased for dose-response analyses. Those compounds binding to MCL-1 (via displacement of MCL-1 SAHB$_A$) with a potency of less than 30 μM were advanced to dose-responsive specificity testing.

Figure 2.2 (continued)

71,296

High-throughput competitive FP screen:
FITC-MCL-1 SAHB$_A$/MCL-1ΔNΔC vs.
FITC-BAD BH3/BCL-X$_L$ΔC

208

Confirmatory repeat screen

■ % MCL-1 SAHB$_D$ bound to MCL-1ΔNΔC
■ % BAD BH3 bound to BCL-X$_L$ΔC

130

Confirm specificity by alternative competitive
FP: FITC-BID BH3/MCL-1ΔNΔC vs. BCL-X$_L$ΔC

■ % BID BH3 bound to MCL-1ΔNΔC
■ % BID BH3 bound to BCL-X$_L$ΔC

64

Dose-responsive competitive FP analysis:
FITC-MCL-1 SAHB$_A$/MCL-1ΔNΔC

28

Dose-responsive specificity testing:
FITC-BID BH3/MCL-1ΔNΔC vs. BCL-X$_L$ΔC

● MCL-1ΔNΔC
● BCL-X$_L$ΔC

as defined both by > 50% displacement of the FITC-MCL-1 SAHB$_A$/MCL-1ΔNΔC interaction

and a > 45% difference in peptide displacement from MCL-1ΔNΔC vs. BCL-X$_L$ΔC were

advanced to increasingly stringent confirmatory *in vitro* binding assays including: (1) repeat

single-dose testing of 208 molecules in the differential competitive FP screen; (2) alternative

single-dose selectivity screen for 130 confirmed MCL-1-directed antagonists comparing relative

displacement of FITC-BID BH3, a dual binder[35], from MCL-1ΔNΔC vs. BCL-X$_L$ΔC; and then

(3) dose-responsive competitive binding of the 64 most selective molecules against the FITC-

MCL-1 SAHB$_A$/MCL-1ΔNΔC complex (**Figure 2.2**). The identification of gossypol, a

compound known to bind MCL-1 with a two-fold greater affinity than BCL-X$_L$[35], as an initial hit

served as a reassuring internal validation of the screen design.

*Structural classification, binding validation, and preliminary docking analysis of MCL-1-
selective small molecules*

The 64 identified small molecules were categorized into structural classes, as defined by

the specific molecular scaffolds and chemical functionalities for each compound grouping

(**Figure 2.3**). These compounds were purchased from commercial sources and tested in a dose-

responsive competitive FP assay examining displacement of FITC-MCL-1 SAHB$_A$ from MCL-

1ΔNΔC. Those compounds that bound MCL-1 with an IC$_{50}$ value less than 30 μM were

advanced to competitive FP binding assays utilizing the pan-anti-apoptotic binder FITC-BID

BH3. Dose-responsive specificity data from a sample molecule within each class is shown in

Figure 2.4.

47

Classification	Structural Scaffold
Class A	
Class B	Bioactives/ unclassified
Class C	
Class D	
Class E	
Class F	
Class G	
Class H	
Class I	

Figure 2.3. *Structural compound classes that emerged from the screen.* Most small molecules could be classified based on their core structural scaffold (Classes A, C-I). Small molecules that were known bioactives or did not contain similar structural partners were assigned to Class B.

Figure 2.4. *Sampling of compound hits discovered in the initial high-throughput screen.* An example from each structural class (see Figure 2.3) is displayed; competitive FP assay shows displacement of FITC-BID BH3 from MCL-1ΔNΔC and BCL-X$_L$$\Delta$C. Each compound displays differential affinities to MCL-1 but does not bind to BCL-X$_L$ with high affinity.
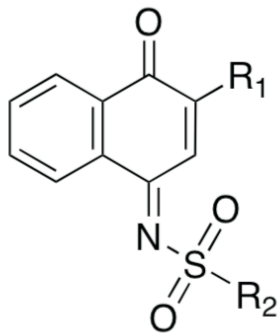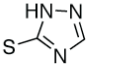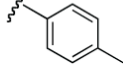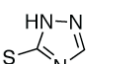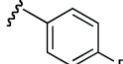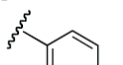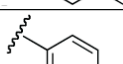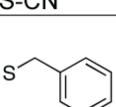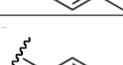
Figure 2.4 (continued)
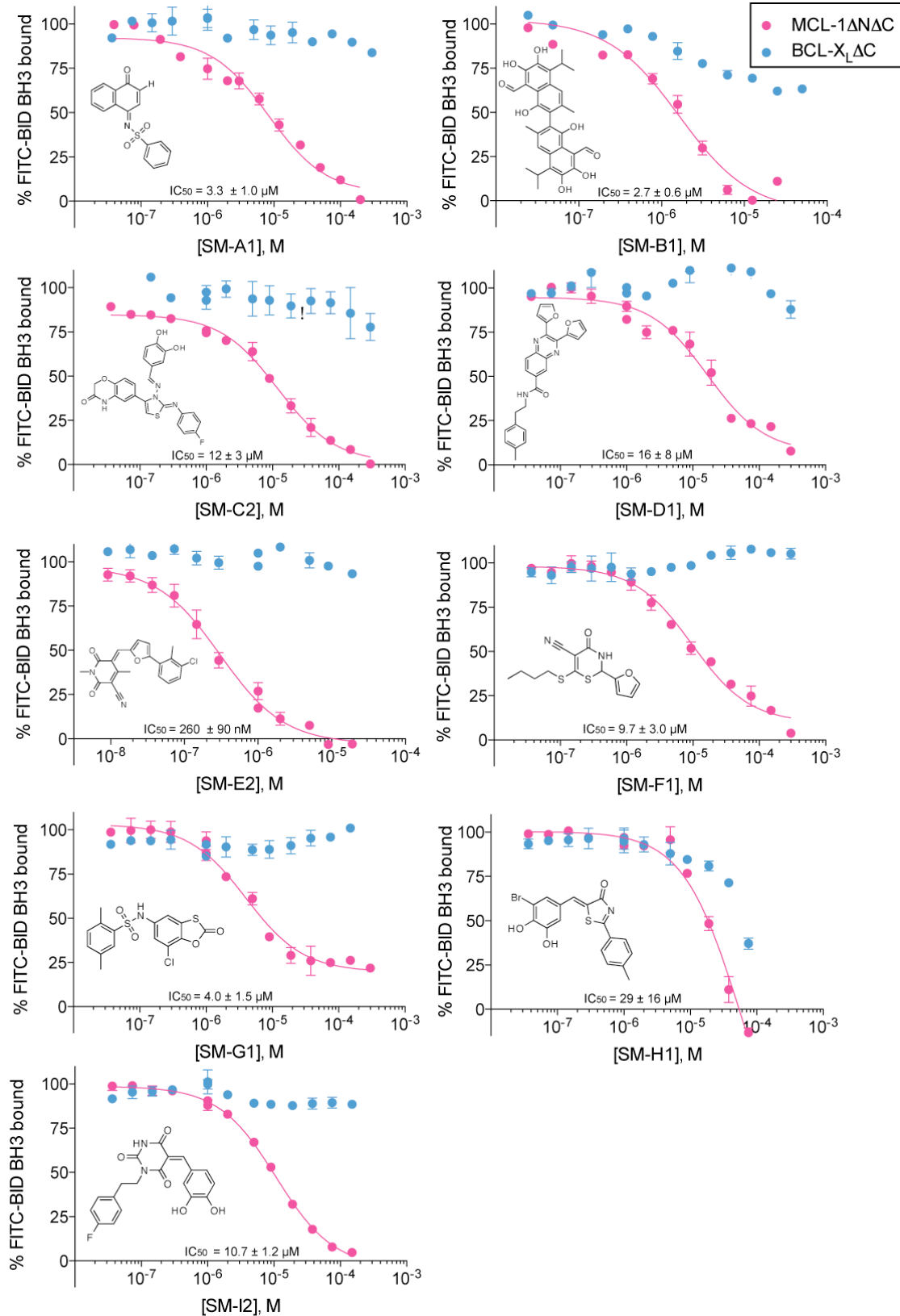
For select classes, preliminary structure-activity relationship (SAR) studies were performed using commercially available derivatives that sampled alternate side groups and scaffold modifications. For example, analysis of Class A compounds revealed particular side group functionalities that either enhanced, had no effect, or impaired MCL-1 binding activity, providing insight into key regions of the interacting scaffold (**Figure 2.5**). Although further medicinal chemistry is necessary to fully dissect the structure-activity relationships that dictate potency and selectivity, the commercial availability of such compounds allowed for preliminary data upon which to generate basic conclusions regarding the importance of discrete functionalities.

To preview potential sites of interaction for the compounds on MCL-1, molecular docking studies using GLIDE XP v.5 were performed. Docking calculations using this program yielded structures highly analogous to published x-ray structures[36]. Coordinates from the MCL-1 SAHB/MCL-1 ΔNΔC co-crystal structure were used as a template, and the hydrophobic groove was selected as the docking site. The program then calculated energetic binding scores for different poses of each ligand in the hydrophobic groove, yielding a rank order of energetically favorable docking solutions. While BH3-only peptides and the MCL-1 SAHB span the entire hydrophobic groove, the small molecules dock to much more specific pockets within the groove. For example, MCL-1 SAHB binding depends on salt bridge interactions at R263, as well as hydrogen bond networks spanning D256 and N260. Based on the energetically favorable docking solutions, R263 is predicted to play a role in forming polar contacts between many of the small molecules and MCL-1ΔNΔC (**Figure 2.6**). Most of the small molecules dock directly into a deep hydrophobic pocket lined by residues L246, V249, L267, and F269, and the more distant H224 also appears to play a role in positioning the compounds into the groove.

R_1	R_2	IC_{50}
triazole-thiol (HN–N, S)	4-methylphenyl	14 ± 9 nM
triazole-thiol (HN–N, S)	4-fluorophenyl	100 ± 80 nM
Cl	4-methylphenyl	3.2 ± 1.6 μM
S-CN	4-methylphenyl	3.8 ± 0.8 μM
S-benzyl	4-methylphenyl	> 10 μM
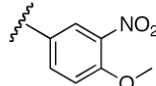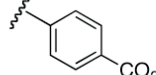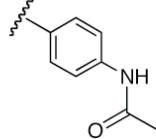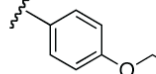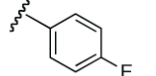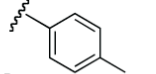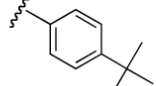
R_1	R_2	IC_{50}
H	3-NO_2, 4-O-methyl phenyl	1.5 ± 1.0 μM
H	phenyl	1.7 ± 0.4 μM
H	4-CO_2H phenyl	2.2 ± 0.5 μM
H	4-(NH–C(O)CH₃) phenyl	2.9 ± 0.7 μM
H	4-ethoxy phenyl	3.1 ± 1.5 μM
H	4-F phenyl	3.6 ± 2.6 μM
H	4-methyl phenyl	4.8 ± 3.0 μM
H	4-tert-butyl phenyl	> 10 μM

Figure 2.5. *SAR binding analysis of Class A compounds.* Structural analogs were purchased, and their binding affinities examined by competitive FP assay in which FITC-BID BH3 is displaced from recombinant MCL-1. Compounds were ranked by IC_{50} value, with the structures of distinguishing R groups also displayed.
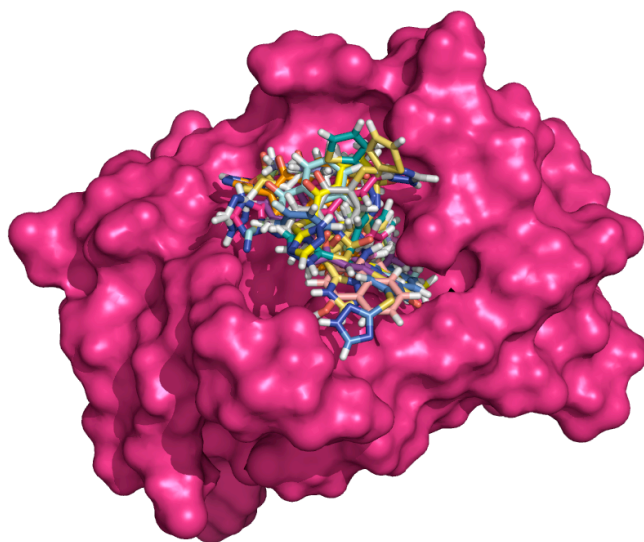
Figure 2.6. *Molecular docking studies reveal predicted MCL-1 pocket binding of top scoring small molecules.* Structural modeling was performed by defining the small molecule interaction surface as the canonical BH3-binding groove of MCL-1; the structures of all compounds identified in the screen were loaded into the docking program, GLIDE XP v.5. The top scoring compounds based on energetically favorable docking calculations are displayed on the MCL-1ΔNΔC structure.

Cellular screening of MCL-1-selective small molecules

To explore the specificity of the top small molecule hits in a genetically controlled system, a panel of mouse embryo fibroblasts (MEFs) was assembled for small molecule testing. Cellular responses to the molecules were compared in wild-type and *Bax^{-/-}Bak^{-/-}* (DKO) MEFs to distinguish among compounds that induce cell death in a BAX/BAK-dependent manner. To validate the cellular screen, the pro-apoptotic activity of the selective BCL-2/BCL-X$_L$ inhibitor ABT-737, which is known to impair the viability of *Mcl-1^{-/-}* MEFs, but has no significant effect on wild-type, *Bcl-x$_L$^{-/-}*, or DKO MEFs, was examined (**Figure 2.7**). Importantly, ABT-737 showed no cytotoxic effect in wild-type or DKO MEFs, and these results were benchmarked against the small molecules arising from the high-throughput screen to eliminate compounds with inherent non-specific toxicity based on potential off-target effects. Compounds with a favorable, non-toxic profile in MEFs were advanced to further testing (**Table 2.2**).

The MCL-1-selective small molecules were next applied to cancer cells that overexpress MCL-1 to screen for pro-apoptotic activity. For example, OPM2 multiple myeloma cells demonstrated varying sensitivity to all of the selected compounds, with IC$_{50}$ values ranging from 500 nM to 50 µM. Moreover, 18 of the small molecules displayed synergistic killing when combined with TRAIL, as determined by CalcuSyn analysis (combination index < 1)[37] (**Table 2.2**). Interestingly, MCL-1 siRNA[38] and MCL-1 SAHB also sensitize TRAIL-mediated cell death, suggesting that the small molecules may likewise induce cell death as a result of MCL-1 inhibition.
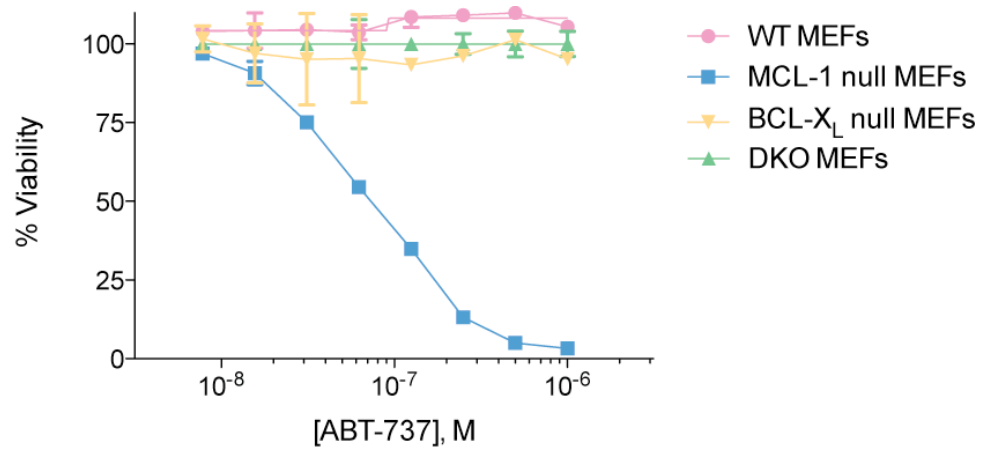
Figure 2.7. *ABT-737 selectively impairs viability of Mcl-1^{-/-} MEFs but exhibits no cytotoxicity in wild-type, DKO, or Bcl-x_L^{-/-} MEFs.* Cell viability was measured at 24 hours post-treatment.

Table 2.2. *Cellular screens were applied to advance small molecules that induced cancer cell death in MCL-1-expressing OPM2 cells but were not cytotoxic to MEFs.* Combination effects with TRAIL in OPM2 cells are indicated by + for synergy, - for antagonism, and +/- for additive effects based on previously published combination index value ranges[37].

Compound	WT MEF EC_{50}	DKO MEF EC_{50}	TRAIL synergy in OPM2
SM-C4	~40 µM	~40 µM	++
SM-D1	>100 µM	>100 µM	+++
SM-E3	~80 µM	~80 µM	+
SM-F3	>100 µM	>100 µM	++
SM-H1	~50 µM	~75 µM	+++

Discussion

A novel FP-based competitive binding assay was established using the MCL-1-selective stapled peptide MCL-1 SAHB$_A$, with the goal of identifying potent and selective small molecule MCL-1 inhibitors by competing with a high affinity and high specificity stapled peptide ligand. This screen yielded 28 small molecules that selectively bound to MCL-1 with high affinity based on a competitive FP binding displacement assay. A variety of distinct structural classes were identified, and their binding activity was interrogated in a variety of *in vitro* assays. The results of initial cellular testing were consistent with specific induction of cell death in the context of MCL-1 expression, lacking non-specific toxicity as assayed by parallel screening in MEFs. These findings highlight the utility of the MCL-1/MCL-1 SAHB-based small molecule screen, which yielded a novel cohort of compounds for advancement to a rigorous battery of mechanistic studies designed to identify potent and selective MCL-1 inhibitors with the capacity to reactivate cancer cell apoptosis in the specific context of MCL-1 dependence.

Methods

SAHB synthesis

Hydrocarbon-stapled peptides corresponding to BCL-2 family BH3 domains and their FITC-βAla derivatives were synthesized, purified, and characterized according to previously described methods[14,31,39]. The sequence compositions of all SAHBs used in this study are listed in **Table 2.1**.

BCL-2 family protein production

Recombinant MCL-1ΔNΔC and BCL-X$_L$ΔC were expressed and purified as previously reported[29,40]. Transformed *Escherichia coli* BL21 (DE3) were cultured in ampicillin-containing Luria Broth, and protein expression was induced with 0.5 mM isopropyl β-D-1-thiogalactopyranoside (IPTG). The bacterial pellets were resuspended in buffer (1% Triton X-100 in PBS, complete protease inhibitor tablet), sonicated, and after centrifugation at 45,000x*g* for 45 min, the supernatants were applied to glutathione-sepharose columns (GE Healthcare). On-bead digestion of GST-tagged protein was accomplished by overnight incubation at room temperature in the presence of thrombin (75 units) in PBS (3 mL). The tagless recombinant proteins were purified by size exclusion chromatography (SEC) using a Superdex-75 column (GE Healthcare) with 150 mM NaCl, 50 mM Tris, pH 7.4 buffer conditions.

Fluorescence polarization binding assays

Fluorescence polarization assays (FPA) were performed as previously described[40,41]. Briefly, direct binding curves were first generated by incubating FITC-MCL-1 SAHB$_A$, FITC-BID BH3,

or FITC-BAD BH3 (15 nM) with serial dilutions of anti-apoptotic protein in FPA buffer (150 mM NaCl, 50 mM Tris, pH 8.0, 0.0625% CHAPS), and fluorescence polarization measured at 5 min on a SpectraMax M5 microplate reader (Molecular Devices). For competition assays, a serial dilution of small molecule or acetylated peptide was added to recombinant protein at ~EC_{75} concentration, as determined by the direct binding assay (MCL-1ΔNΔC, 45 nM; BCL-X$_L$$\Delta$C, 300 nM). Fluorescence polarization was measured at equilibrium and IC_{50} values calculated by nonlinear regression analysis of competitive binding curves using Prism software (Graphpad).

High-throughput screening

Small molecule screening was performed at the Institute for Chemistry and Cellular Biology-Longwood (ICCB-Longwood) at Harvard Medical School, utilizing the commercial libraries Asinex1 (12,378 molecules), Chembridge3 (10,560 molecules), ChemDiv4 (14,677 molecules), Enamine2 (26,576), Life Chemicals1 (3,893 molecules), and Maybridge5 (3,212 molecules). High-throughput competitive FP binding assays were employed to screen for small molecules that disrupted the FITC-MCL-1 SAHB$_A$/MCL-1ΔNΔC, but not the FITC-BAD BH3/BCL-X$_L$$\Delta$C, interaction. SEC-purified MCL-1ΔNΔC or BCL-X$_L$$\Delta$C (see above) was delivered by automated liquid handler (WellMate, Matrix) to 384 well plates, followed by addition of small molecule libraries (~5 mg/mL, 100 nL). After a 15 min incubation at room temperature, the corresponding FITC-SAHB (15 nM) was added to each well by liquid handler and FP read at 1 h using a PerkinElmer Envision plate reader (λ_{ex} 480 nm, λ_{em} 535 nm).

Structural modeling

Docked structures of MCL-1ΔNΔC and all small molecule hits were generated using GLIDE XP v.5 and analyzed using PYMOL[42].

Cellular viability assays

OPM2 cells were maintained in RPMI 1640 (ATCC) supplemented with 10% (v/v) FBS, 100 U/mL penicillin, 100 mg/mL streptomycin, 0.1 mM MEM non-essential amino acids, and 50 mM ß-mercaptoethanol. Mouse embryonic fibroblasts (MEFs) cells were maintained in DMEM high glucose (Invitrogen) supplemented with 10% (v/v) FBS, 100 U/mL penicillin, 100 mg/mL streptomycin, 2 mM L-glutamine, 50 mM HEPES, 0.1 mM MEM non-essential amino acids, and 50 mM ß -mercaptoethanol. OPM2 cells ($5x10^4$/well) were seeded in 96-well opaque plates and incubated with the indicated serial dilutions of vehicle (0.4% DMSO), compound, TRAIL, or the combination in RPMI at 37°C in a final volume of 100 mL. For MEF experiments, cells ($5x10^3$/well) were seeded in 96-well opaque plates for 24 h and then incubated with the indicated serial dilutions of vehicle (0.4% DMSO), compound, or ABT-737 in DMEM at 37°C in a final volume of 100 mL. Cell viability was assayed at 24 h by addition of CellTiter-Glo reagent according to the manufacturer's protocol (Promega), and luminescence was measured using a SpectraMax M5 microplate reader (Molecular Devices).

Contributions

M. Stewart and G. Bird synthesized the stapled peptides applied in these studies. N. Cohen performed the high-throughout screen and all biochemical and cellular experiments, with guidance from L. Walensky. Small molecule screening was conducted by N. Cohen at Harvard Medical School's Institute for Chemistry and Cell Biology (ICCB), with equipment and screen design assistance provided by ICCB staff. N. Cohen and M. Stewart analyzed screening data and determined initial hit guidelines, with supervision from L. Walensky. E. Gavathiotis performed molecular docking studies. This chapter was written by N. Cohen and reviewed by L. Walensky. Assistance in generating figures was provided by E. Smith.

References

1.   Stewart, M.L., Fire, E., Keating, A.E. & Walensky, L.D. The MCL-1 BH3 helix is an exclusive MCL-1 inhibitor and apoptosis sensitizer. *Nature Chem Biol* **6**, 595-601 (2010).

2.   Tsujimoto, Y., Finger, L.R., Yunis, J., Nowell, P.C. & Croce, C.M. Cloning of the chromosome breakpoint of neoplastic B cells with the t(14;18) chromosome translocation. *Science* **226**, 1097-1099 (1984).

3.   Tsujimoto, Y., Cossman, J., Jaffe, E. & Croce, C.M. Involvement of the bcl-2 Gene in Human Follicular Lymphoma. *Science* **228**, 1440-1443 (1985).

4.   Vaux, D.L., Cory, S. & Adams, J.M. Bcl-2 gene promotes haemopoietic cell survival and cooperates with c-myc to immortalize pre-B cells. *Nature* **335**, 440-442 (1988).

5.   Sattler, M. et al. Structure of Bcl-xL-Bak peptide complex: Recoginition between regulators of apoptosis. *Science* **275**, 983-986 (1997).

6.   Kang, M.H. & Reynolds, C.P. BCL-2 inhibitors: targeting mitochondrial apoptotic pathways in cancer therapy. *Clin. Cancer Res.* **15**, 1126-1132 (2009).

7.   Degterev, A. et al. Identification of small-molecule inhibitors of interaction between the BH3 domain and Bcl-xL. *Nat Cell Biol* **3**, 173-82 (2001).

8.   Enyedy, I.J. et al. Discovery of small-molecule inhibitors of Bcl-2 through structure-based computer screening. *J Med Chem* **44**, 4313-24 (2001).

9.   Kitada, S. et al. Discovery, characterization, and structure-activity relationships studies of proapoptotic polyphenols targeting B-cell lymphocyte/leukemia-2 proteins. *J Med Chem* **46**, 4259-64 (2003).

10.   Nguyen, M. et al. Small molecule obatoclax (GX15-070) antagonizes MCL-1 and overcomes MCL-1-mediated resistance to apoptosis. *Proc Natl Acad Sci U S A* **104**, 19512-7 (2007).

11.   Oltersdorf, T. et al. An inhbitor of Bcl-2 family proteins induces regression of solid tumours. *Nature* **435**, 677-681 (2005).

12.   Petros, A.M. et al. Discovery of a potent and selective Bcl-2 inhibitor using SAR by NMR. *Bioorg Med Chem Lett* **20**, 6587-91 (2010).

13.   Tzung, S.P. et al. Antimycin A mimics a cell-death-inducing Bcl-2 homology domain 3. *Nat Cell Biol* **3**, 183-91 (2001).

14.   Walensky, L.D. et al. Activation of apoptosis in vivo by a hydrocarbon-stapled BH3 helix. *Science* **305**, 1466-70 (2004).

15.   Wang, G. et al. Structure-based design of potent small-molecule inhibitors of anti-apoptotic Bcl-2 proteins. *J Med Chem* **49**, 6139-42 (2006).

16.   Wang, J.L. et al. Structure-based discovery of an organic compound that binds Bcl-2 protein and induces apoptosis of tumor cells. *Proc Natl Acad Sci U S A* **97**, 7124-9 (2000).

17.   Berg, T. Small-molecule inhibitors of protein-protein interactions. *Curr. Op. Drug Disc. Dev.* **11**, 666-674 (2008).

18.   Degeretev, A. et al. Identification of small molecule inhibitors of interaction between the BH3 domain and BCL-X$_L$. *Nature Cell Biol.* **3**, 173-182 (2001).

19.   Qian, J. et al. Discovery of novel inhibitors of Bcl-xL using multiple high-throughput screening platforms. *Anal. Biochem.* **328**, 131-138 (2004).

20.   Zhai, D. et al. High-throughput fluorescence polarization assay for chemical library screening against anti-apoptotic Bcl-2 family member Bcl-2. *Journal of Biomolecular Screening* **17**, 350-360 (2012).

21.   Tse, C. et al. ABT-263: a potent and orally bioavailable Bcl-2 family inhibitor. *Cancer Res* **68**, 3421-8 (2008).

22.   Wilson, W.H. et al. Navitoclax, a targeted high-affinity inhibitor of BCL-2, in lymphoid malignancies: a phase 1 dose-escalation study of safety, pharmacokinetics, pharmacodynamics, and antitumour activity. *Lancet Oncol* **11**, 1149-59 (2010).

23.   Gandhi, L. et al. Phase I study of Navitoclax (ABT-263), a novel Bcl-2 family inhibitor, in patients with small-cell lung cancer and other solid tumors. *J Clin Oncol* **29**, 909-16 (2011).

24.   Roberts, A.W. et al. Substantial susceptibility of chronic lymphocytic leukemia to BCL2 inhibitio: Results of Phase 1 study of navitoclax (ABT-263) in patients with relapsed or refractory disease. *J Clin Onc* (2011).

25.   Konopleva, M. et al. Mechanisms of apoptosis sensitivity and resistance to the BH3 mimetic ABT-737 in acute myeloid leukemia. *Cancer Cell* **10**, 375-388 (2006).

26.   Lin, X. et al. "Seed" analysis of off-target siRNAs reveals an essential role of MCL-1 in resistance to the small-molecule Bcl-2/Bcl-xL inhibitor ABT-737. *Oncogene* **26**, 3972-3979 (2007).

27.   van Delft, M.F. et al. The BH3 mimetic ABT-737 targets selective Bcl-2 proteins and efficiently induces apoptosis via Bak/Bax if Mcl-1 is neutralized. *Cancer Cell* **10**, 389-399 (2006).

28.   Yecies, D., Carlson, N.E., Deng, J. & Letai, A. Acquired resistance to ABT-737 in lymphoma cells that up-regulate MCL-1 and BFL-1. *Blood* **115**, 3304-13 (2010).

29.   Gavathiotis, E. et al. BAX activation is initiated at a novel interaction site. *Nature* **455**, 1076-81 (2008).

30.   Walensky, L.D. et al. Activation of apoptosis in vivo by a hydrocarbon stapled BH3 helix. *Science* **305**, 1466-1470 (2004).

31.   Walensky, L.D. et al. A stapled BID BH3 helix directly binds and activates BAX. *Mol Cell* **24**, 199-210 (2006).

32.   Beroukhim, R. et al. The landscape of somatic copy-number alteration across human cancers. *Nature* **463**, 899-905 (2010).

33.   Zhang, J.-H., Chung, T.D.Y. & Oldenburg, K.R. A simple statistical parameter for use in evaluation and validation of high throughput screening assays. *J. Biomolec. Screening* **4**, 67-73 (1999).

34.   Zhang, H., Nimmer, P.M., Rosenberg, S.H., Ng, S. & Joseph, M.K. Development of a high-throughput fluorescence polarization assay for Bcl-xL. *Anal. Biochem.* **307**, 70-75 (2002).

35.   Zhai, D., Jin, C., Satterthwait, A.C. & Reed, J.C. Comparison of chemical inhibitors of antiapoptotic BCL-2 family proteins. *Cell Death Diff.* **13**, 1419-1421 (2006).

36.   Cross, J.B. et al. Comparison of Several Molecular Docking Programs: Pose Prediction and Virtual Screening Accuracy. *J. Chem. Inf. Model.* **49**, 1455-1474 (2009).

37.   Chou, T.-C. Theoretical basis, experimental design, and computerized simulation of synergism and antagonism in drug combination studies. *Pharmacol. Rev.* **58**, 621-681 (2006).

38.   Kim, S.-H., Ricci, M.S. & El-Deiry, W.S. Mcl-1: A Gateway to TRAIL Sensitization. *Cancer Res.* **68**, 2062-2064 (2008).

39.   Bird, G.H., Bernal, F., Pitter, K. & Walensky, L.D. Chapter 22 Synthesis and Biophysical Characterization of Stabilized alpha-Helices of BCL-2 Domains. *Methods Enzymol* **446**, 369-86 (2008).

40.   Pitter, K., Bernal, F., Labelle, J. & Walensky, L.D. Dissection of the BCL-2 family signaling network with stabilized alpha-helices of BCL-2 domains. *Methods Enzymol* **446**, 387-408 (2008).

41.   Bernal, F. et al. A stapled p53 helix overcomes HDMX-mediated suppression of p53. *Cancer Cell* **18**, 411-22 (2010).

42.   DeLano, W.L. *The PyMOL Molecular Graphics System*, (DeLano Scientific, San Carlos, 2002).

Chapter 3

MIM1 is an MCL-1-Selective Small Molecule Inhibitor That Targets MCL-1 *in vitro* and

Induces Cancer Cell Apoptosis in the Context of MCL-1 Dependence

Abstract

Cancer cells hijack BCL-2 family survival proteins to suppress the death effectors and thereby enforce an immortal state. This is accomplished biochemically by an anti-apoptotic surface groove that neutralizes the pro-apoptotic BH3 α-helix of death proteins. Anti-apoptotic MCL-1 in particular has emerged as a ubiquitous resistance factor in cancer. Whereas targeting the BCL-2 anti-apoptotic subclass effectively restores the death pathway in BCL-2-dependent cancer, the development of molecules tailored to the binding specificity of MCL-1 has lagged. We previously discovered that a hydrocarbon-stapled MCL-1 BH3 helix is an exquisitely selective MCL-1 antagonist. By deploying this unique reagent in a competitive screen, we identified an MCL-1 inhibitor molecule that selectively targets the BH3-binding groove of MCL-1, neutralizes its biochemical lockhold on apoptosis, and induces caspase activation and leukemia cell death in the specific context of MCL-1 dependence.

Introduction: From Selective Stapled Peptide to Selective Small Molecule

MCL-1 SAHBs are hydrocarbon-stapled MCL-1 BH3 helices that were previously shown using chemical, structural, and biological methods to selectively target MCL-1 and sensitize cancer cells to caspase-dependent apoptosis[1]. Here, we utilized MCL-1 SAHB$_A$ as a screening tool to discover selective small molecules that target MCL-1. As described in Chapter 2, a high-throughput competitive fluorescence polarization (FP) screening assay was developed based on the direct binding interaction between FITC-MCL-1 SAHB$_A$ and MCL-1ΔNΔC; a counter-screen was performed based on the direct and selective interaction between FITC-BAD BH3 and BCL-X$_L$. Multiple commercial libraries (71,296 small molecules) were screened for the capacity to displace FITC-MCL-1 SAHB$_A$ from recombinant MCL-1ΔNΔC while leaving the BCL-X$_L$/BAD BH3 interaction intact (**Figure 3.1**).

Based on the analysis of this primary screening data, which compared peptide displacement from MCL-1ΔNΔC and BCL-X$_L$ΔC, 208 compounds with the capacity to selectively displace MCL-1 SAHB from MCL-1 were advanced through rigorous confirmatory *in vitro* binding assays, including repeat single-dose testing in the initial differential competitive FP screen, an alternative single-dose selectivity screen for 130 confirmed MCL-1-directed antagonists comparing relative displacement of FITC-BID BH3, a pan-anti-apoptotic binder[2], from MCL-1ΔNΔC and BCL-X$_L$ΔC, and lastly, competitive dose-responsive binding of the top 64 compounds, examining displacement of FITC-MCL-1 SAHB$_A$ from MCL-1ΔNΔC. Of the 64 compounds that competed with FITC-MCL-1 SAHB$_A$ for MCL-1ΔNΔC binding at IC$_{50}$ potencies of < 30 μM, 28 small molecules were subjected to dose-responsive target selectivity analysis in the comparative FITC-BID BH3/MCL-1ΔNΔC vs. FITC-BID BH3/BCL-X$_L$ΔC competition FP assay, and then to screening liposomal release and *Bax$^{-/-}$Bak$^{-/-}$* mouse embryonic

67
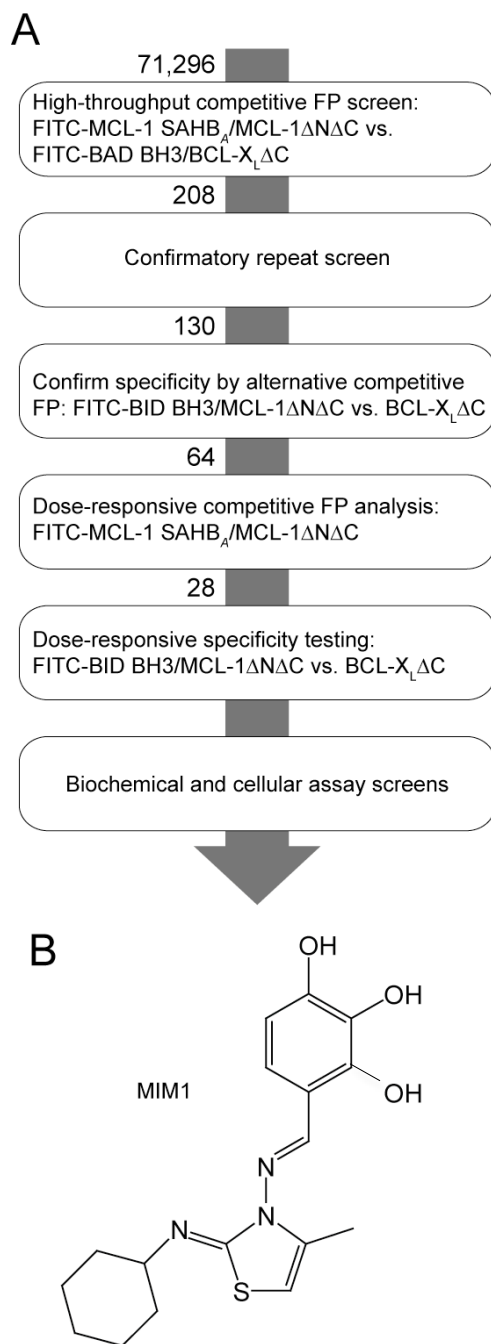
Figure 3.1. *Identification of MIM1, a selective inhibitor of anti-apoptotic MCL-1.* A high-throughput stapled peptide-based screen for small molecules that selectively target MCL-1ΔNΔC identified MIM1. (B) The molecular structure of MIM1 is characterized by a thiazolyl core substituted with methyl, cyclohexylimino, and benzenetriol R groups.

fibroblast (MEF) cytotoxicity assays. Ultimately, we selected 4-((E)-(((Z)-2(cyclohexylimino)-4-methylthiazol-3(2H)-yl)imino)methyl)benzene-1,2,3-triol, termed MCL-1 inhibitor molecule 1 (MIM1), as our prototype compound due to a combination of favorable biophysical and biological properties that included MW > 200, solubility, MCL-1 binding potency and selectivity, compatibility with and activity in a BAX-mediated liposomal release assay, and relatively little to no toxicity in $Bax^{-/-}Bak^{-/-}$ MEFs. This chapter will focus on our detailed characterization of MIM1 as a potent and selective lead inhibitor of MCL-1 for reactivation of apoptosis in MCL-1-dependent cancer.

Results

Identification of MIM1, a potent and selective MCL-1 inhibitor molecule

The molecular structure of MIM1 (MW 347) is characterized by a thiazolyl core substituted with methyl, cyclohexylimino, and benzenetriol R groups (**Figure 3.1**), and the compound's structure was verified by ^{1}H NMR (**Figure 3.2**). We chose to vet the anti-apoptotic binding selectivity of MIM1 in competitive FP assays by comparison with ABT-737, a selective BCL-2/BCL-X$_L$ inhibitor molecule[3]. Whereas MIM1 effectively competed with FITC-MCL-1 SAHB$_A$ and FITC-BID BH3 for MCL-1ΔNΔC binding with respective IC$_{50}$ values of 4.7 and 4.8 µM, the compound showed no capacity to displace FITC-BID BH3 from BCL-X$_L$ΔC (IC$_{50}$ > 50 µM), mirroring the selectivity of Ac-MCL-1 SAHB$_D$ (**Figure 3.3**). In striking contrast, ABT-737 competed with FITC-BID BH3 for BCL-X$_L$ΔC binding, but showed no activity toward MCL-1ΔNΔC. Although Ac-MCL-1 SAHB$_D$ was a 30- to 60-fold more potent competitor for MCL-1ΔNΔC binding than MIM1, the MCL-1-selective small molecule is one-seventh the size of the stapled peptide and exhibits an IC$_{50}$ for its target (4.8 µM) in the same range as that of ABT-737 for BCL-X$_L$ΔC (2.3 µM) upon competition with FITC-BID BH3. Thus, MIM1 emerged from the competitive screen with a marked MCL-1ΔNΔC preference that reflects the binding specificity of the stapled peptide ligand and the opposite interaction profile of ABT-737.

Structural analysis of the MIM1/MCL-1ΔNΔC interaction

To localize the protein interaction site that accounts for competitive small molecule binding activity, we performed NMR analysis of ^{15}N-MCL-1ΔNΔC upon MIM1 titration. The addition of MIM1 up to a 2:1 molecule:protein ratio induced significant backbone amide chemical shift changes in those MCL-1ΔNΔC residues concentrated in a subregion of the
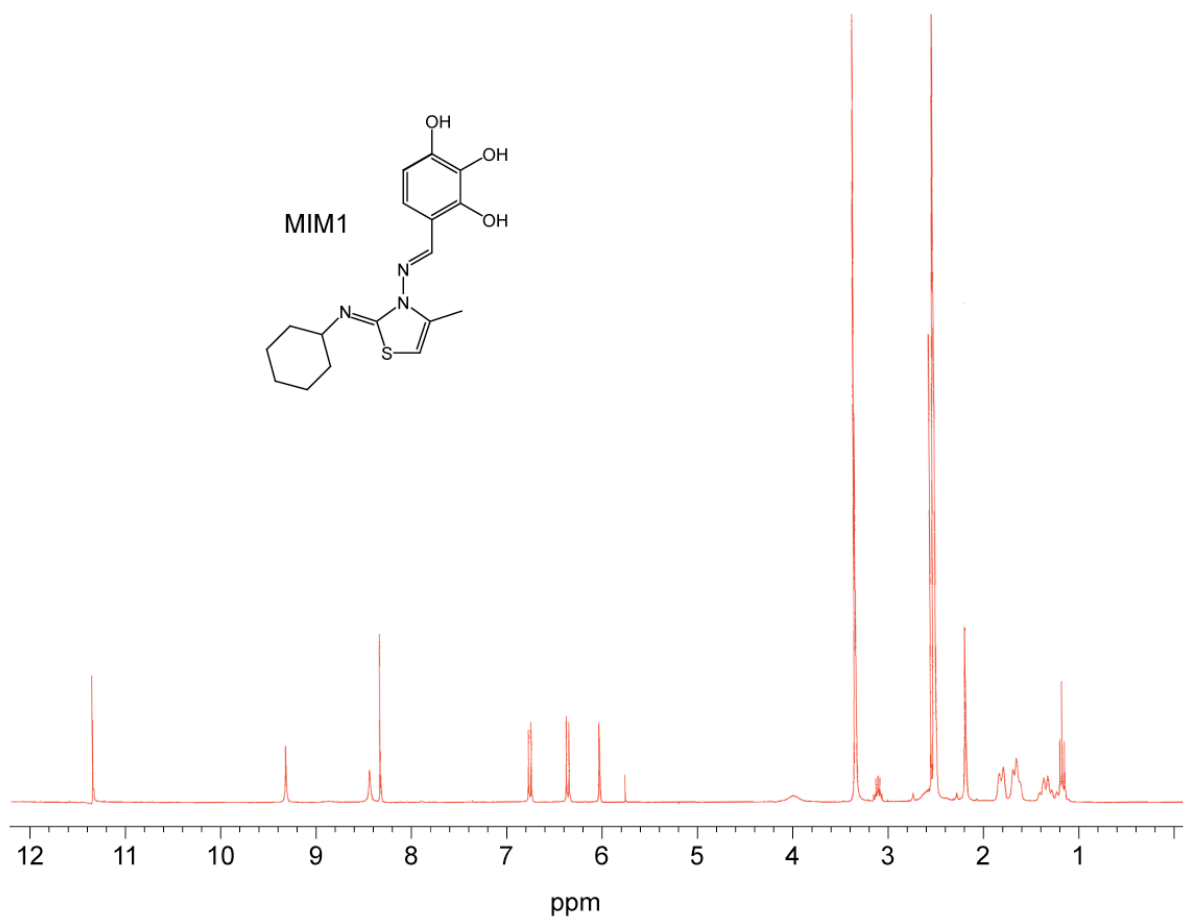
Figure 3.2. *¹H NMR spectrum of MIM1.*

Figure 3.3. *MIM1 selectively binds MCL-1 over BCL-X_L by competitive FP assay, with an opposite binding profile to ABT-737.* (A) MCL-1 SAHB$_D$ and MIM1 dose-responsively competed with FITC-MCL-1 SAHB$_A$ for binding to MCL-1ΔNΔC, whereas the BCL-2/BCL-X_L-selective antagonist ABT-737 had no effect. (B) Similarly, MCL-1 SAHB$_D$ and MIM1, but not ABT-737, effectively competed with FITC-BID BH3 peptide for binding to MCL-1ΔNΔC. (C) In contrast, ABT-737 dose-responsively competed with FITC-BID BH3 for binding to BCL-X_LΔC, whereas MCL-1 SAHB$_D$ and MIM1 showed no BCL-X_LΔC-binding activity. Data are mean ± SEM for FP assays performed in at least duplicate and then repeated twice with independent protein preparations with similar results. CI, confidence intervals

Figure 3.3 (continued)

A

Compound	IC_{50}	95% CI
MCL-1 SAHB$_D$	0.078 μM	0.067-0.091
ABT-737	> 50 μM	---
MIM1	4.72 μM	3.72-5.99

B

Compound	IC_{50}	95% CI
MCL-1 SAHB$_D$	0.171 μM	0.131-0.225
ABT-737	> 50 μM	---
MIM1	4.78 μM	3.87-5.82

C

Compound	IC_{50}	95% CI
MCL-1 SAHB$_D$	> 50 μM	---
ABT-737	2.31 μM	2.10-2.54
MIM1	> 50 μM	---
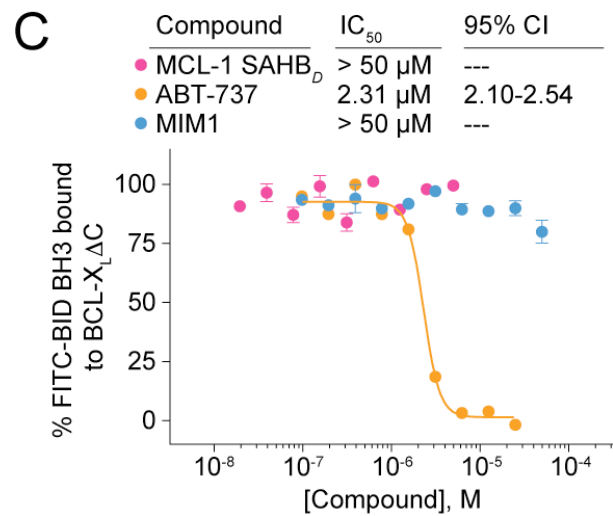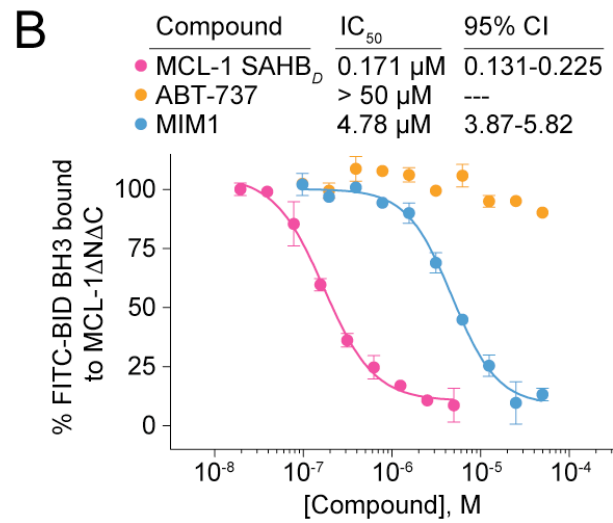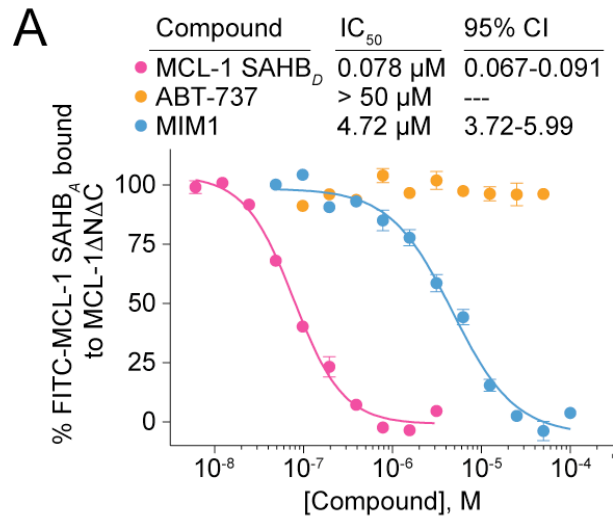
canonical BH3-binding pocket, which is comprised of residues from α2 (BH3) and portions of

α3, α4, α5 (BH1) and α8 (BH2) (**Figure 3.4A**). These data are consistent with a direct

interaction between MIM1 and MCL-1ΔNΔC at the very surface employed by BH3 helices to

engage MCL-1.

We next performed molecular docking analysis to examine the predicted interactions

between MIM1 and MCL-1ΔNΔC at the BH3-binding pocket. Interestingly, MIM1 is predicted

to occupy that portion of the BH3-binding site engaged by residues 211-216 ETLRRV (aa 211-

216) of MCL-1 SAHB$_D$ (**Figure 3.4B-C**, PDB 3MK8[1]). Whereas the cyclohexyl group makes

complementary hydrophobic contacts with the region of the protein interface flanked by MCL-1

SAHB$_D$ residues L213 and V216, the thiazolyl core and its methyl substituent point directly into

a deep crevice occupied in the MCL-1 SAHB$_D$/MCL-1ΔNΔC complex by the highly conserved

leucine (MCL-1 SAHB$_D$ L213) of BH3 domains. Interestingly, the benzene-1,2,3-triol (or

pyrogallol) moiety engages in hydrophilic contacts with D256 and R263, two charged MCL-1

residues implicated in complementary electrostatic interactions with a variety of BH3 domain

R/D pairs (e.g., aa R214, D218 of MCL-1 SAHB$_D$). Thus, MIM1 appears to simulate the key

molecular features of approximately 1.5 turns of the MCL-1 BH3 helix at a potential selectivity

hot-spot on the MCL-1 binding surface.

MIM1 blocks MCL-1-mediated suppression of pro-apoptotic BAX

We next examined whether MIM1 could selectively block MCL-1ΔNΔC-based

suppression of BAX activation, as monitored by a BAX-mediated liposomal release assay

tailored to distinguish between pharmacologic regulation by MCL-1ΔNΔC vs. BCL-X$_L$ΔC.

Whereas the BH3-only protein tBID directly triggers the transformation of monomeric BAX to a

Figure 3.4. *MIM1 targets the canonical BH3-binding pocket of MCL-1.* (A) Measured chemical shift changes of ^{15}N-MCL-1ΔNΔC upon MIM1 titration up to a ratio of 2:1 MIM1:MCL-1 are plotted as a function of MCL-1ΔNΔC residue. Affected residues are represented as purple bars in the plot (calculated significance threshold > 0.0197 p.p.m.). Residues with significant backbone amide chemical shift changes (purple) are concentrated in a subregion of the canonical BH3-binding pocket (green). MCL-1ΔNΔC residues M250, V253, F254, S255, D256, G257, G262, and R263 are unassigned. (B, C) The docked structure of MIM1 at the canonical BH3-binding pocket of MCL-1ΔNΔC predicts that (1) the cyclohexyl group makes complementary hydrophobic contacts with the region of the protein interface flanked by MCL-1 SAHB$_D$ residues L213 and V216, (2) the thiazolyl core and its methyl substituent point directly into a deep crevice occupied by MCL-1 SAHB$_D$ L213 in the stapled peptide/protein complex, and (3) the benzene-1,2,3-triol (or pyrogallol) moiety engages in hydrophilic contacts with D256 and R263, two charged MCL-1 residues implicated in complementary electrostatic interactions with R214 and D218 of MCL-1 SAHB$_D$.

Figure 3.4 (continued)
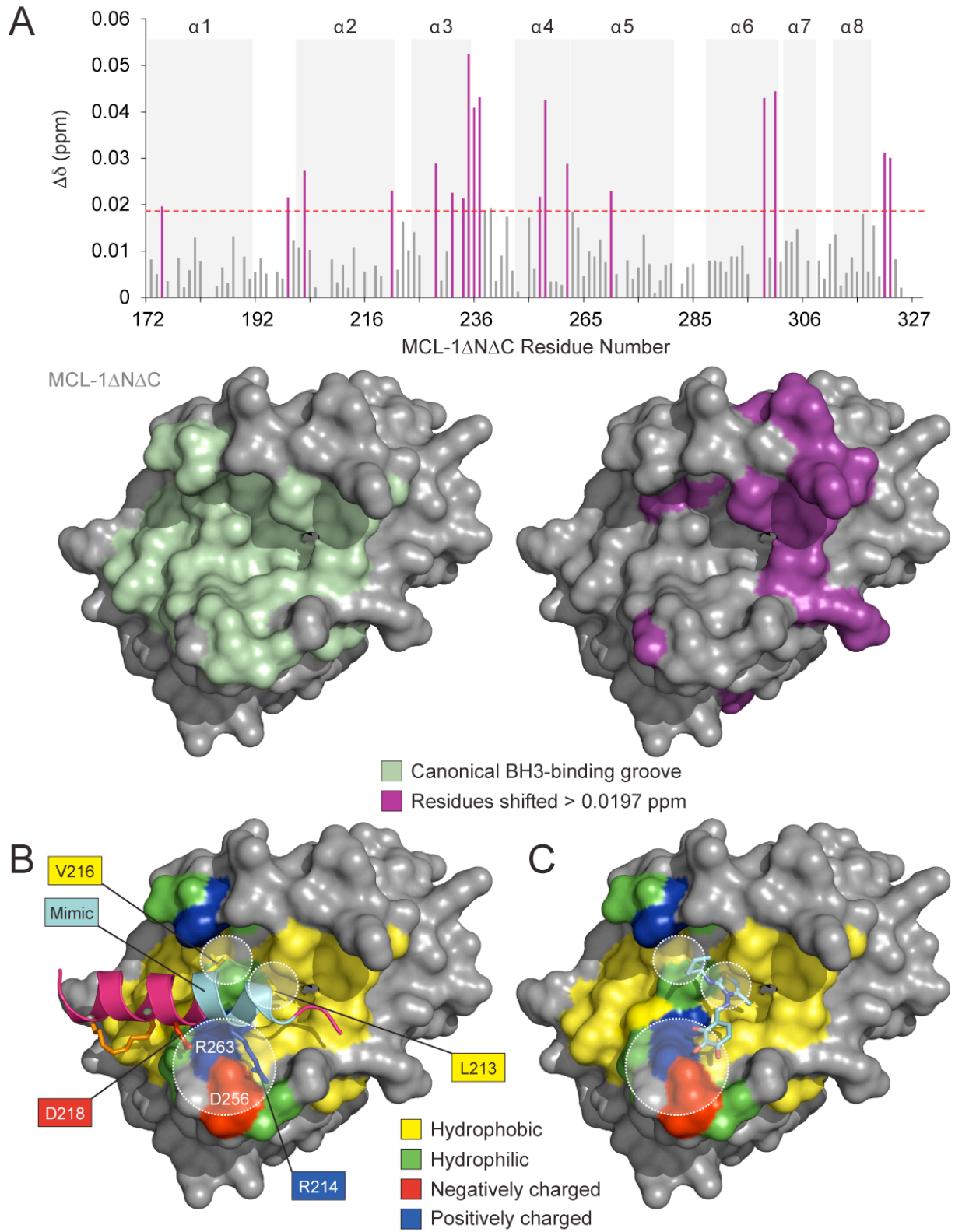
membrane-embedded oligomer that porates liposomal vesicles and releases encapsulated fluorophore, the addition of anti-apoptotic proteins, such as MCL-1ΔNΔC or BCL-X$_L$ΔC, blocks tBID-induced BAX activation and liposomal release (**Figure 3.5A**). While the BAX-suppressive effects of MCL-1ΔNΔC are completely eliminated by pre-incubation with MCL-1 SAHB$_D$, BCL-X$_L$ΔC-based inhibition of BAX activation is unimpeded by the MCL-1-selective stapled peptide (**Figure 3.5B**). Conversely, ABT-737, which selectively blocks BCL-X$_L$ΔC, negates BCL-X$_L$ΔC-mediated suppression of BAX activation but has no effect on MCL-1ΔNΔC activity (**Figure 3.5C**). Having documented the high fidelity of this tailored liposomal assay for distinguishing between anti-apoptotic selectivities, we next evaluated the functional activity of MIM1. Indeed, we find that MIM1 simulates the pharmacologic activity of MCL-1 SAHB$_D$, preventing BAX suppression by MCL-1ΔNΔC but not by BCL-X$_L$ΔC (**Figure 3.5D**). Consistent with the reduced molecular weight and competitive binding activity of MIM1 compared to MCL-1 SAHB$_D$, the kinetics of MIM1 inhibition of MCL-1ΔNΔC-mediated BAX suppression are correspondingly slower (**Figures 3.2C-D, 3.5B, 3.5D**). Thus, these data explicitly link the selective MCL-1ΔNΔC binding activity of MIM1 with functional blockade of MCL-1ΔNΔC-mediated inhibition of BAX activation.

Selective activation of MCL-1-dependent leukemia cell death by MIM1

One of the key challenges in developing and applying molecular antagonists for BCL-2 family anti-apoptotic proteins is the variable expression of multiple homologues. That is, a cancer cell will only be susceptible to a selective anti-apoptotic inhibitor if the cell is especially dependent on that particular survival protein. Thus, the mere expression of MCL-1 does not predict cancer cell sensitivity to an MCL-1-selective inhibitor, as other anti-apoptotics lying
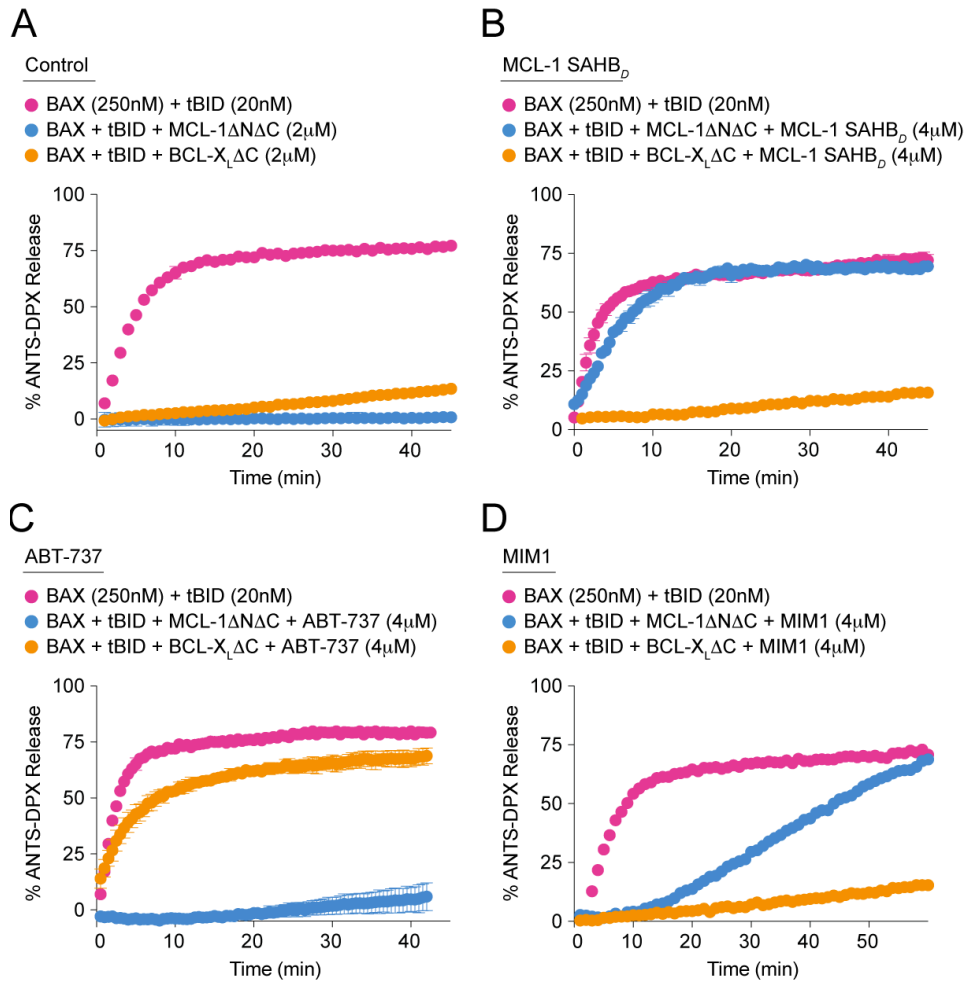
Figure 3.5. *Selective blockade of MCL-1-mediated suppression of BAX activation by MIM1.*
(A) BH3-only protein tBID directly activates BAX-mediated liposomal release, which is
effectively suppressed by treatment with anti-apoptotic MCL-1ΔNΔC and BCL-X$_L$ΔC. (B)
MCL-1 SAHB$_D$ selectively inhibited MCL-1ΔNΔC suppression of tBID-induced BAX
activation. (C) ABT-737 selectively inhibited BCL-X$_L$ΔC suppression of tBID-induced BAX
activation. (D) The activity profile of MIM1 in the liposomal release assay mirrored the MCL-1
selectivity of MCL-1 SAHB$_D$. Liposomal assays were conducted in triplicate for each condition
and repeated with an independent preparation of recombinant BAX with similar results.

outside its binding spectrum may continue to effectively suppress BAX/BAK. To test MIM1's activity and specificity in cancer cells, we employed murine BCR-ABL(p185)-transformed, *Arf*-null, B-lineage acute lymphoblastic leukemia (*p185^{+}Arf$^{/-}$* B-ALL) cells that are unable to survive upon *Mcl-1* deletion unless reconstituted with anti-apoptotic protein, reflecting a stringent system for assessing anti-apoptotic dependence. To validate the cellular assay, we first compared the effect of ABT-737 on *p185^{+}Arf$^{/-}$*/*Mcl-1*-deleted B-ALL cells rescued by overexpression of MCL-1 or BCL-X$_L$ (**Figure 3.6)** and observed dose-responsive impairment of cancer cell viability (IC$_{50}$, 1.6 µM) that coincided with dose-responsive caspase 3/7 activation in the BCL-X$_L$-dependent cells, but no effect on the MCL-1-dependent cells (**Figure 3.7A**). Strikingly, MIM1 had the exact opposite effect, negatively impacting the viability of the MCL-1-dependent cells (IC$_{50}$, 4.2 µM), including dose-dependent induction of caspase 3/7 activity, but having little to no effect on the BCL-X$_L$-dependent cells (**Figure 3.7B**). Importantly, ABT-737 and MIM1 had no significant effect on the viability of wild-type or *Bax$^{-/-}$Bak$^{-/-}$* MEFs over the same dose range, with no observed caspase 3/7 activation (**Figure 3.8**).

To interrogate the mechanism underlying MIM-1-selective killing, we performed anti-MCL-1 co-immunoprecipitations from the MCL-1 rescued *p185^{+}Arf$^{/-}$*/*Mcl-1*-deleted B-ALL cells treated with escalating doses of MIM1. By 6 hours, we observed dose-responsive dissociation of the MCL-1/BAK complex in the MIM-1 treated cells (**Figure 3.9**). Notably, BCL-X$_L$ /BAK dissociation was not observed when the identical experiment was performed on the BCL-X$_L$-rescued *p185^{+}Arf$^{/-}$*/*Mcl-1*-deleted B-ALL cells. These results provide important insight into the mechanistic basis for MIM1's MCL-1-selective anti-leukemia activity, as MIM1 effectively reduces the apoptotic threshold by disruption of the inhibitory MCL-1/BAK interaction.
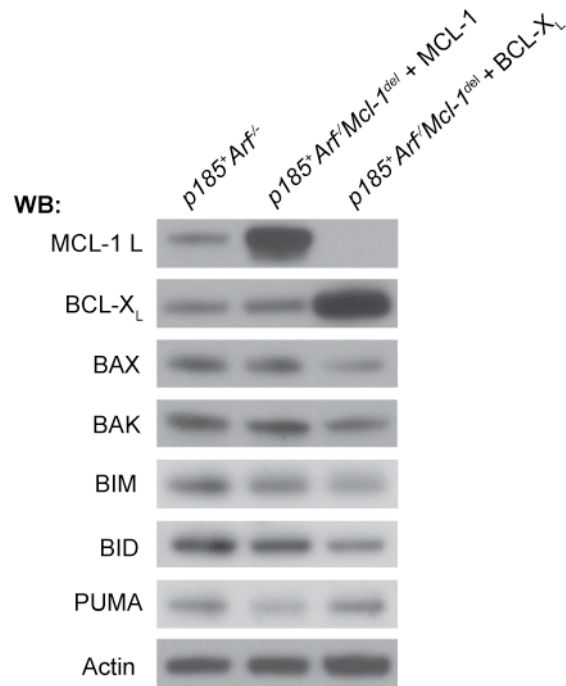
Figure 3.6 *Western blot analysis of genetically-defined p185$^+$Arf$^{/-}$ B-ALL cells.* Whereas the parental *p185$^+$Arf$^{/-}$* B-ALL cells express both MCL-1 and BCL-X$_L$, MCL-1- and BCL-X$_L$- rescued *p185$^+$Arf$^{/-}$/Mcl-1*-deleted B-ALL cells demonstrate overexpression of MCL-1 or BCL-X$_L$, respectively. Pro-apoptotic effectors, such as BAX, BAK, and BH3-only proteins, are expressed at relatively similar levels in all three cell lines.
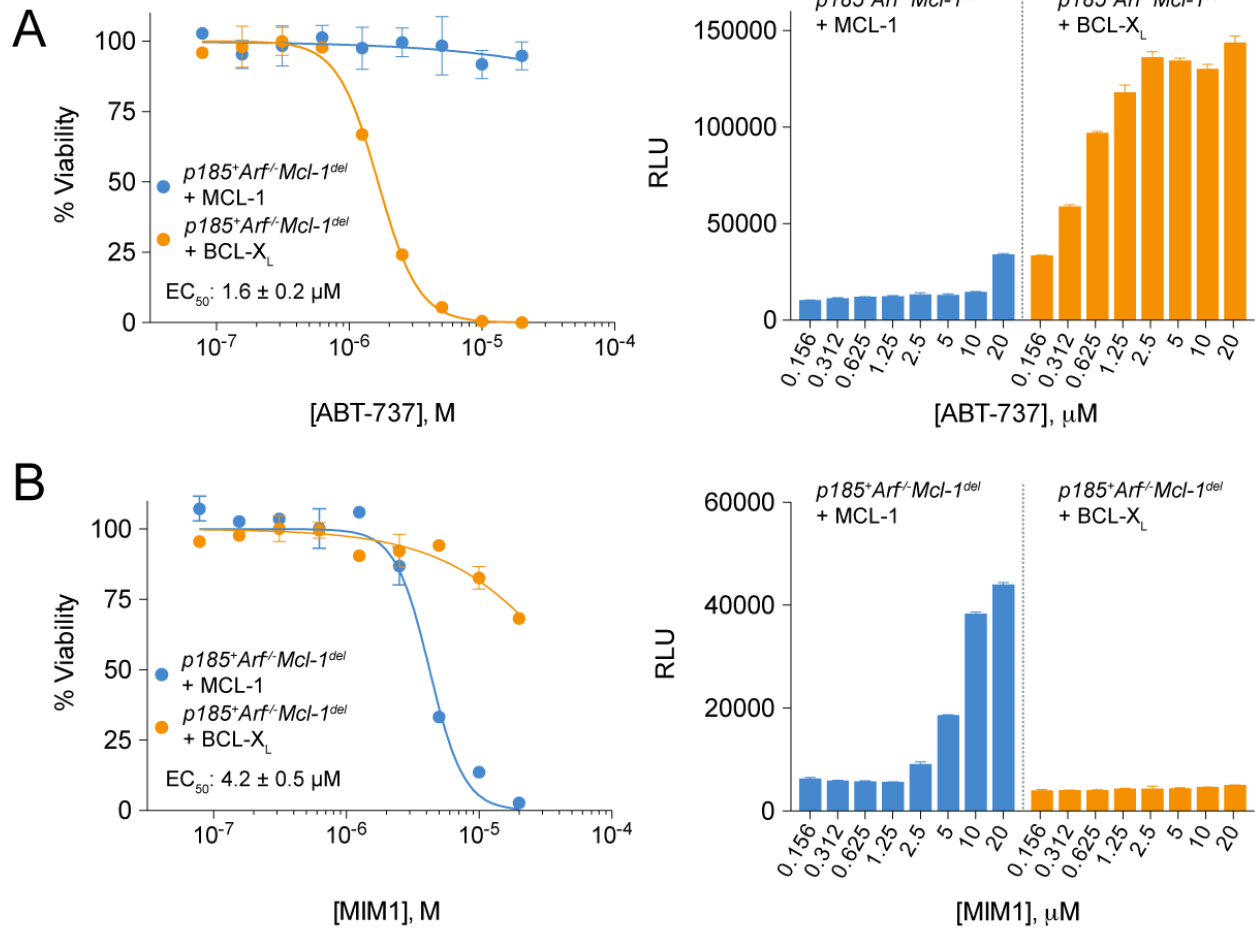
Figure 3.7. *MCL-1-dependent anti-leukemia activity of MIM.* (A) ABT-737 selectively impaired the viability of *p185⁺Arf⁻/⁻/Mcl-1*-deleted B-ALL cells rescued by BCL-X$_L$, but not MCL-1, as measured by CellTiter-Glo assay at 24 h. The selective cytotoxic effect of ABT-737 was accompanied by dose-responsive caspase 3/7 activation in the BCL-X$_L$-rescued leukemia cell line, as measured at 8 h post-treatment. (B) MIM1 exhibited the opposite cellular activity profile of ABT-737, selectively impairing the viability of *p185⁺Arf⁻/⁻/Mcl-1*-deleted B-ALL cells rescued by MCL-1, but not BCL-X$_L$. Correspondingly, the selective cytotoxic effect of MIM1 was accompanied by dose-responsive caspase 3/7 activation only in the MCL-1-rescued leukemia cell line.
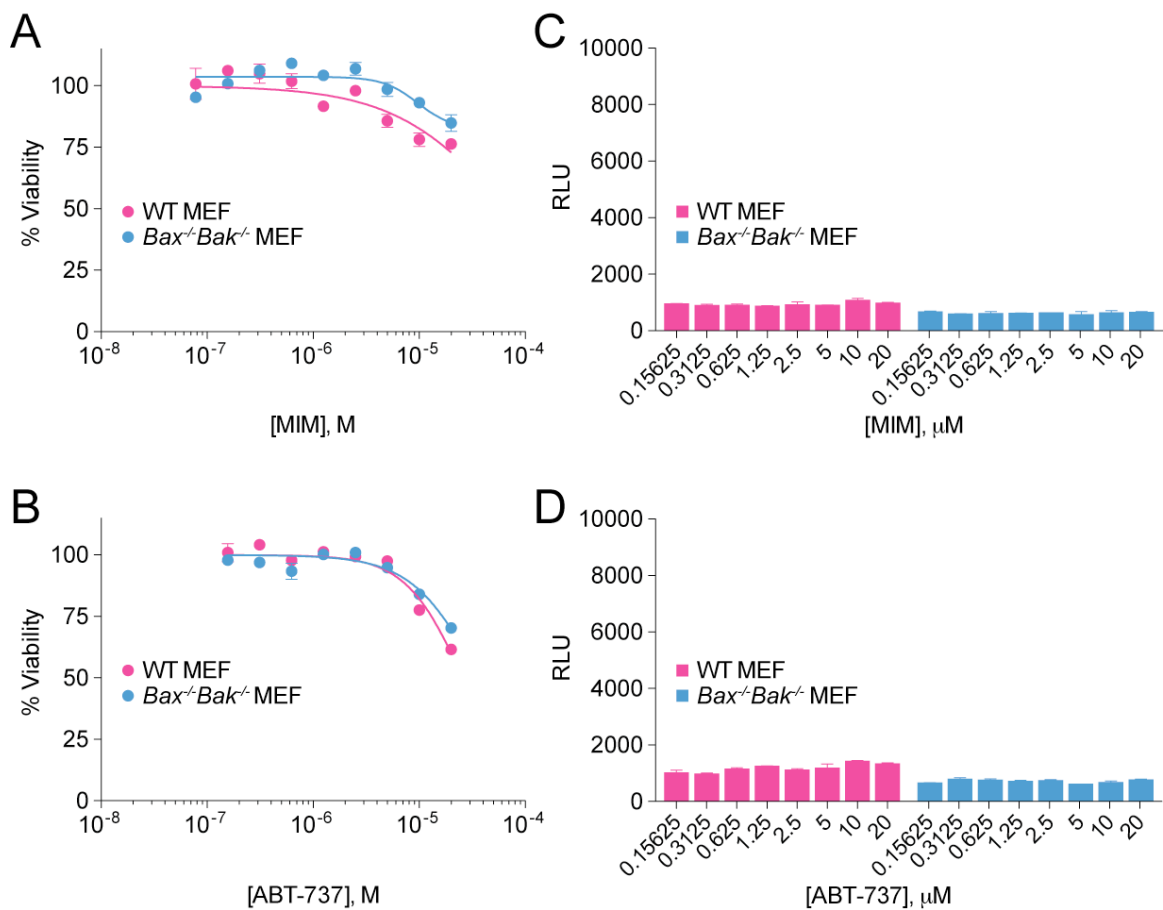
Figure 3.8. *Effect of MIM1 and ABT-737 on MEFs.* MIM1 and ABT-737 induce little to no cytotoxicity (24 h) (A, B) or caspase 3/7 activation (8 h) (C, D) in wild-type or $Bax^{-/-}Bak^{-/-}$ MEFs treated with the same dose range that caused selective viability impairment of MCL-1- or BCL-X_L-rescued $p185^+Arf^{-/-}/Mcl-1$-deleted B-ALL cells. Data are mean $\pm$ SEM for experiments performed in at least duplicate, normalized to vehicle control, and repeated twice with independent cell cultures with similar results.
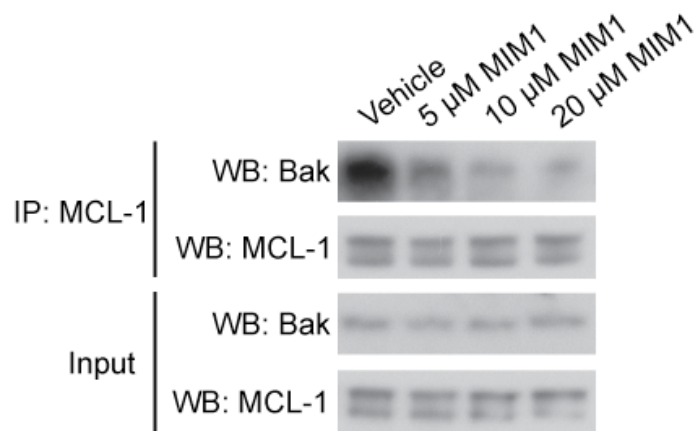
Figure 3.9. *Co-immunoprecipitation of MCL-1 and BAK shows MIM1-induced complex disruption in leukemia cells. p185$^+$Arf$^{/-}$Mcl-1*-deleted leukemia cells rescued by MCL-1 overexpression were treated with varying doses of MIM1 for 6 hours, followed by immunoprecipitation of MCL-1. Equal loading is documented by the cellular inputs, and a MIM1 dose-dependent decrease in BAK was co-immunoprecipitated with MCL-1, supporting a mechanistic association between MIM1-induced leukemia cell apoptosis and the molecule's capacity to displace pro-apoptotic BAK from MCL-1.

We next examined the functional impact of combining ABT-737 and MIM1 in isogenic $p185^+Arf^{/-}$ B-ALL cells differing only in their expression of MCL-1 and BCL-X$_L$ (**Figure 3.6**). In parental $p185^+Arf^{/-}$ B-ALL cells that express both endogenous MCL-1 and BCL-X$_L$, the combination of ABT-737 (EC$_{50}$, 5.1 µM) and MIM1 (EC$_{50}$, 10.6 µM) resulted in synergistic cytotoxicity, as determined by CalcuSyn analysis[4] (EC$_{50}$, 1.4 µM; CI this dose, 0.47) (**Figure 3.10A)**. Strikingly, when the combination was applied to MCL-1-reconstituted $p185^+Arf^{/-}/Mcl$-1-deleted B-ALL cells, the addition of ABT-737 had little effect (**Figure 3.10B**). Similarly, the cytotoxic effects of single agent ABT-737 and the combination on BCL-X$_L$-reconstituted $p185^+Arf^{/-}/Mcl$-1-deleted B-ALL cells were identical, reflecting no added benefit of MIM1 in the absence of MCL-1 (**Figure 3.10C**). These data underscore the selectivity of MIM1 and ABT-737 for their respective targets in the context of high stringency cancer cell dependence on MCL-1 or BCL-X$_L$. Importantly, the relative resistance of non-malignant fibroblasts to MIM1 treatment, as previously observed for ABT-737[5], suggests that a therapeutic window may exist, with preferential toxicity to cells driven by discrete anti-apoptotic blockades.

Structure-activity relationship studies

The discovery of MIM1 from a high-throughput screen employing MCL-1 SAHB yielded a novel therapeutic prototype for molecular targeting of MCL-1. We performed preliminary SAR studies to examine MIM1's structural analogs and determine which R groups are required to maintain specific MCL-1 binding activity. Commercially available analogs were purchased and tested for their ability to displace FITC-BID BH3 from MCL-1. **Figure 3.11** shows a structural comparison of MIM1 and its analogs, all of which were less potent than the parental MIM1. Comparative binding analyses revealed two major insights: (1) the pyrogallol moiety appears

Figure 3.10 *MCL-1-dependent synergy of MIM1 and ABT-737 in leukemia cells.*

(A) Combination treatment with MIM1 and ABT-737 induced synergistic killing of parental *p185$^+$Arf$^{/-}$* B-ALL cells that express endogenous MCL-1 and BCL-X$_L$, as reflected by a leftward shift of the viability isotherm (left) and the CalcuSyn dose effect curve (right), with calculated CI values of < 1 at ED$_{50}$, ED$_{75}$, and ED$_{90}$. CI, combination index; ED, effective dose. (B) The addition of ABT-737 to MIM1 treatment of MCL-1-rescued *p185$^+$Arf$^{/-}$/Mcl-1*-deleted B-ALL cells had little to no additional cytotoxic effect, consistent with the relative inactivity of ABT-737 in the context of MCL-1-dependence. (C) Correspondingly, the addition of MIM1 to ABT-737 treatment of BCL-X$_L$-rescued *p185$^+$Arf$^{/-}$/Mcl-1*-deleted B-ALL cells provided no additional cytotoxic effect, consistent with the relative inactivity of MIM1 in the context of BCL-X$_L$-dependence. Data are mean $\pm$ SEM for experiments performed in at least duplicate, normalized to vehicle control, and repeated twice with independent cell cultures with similar results.

Figure 3.10 (continued)

A

p185+Arf-/-

	EC$_{50}$
MIM1	10.6 μM
ABT-737	5.1 μM
1:MIM1:ABT-737	1.4 μM

p185+Arf-/-

MIM1
ABT-737
1:MIM1:ABT-737

EC$_X$	CI
50	0.47
75	0.35
90	0.27

B

p185+Arf-/-Mcl-1del + MCL-1

	EC$_{50}$
MIM1	4.0 μM
ABT-737	>10 μM
1:MIM1:ABT-737	3.4 μM

C

p185+Arf-/-Mcl-1del + BCL-X$_L$

	EC$_{50}$
MIM1	>10 μM
ABT-737	0.5 μM
1:MIM1:ABT-737	0.5 μM

Figure 3.11 *SAR of MIM1 reveals key structural elements for MCL-1 binding.* MIM1 analogs were purchased and tested for their ability to displace FITC-BID BH3 from MCL-1, as assessed by competitive FP assay. The IC_{50} values corresponding to the tabulated MIM1 analogs are plotted as a bar graph. Data are mean $\pm$ SEM for FP assays performed in at least duplicate.

essential for MCL-1 binding, and (2) at least one of the two indicated R groups requires a degree of hydrophobic bulk, in accordance with the presence of cyclohexyl and methyl R groups in MIM1. Future SAR studies will focus on expanding the library of *de novo* synthesized MIM1 analogs in an effort to enhance the potency of binding and cellular activity.

MIMx4, a MIM1 analog that does not bind MCL-1, was utilized as a negative control to further confirm the specificity-of-action of MIM1. **Figure 3.12** demonstrates that MIMx4 does not bind MCL-1 or BCL-X_L by competitive FP assay. In addition, the compound shows no activity in promoting release of tBID from MCL-1, and thus does not induce BAX-mediated liposomal release. Furthermore, specific cellular killing is not seen in MCL-1-dependent leukemia cells, with cell death only occurring due to non-specific cytotoxicity at high doses. These data highlight that a negative control molecule containing the core structure of MIM1 but without essential MCL-1 binding features does not recapitulate any of the biochemical or cellular activity of the MCL-1-selective MIM1 compound.
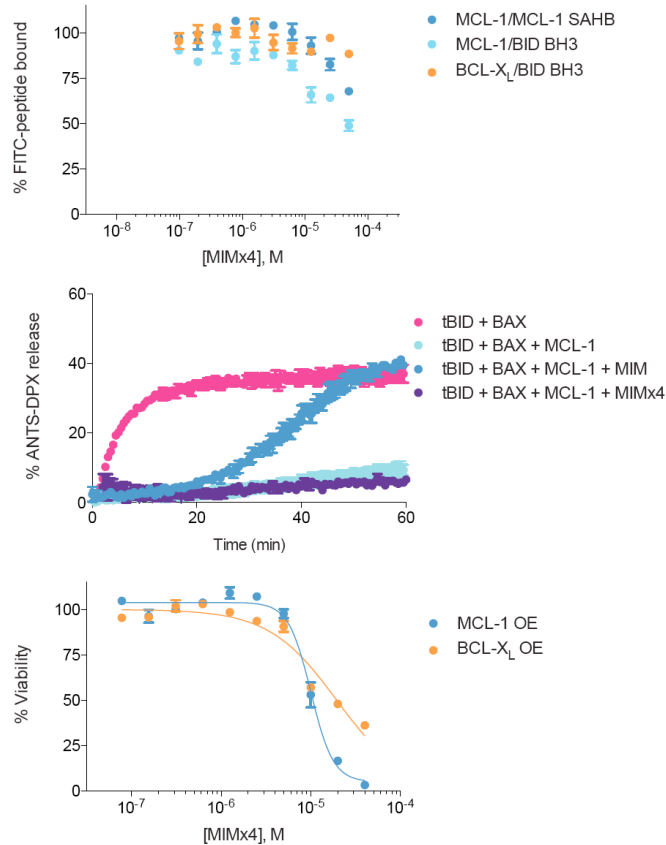
Figure 3.12. *MIMx4 does not bind MCL-1 and shows no activity in liposomal release or cellular specificity assays.* (A) MIMx4 does not displace FITC-MCL-1 SAHB or FITC-BID BH3 from MCL-1 or BCL-X_L as assessed by competitive FP assay. (B) MIM1 triggers liposomal release in the presence of MCL-1, whereas MIMx4 shows no effect. (C) MIMx4 manifests non-specific toxicity in both leukemia cell types at high doses, with no specificity for the MCL-1-dependent leukemia cells.

Discussion

Cancer cells are empowered by the combination of proliferative drives and apoptotic blockades. Under homeostatic conditions, BCL-2 family anti-apoptotic proteins guard against premature or unwanted cellular death, but in the context of cancer, their overexpression subverts the natural death pathway and promotes tumor development, maintenance, recurrence, and chemoresistance. To reduce the apoptotic threshold in cancer and thereby facilitate the efficacy of chemotherapy and radiation treatment, an ideal collection of targeted apoptotic therapies would include agents with specificities tailored to individual, subsets of, and all anti-apoptotic proteins. The BH3 helix-binding groove on the surface of anti-apoptotic proteins represents the pharmacologic bull's-eye for such targeted therapies. The first structure of a pro-apoptotic BH3 helix in complex with anti-apoptotic BCL-X_L[6] provided the blueprint for developing such molecules and designer peptides. The bench-to-bedside learnings from ABT-737 and ABT-263 have yielded enormous insight into the remarkable potential and remaining challenges of this pharmacologic strategy. Deciphering the topographic hot-spots that dictate similarities and differences among the BH3-binding sites of numerous anti-apoptotic proteins presents a considerable drug design challenge. However, the advancement of ABT-263 and a growing diversity of small molecules and peptides that address the variety of BCL-2 family targets[1,7-21] predicts that this pharmacologic puzzle can ultimately be solved.

With BCL-2/BCL-X_L-selective inhibitors having led the field, significant attention has shifted to expanding the scope of anti-apoptotic targeting, with a special emphasis on MCL-1, a ubiquitous pathogenic and resistance factor in cancer. To uncover the binding and specificity determinants for MCL-1, we generated a library of hydrocarbon-stapled BH3 helices to screen for a naturally selective MCL-1 inhibitor. Ironically, the BH3 helix of MCL-1 itself emerged as

the most potent and selective antagonist. Biochemical and structural analysis of the MCL-1 SAHB$_D$/MCL-1ΔNΔC interaction provided new insight into key distinguishing features of the binding interface and how they could potentially be harnessed for drug development. Here, we applied this uniquely selective, high affinity stapled peptide to screen for small molecules that could effectively displace it from the BH3-binding groove of MCL-1ΔNΔC, yet not target BCL-X$_L$. MIM1 emerged as a potent and selective small molecule inhibitor of MCL-1ΔNΔC, capable of targeting the canonical BH3-binding pocket of MCL-1, blocking MCL-1-mediated suppression of tBID-induced BAX activation *in vitro*, and inducing caspase 3/7 activation and cell death in MCL-1-dependent, but not BCL-X$_L$-dependent, leukemia cells. In each case, ABT-737 had the opposite biochemical and cellular activity profile of MIM1, and synergized with MIM1 only in the context of dual MCL-1 and BCL-X$_L$ expression. These data indicate that MIM1 may serve as a prototype for the development of next generation small molecules that effectively reduce the apoptotic threshold in cancers specifically driven by anti-apoptotic MCL-1.

Methods

SAHB synthesis

Hydrocarbon-stapled peptides corresponding to BCL-2 family BH3 domains and their FITC-βAla derivatives were synthesized, purified, and characterized according to previously described methods[22-24]. The sequence compositions of all SAHBs used in this study are indicated in Table 2.1.

BCL-2 family protein production

Recombinant MCL-1ΔNΔC, BCL-X$_L$ΔC, and full-length BAX were expressed and purified as previously reported[25,26]. Transformed *Escherichia coli* BL21 (DE3) were cultured in ampicillin-containing Luria Broth, and protein expression was induced with 0.5 mM isopropyl β-D-1-thiogalactopyranoside (IPTG). The bacterial pellets were resuspended in buffer (1% Triton X-100 in PBS, complete protease inhibitor tablet for MCL-1ΔNΔC and BCL- X$_L$ΔC, and 250 mM NaCl, 20 mM Tris, complete protease inhibitor tablet, pH 7.2 for BAX), sonicated, and after centrifugation at 45,000x*g* for 45 min, the supernatants were applied to glutathione-sepharose columns (GE Healthcare) for GST-MCL-1ΔNΔC and BCL-X$_L$ΔC, or a chitin column (BioLabs) for Intein-BAX. On-bead digestion of GST-tagged protein was accomplished by overnight incubation at room temperature in the presence of thrombin (75 units) in PBS (3 mL), whereas the intein tag was cleaved from BAX by overnight incubation of the chitin beads at 4°C with 50 mM DTT. The tagless recombinant proteins were purified by size exclusion chromatography (SEC) using a Superdex-75 column (GE Healthcare) with 150 mM NaCl, 50 mM Tris, pH 7.4

buffer conditions for MCL-1ΔNΔC and BCL-X_LΔC, and 20 mM HEPES pH 7.2, 150 mM KCl

buffer conditions for full-length monomeric BAX protein.

Fluorescence polarization binding assays

Fluorescence polarization assays (FPA) were performed as previously described[25,27]. Briefly,

direct binding curves were first generated by incubating FITC-MCL-1 SAHB$_A$, FITC-BID BH3,

or FITC-BAD BH3 (15 nM) with serial dilutions of anti-apoptotic protein, and fluorescence

polarization measured at 5 min on a SpectraMax M5 microplate reader (Molecular Devices). For

competition assays, a serial dilution of small molecule or acetylated peptide was added to

recombinant protein at ~EC_{75} concentration, as determined by the direct binding assay (MCL-

1ΔNΔC, 45 nM; BCL-X_LΔC, 300 nM). Fluorescence polarization was measured at equilibrium

and IC_{50} values calculated by nonlinear regression analysis of competitive binding curves using

Prism software (Graphpad).

MIM1 characterization by mass spectrometry and ^{1}H-NMR spectroscopy

4-((*E*)-(((*Z*)-2-(cyclohexylimino)-4-methylthiazol-3(2*H*)-yl)imino)methyl)benzene-1,2,3-triol.

LC-MS: 348(M+1,ES+); 346(M-1, ES-). ^{1}H NMR (300 MHz, *DMSO-d6*): d 11.35 (s, 1H, -O<u>H</u>);

9.3 (s, 1H, -O<u>H</u>); 8.42 (s, 1H, -O<u>H</u>); 8.31(s, 1H*)*; 6.73 (d, 1H, *J=8.4 Hz*); 6.34(d, 1H, *J=8.4 Hz*);

6.01(s, 1H); 3.09-3.05 (m, 1H); 2.15 (s, 3H); 1.81-1.60 (m, 5H); 1.40-1.2 (m, 3H), 1.15 (t, 2H).

NMR samples and spectroscopy

Uniformly ^{15}N-labeled MCL-1ΔNΔC was generated by modifying its expression and purification

scheme in accordance with the method for producing ^{15}N-BAX[26,28]. Protein samples were

prepared in 20 mM HEPES solution at pH 6.5 in 5% D_2O. MIM1 (20 mM stock) was titrated

into a solution of 100 μM MCL-1ΔNΔC to achieve the indicated molar ratio concentration.

Correlation ^{1}H-^{15}N HSQC spectra[29] were acquired at 25°C on a Bruker 800 MHz NMR

spectrometer equipped with a cryogenic probe, processed using NMRPipe[30], and analyzed with

NMRView[31]. The weighted average chemical shift difference Δ at the indicated molar ratio was

calculated as $\sqrt{\{(\Delta H)^2 + (\Delta N/5)^2\}/2}$ in p.p.m. The absence of a bar indicates no chemical shift

difference, or the presence of a proline or residue that is overlapped or not assigned. MCL-

1ΔNΔC cross-peak assignments were applied as previously reported[28]. The significance

threshold for backbone amide chemical shift changes was calculated based on the average

chemical shift across all residues plus the standard deviation, in accordance with standard

methods[32].

Structural modeling

Docked structures of MCL-1ΔNΔC and MIM1 were generated using *Glide* and analyzed using

PYMOL[33].

Liposomal release assay

Liposomes were prepared and release assays performed as previously described[34,35]. Liposomal

composition reflects a mixture of the following molar percentages of lipids (Avanti Polar

Lipids): phosphatidylcholine, 48%; phosphatidylethanolamine, 28%; phosphatidylinositol, 10%;

dioleoyl phosphatidylserine, 10%; and tetraoleoyl cardiolipin, 4%. Aliquots of mixed lipids (1

mg total) are stored in glass at -20°C under nitrogen, and before use, resuspended in liposome

assay buffer (10 mM HEPES, 200 mM KCl, 1 mM $MgCl_2$, pH 7) containing 12.5 mM of the

fluorescent dye ANTS (8-aminonaphthalene-1,3,6-trisulfonic acid, disodium salt) and 45 mM of

the quencher DPX (p-xylene-bis-pyridinium bromide). The resulting slurry is vortexed for 10

min and freeze-thawed five times in liquid nitrogen and a 40°C water bath, respectively. The

solution is then passed through an Avanti Mini-Extruder Set (#610000) equipped with a 100 nm

filter, followed by passage through a Sepharose column (GE Healthcare) to remove residual

ANTS/DPX. The liposomes are brought up to a volume of 3 mL to produce a final liposome

stock. For the liposomal release assay, a total volume of 30 μL is used in 384 well black flat-

bottom plates (Costar), and baseline fluorescent measurements of 8 μL liposomes are made for

10 min using a Tecan Infinite M1000 (λ_{ex} 355 nm, λ_{em} 520 nm). Following the baseline read,

recombinant anti-apoptotic protein, with or without pre-incubated small molecule or peptide, is

added to the liposomes. Subsequently, 20 nM caspase-cleaved mouse BID (R&D systems) and

250 nM purified recombinant monomeric BAX is added, and fluorescence measurements are

recorded each minute until the release measurements plateau, at which point the liposomes are

quenched with 0.2% Triton X-100 (100% release). The percentage release of ANTS/DPX was

calculated according to the equation ($[F - F0]/[F100 - F0]) \times 100$, where F0 and F100 are

baseline and maximal fluorescence, respectively.

Cell viability and caspase 3/7 activation assays

BCR-ABL(p185)-transformed *Arf*$^{/-}$ B-ALL cells were generated by transducing *Mcl-1*$^{+/+}$*Arf*$^{/-}$

mouse bone marrow with BCR-ABL(p185)-IRES-Luciferase vector and then removing the cells

from growth factor and stromal support[36]. MCL-1 or BCL-X$_L$-rescued *p185*$^+$*Arf*$^{/-}$/*Mcl-1*-deleted

B-ALL cells were generated by transducing *Mcl-1*$^{f/f}$*Arf*$^{/-}$ mouse bone marrow with p185-IRES-

Luciferase. Transformed *p185*$^+$*Mcl-1*$^{f/f}$*Arf*$^{/-}$ B-ALL cells were then transduced with MSCV-

Puro-*Mcl-1* or MSCV-Puro-*Bcl-X$_L$* and selected to produce stable clones, which were subsequently transduced with MSCV-*Cre*-IRES-GFP to delete the endogenous *Mcl-1* alleles. B-ALL cells were maintained in RPMI 1640 (ATCC) supplemented with 10% (v/v) FBS, 100 U/mL penicillin, 100 mg/mL streptomycin, 0.1 mM MEM non-essential amino acids, and 50 mM b-mercaptoethanol. Mouse embryonic fibroblasts (MEFs) cells were maintained in DMEM high glucose (Invitrogen) supplemented with 10% (v/v) FBS, 100 U/mL penicillin, 100 mg/mL streptomycin, 2 mM L-glutamine, 50 mM HEPES, 0.1 mM MEM non-essential amino acids, and 50 mM b-mercaptoethanol. Leukemia cells ($4x10^4$/well) were seeded in 96-well opaque plates and incubated with the indicated serial dilutions of vehicle (0.4% DMSO), MIM1, ABT-737, or the combination in DMEM at 37°C in a final volume of 100 ml. For MEF experiments, cells ($5x10^3$/well) were seeded in 96-well opaque plates for 24 h and then incubated with the indicated serial dilutions of vehicle (0.4% DMSO), MIM1, or ABT-737. Cell viability was assayed at 24 h by addition of CellTiter-Glo reagent according to the manufacturer's protocol (Promega), and luminescence was measured using a SpectraMax M5 microplate reader (Molecular Devices). Caspase 3/7 activation was assayed at 8 h by addition of Caspase-Glo 3/7 reagent according to the manufacturer's protocol (Promega), and luminescence measured using a SpectraMax M5 microplate reader. Synergy of the MIM1/ABT-737 combination in leukemia cells was calculated using the CalcuSyn software package[4].

Co-immunoprecipitation assay

p185$^+$*Arf*$^{-/-}$/*Mcl-1*-deleted B-ALL cells rescued by MCL-1 overexpression ($5x10^6$ cells) were incubated with MIM1 or vehicle in the above-indicated culture media at 37°C for 6 h. After cellular lysis in 50 mM Tris (pH 7.4), 150 mM NaCl, 2.5 mM MgCl$_2$, 0.5% NP40 and complete

protease inhibitor tablet, cellular debris was pelleted at 14,000g for 10 min at 4ºC. The supernatant was exposed to pre-equilibrated protein A/G sepharose beads and the pre-cleared supernatant subsequently incubated with anti-MCL-1 antibody (anti-MCL-1, Rockland Immunochemical) overnight at 4ºC, followed by the addition of protein A/G sepharose beads for 1 h. The beads were pelleted and washed with lysis buffer 3 times for 10 min at 4ºC. The washed beads were then pelleted, heated to 90ºC for 10 min in SDS loading buffer, analyzed by SDS/PAGE, and then immunoblotted for MCL-1 and BAK (anti-BAK-NT, Millipore).

Contributions

M. Stewart and G. Bird synthesized the stapled peptides applied in these studies. N. Cohen performed the high-throughput screen and secondary biochemical validation, including binding assays and liposomal assays, with guidance from L. Walensky. E. Gavathiotis performed the NMR analysis and structural modeling studies. J. Opferman kindly provided the genetically defined murine leukemia cells used in this study, and J. Tepper characterized the cells and performed immunoprecipitation experiments. N. Cohen performed cell viability and compound synergy experiments with guidance from L. Walensky. L. Walensky and N. Cohen wrote the submitted manuscript, which was reviewed by J. Opferman. Assistance in generating figures was provided by E. Smith.

References

1.   Stewart, M.L., Fire, E., Keating, A.E. & Walensky, L.D. The MCL-1 BH3 helix is an exclusive MCL-1 inhibitor and apoptosis sensitizer. *Nature Chem Biol* **6**, 595-601 (2010).

2.   Zhai, D., Jin, C., Satterthwait, A.C. & Reed, J.C. Comparison of chemical inhibitors of antiapoptotic BCL-2 family proteins. *Cell Death Diff.* **13**, 1419-1421 (2006).

3.   Oltersdorf, T. et al. An inhbitor of Bcl-2 family proteins induces regression of solid tumours. *Nature* **435**, 677-681 (2005).

4.   Chou, T.C. Theoretical basis, experimental design, and computerized simulation of synergism and antagonism in drug combination studies. *Pharmacol. Rev.* **58**, 621-681 (2006).

5.   van Delft, M.F. et al. The BH3 mimetic ABT-737 targets selective Bcl-2 proteins and efficiently induces apoptosis via Bak/Bax if Mcl-1 is neutralized. *Cancer Cell* **10**, 389-399 (2006).

6.   Sattler, M. et al. Structure of Bcl-xL-Bak peptide complex: recognition between regulators of apoptosis. *Science* **275**, 983-6 (1997).

7.   Arnold, A.A. et al. Preclinical studies of Apogossypolone: a new nonpeptidic pan small-molecule inhibitor of Bcl-2, Bcl-XL and Mcl-1 proteins in follicular small cleaved cell lymphoma model. *Mol Cancer* **7,** 20 (2008).

8.   Doi, K. et al. Discovery of Marinopyrrole A (Maritoclax) as a Selective Mcl-1 Antagonist that Overcomes ABT-737 Resistance by Binding to and Targeting Mcl-1 for Proteasomal Degradation. *J Biol Chem* (2012).

9.   Feng, Y. et al. Design, synthesis and interaction study of quinazoline-2(1H)-thione derivatives as novel potential Bcl-xL inhibitors. *J Med Chem* **53**, 3465-79 (2010).

10.   Kazi, A. et al. The BH3 alpha-helical mimic BH3-M6 disrupts Bcl-X(L), Bcl-2, and MCL-1 protein-protein interactions with Bax, Bak, Bad, or Bim and induced apoptosis in a Bax- and Bim- dependent manner. *J Biol Chem* **286**, 9382-92 (2011).

11.   Lee, E.F. et al. A novel BH3 ligand the selectively targets Mcl-1 reveals that apoptosis can proceed without Mcl-1 degradation. *J Cell Biol* **180**, 341-55 (2008).

12.   M.D., B. et al. Evaluation of diverse alpha/beta-backbone patterns for functional alpha helix mimicry: analogues of the Bim BH3 domain. *J Am Chem Soc* **134**, 315-23 (2012).

13.   Mohammad, R.M. et al. Preclinical studies of TW-37, a new nonpeptidic small molecule inhibitor of Bcl-2, in diffuse large cell lymphoma xenograft model reveal drug action on both Bcl-2 and Mcl-1. *Clin Cancer Res* **13**, 2226-35 (2007).

14.   Nguyen, M. et al. Small molecule obatoclax (GX15-070) antagonizes MCL-1 and overcomes MCL-1-mediated resistance to apoptosis. *PNAS* **104**, 19512-19517 (2007).

15.   Oh, H. et al. Cryptosphaerolide, a cytotoxic Mcl-1 inhibitor from a marine-derived ascomycete related to the genus Cryptosphaeria. *J Nat Prod* **73**, 998-1001 (2010).

16.   Paoluzzi, L. et al. Targeting Bcl-2 family members with the BH3 mimetic AT-101 markedly enhances the therapeutic effects of chemotherapueitc agents in in vitro and in vivo models of B-cell lymphoma. *Blood* **111**, 5350-8 (2008).

17.   Petros, A.M. et al. Discovery of a potent and selective Bcl-2 inhibitor using SAR by NMR. *Bioorg Med Chem Lett* **20**, 6587-91 (2010).

18.   Placzek, W.J. et al. Identification of a novel Mcl-1 protein binding motif. *J Biol Chem* **286**, 39829-35 (2011).

19.   Wang, G. et al. Structure-based design of potent small molecule inhibitors of anti-apoptotic Bcl-2 proteins. *J Med Chem* **49**, 6139-42 (2006).

20.   Zhang, Z. et al. A novel BH3 mimetic S1 potently induces Bax/Bak-depended apoptosis by targeting both Bcl-2 and MCL-1. *Int J Cancer* **128**, 1724-35 (2011).

21.   Zheng, C.H. et al. Design, synthesis and activity evaluation of broad-spectrum small molecule inhibtors of anti-apoptotic Bcl-2 family proteins: characteristics of broad spectrum protein binding and its effects on anti-tumor activity. *Bioorg Med Chem Lett* **22**, 39-44 (2012).

22.   Bird, G.H., Bernal, F., Pitter, K. & Walensky, L.D. Chapter 22 Synthesis and Biophysical Characterization of Stabilized alpha-Helices of BCL-2 Domains. *Methods Enzymol* **446**, 369-86 (2008).

23.   Walensky, L.D. et al. Activation of apoptosis in vivo by a hydrocarbon-stapled BH3 helix. *Science* **305**, 1466-70 (2004).

24.   Walensky, L.D. et al. A stapled BID BH3 helix directly binds and activates BAX. *Mol Cell* **24**, 199-210 (2006).

25.   Pitter, K., Bernal, F., Labelle, J. & Walensky, L.D. Dissection of the BCL-2 family signaling network with stabilized alpha-helices of BCL-2 domains. *Methods Enzymol* **446**, 387-408 (2008).

26.   Gavathiotis, E. et al. BAX activation is initiated at a novel interaction site. *Nature* **455**, 1076-81 (2008).

27.   Bernal, F. et al. A stapled p53 helix overcomes HDMX-mediated suppression of p53. *Cancer Cell* **18**, 411-22 (2010).

28.   Suzuki, M., Youle, R.J. & Tjandra, N. Structure of Bax: coregulation of dimer formation and intracellular localization. *Cell* **103**, 645-54 (2000).

29.   Grzesiek, S. & Bax, A. The importance of not saturating water in protein NMR: application to sensitivity enhancement and NOE measurements. *J Am Chem Soc* **115**, 12593-12594 (1993).

30.   Delaglio, F. et al. NMRPipe: a multidimensional spectral processing system based on UNIX pipes. *J Biomol NMR* **6**, 277-93 (1995).

31.   Johnson, B.A. Using NMRView to visualize and analyze the NMR spectra of macromolecules. *Methods Mol Biol* **278**, 313-52 (2004).

32.   Marintchev, A., Frueh, D. & Wagner, G. NMR methods for studying protein-protein interactions involved in translation initiation. *Methods Enzymol* **430**, 283-331 (2007).

33.   DeLano, W.L. *The PyMOL Molecular Graphics System*, (DeLano Scientific, San Carlos, 2002).

34.   Yethon, J.A., Epand, R.F., Leber, B., Epand, R.M. & Andrews, D.W. Interaction with a membrane surface triggers a reversible conformational change in Bax normally associated with induction of apoptosis. *J Biol Chem* **278**, 48935-41 (2003).

35.   Lovell, J.F. et al. Membrane binding by tBid initiates an ordered series of events culminating in membrane permeabilization by Bax. *Cell* **135**, 1074-84 (2008).

36.   Williams, R.T., Roussel, M.F. & Sherr, C.J. Arf gene loss enhances oncogenicity and limits imatinib response in mouse models of Bcr-Abl-induced acute lymphoblastic leukemia. *Proc Natl Acad Sci U S A* **103**, 6688-93 (2006).

Chapter 4

MCL-1 Cysteine Modification:

Characterization of an Alternative Small Molecule Binding Mechanism

Abstract

BCL-2 family proteins are critical regulators of apoptosis, a form of programmed cell death that is essential to tissue development, homeostasis, and organism longevity. MCL-1 is an anti-apoptotic BCL-2 protein that binds and inhibits select pro-apoptotic members. Loss of MCL-1 function can sensitize cells to apoptosis and lead to premature cell death, whereas overexpression can prolong cell survival in the face of pro-apoptotic stress. MCL-1 is unique among the anti-apoptotics both in its interaction profile and complex post-translational regulation. Whereas small molecules have been developed to target the BCL-2 subclass of anti-apoptotic proteins, selective modulators of MCL-1 have remained out of reach. Because such compounds would be valuable tools to analyze MCL-1 function in health and disease, we undertook a screening assay and identified a class of compounds that bound to MCL-1 selectively and covalently, leading to striking changes in MCL-1 structure and function. In characterizing the binding sites, cysteine modification emerged as a chemical mechanism for MCL-1 modulation with potential physiologic implications. The biochemical and cellular consequences of cysteine modification on MCL-1 activity were studied, revealing a possible new druggable mechanism for maintaining cellular survival in the face of premature or unwanted cell death.

Introduction

BCL-2 family proteins exert their influence over cellular life and death at the level of the mitochondria. As the cell's power plants, mitochondria regulate energy metabolism and cell death, in part by generating and processing reactive oxygen species (ROS), such as superoxide anions, hydrogen peroxide, and hydroxyl radicals[1]. Elevated levels of ROS produce oxidative stress, which is a major contributor to diverse pathologies, including chronic inflammatory diseases, cancer, and neurodegeneration[2]. Oxidative stress leads to chemical derivatization, with mitochondrial proteins as prime targets due to their proximity to the produced ROS; indeed BCL-2 proteins are key targets for reversible and irreversible oxidative modifications[1]. Such oxidative modifications would allow proteins to act as molecular sensors of the cell's overall stress level during disease states and physiological processes[3]. For example, high levels of ROS have been associated with cancer metastasis and promote DNA damage, leading to carcinogenesis[4]. Specifically, BCL-2 was shown to prevent oxidative cell death at the site of free radical generation in response to a number of stimuli[5]. Mechanistically, BCL-2 expression led to an overall reduction in ROS in neural cells[6]. Such findings highlight the importance of BCL-2 family regulation during oxidative stress and the potential to impact cellular life or death through pharmacologic targeting of the proteins themselves or their modes of post-translational modification.

Among the physiologic mechanisms of cysteine modification, S-nitrosylation has previously been reported to impact the functional activity of several apoptotic regulators. Nitric oxide (NO), synthesized from L-arginine by one of three isotypes of nitric oxide synthase (NOS)[7], is a free radical mediator, interacting directly or indirectly with a number of ROS to yield secondary reactive species capable of modifying proteins. NO itself can also act directly on

proteins through S-nitrosylation of free reactive thiol groups[8]. BCL-2 is S-nitrosylated in response to chromium (V), Fas ligand, and stress-induced apoptosis in human lung epithelial cells; this modification inhibits its ubiquitin-mediated proteasomal degradation, thus increasing BCL-2 levels and its anti-apoptotic function[9]. In contrast, S-nitrosylation of X-linked inhibitor of apoptosis (XIAP) inhibits its binding to caspase-3 in neurons and promotes apoptosis[10]. Indeed, S-nitrosylation is an important modifier of a large variety of proteins, promoting alterations in structure and function that have been implicated in disease pathologies ranging from cancer[11] to cardiovascular disease[12] to neurodegeneration[13].

In addition to S-nitrosylation, various other post-translational modifications can affect a protein's reactive cysteines, often taking advantage of electrophilic Michael additions. Physiologic electrophiles that modify cysteines include nitro-fatty acids and α,β-unsaturated aldehydes, such as lipid peroxidation products (e.g., 4-hydroxynonenal).[3] In addition, reactive cysteines may form thiol-protein mixed disulfides with glutathione or free cysteine[14] or undergo reversible and irreversible oxidative modifications with partially reduced oxygen species (e.g., sulfenic acid). All of these modifications are influenced by the redox state of the cell, and alteration in protein structure and function occur as a result.

Rather than targeting proteins at their canonical protein-protein interaction sites or ligand-binding pockets, the potential for targeting post-translational modifications that regulate a protein's function or turnover remains a viable therapeutic option. For example, the deubiquitinase USP9X was recently found to act on MCL-1, stabilizing its protein levels and promoting cell survival[15]. Therefore, targeting this interaction and blocking MCL-1 deubiquitination would be one strategy to overcome cellular survival in cancer. Because aberrant lysine methylation is often involved in carcinogenesis, targeting protein lysine demethylases or

104

methyltransferases that act on proteins such as p53, NFKB, and E2F1 may prevent cancer progression[15]. Proteins that are S-nitrosylated present a unique opportunity for therapeutic targeting: irreversibly inhibiting the nitrosylation event by blocking the reactive cysteine with a covalent inhibitor.

Irreversible small molecule inhibitors have gained attention recently, mainly for covalently modifying residues within enzyme active sites, inhibiting their functions. Covalent inhibitors possess many advantages, such as prolonged pharmacodynamics. This was shown recently by covalent inhibition of specific cysteine residues within the c-Jun N-terminal kinase protein family[16]. Previously, cysteine-modifying small molecules have been discovered to target the fibroblast growth factor receptor tyrosine kinases and Bmx kinase at cysteine residues[17,18]. While covalent inhibition is common for enzymes with ATP binding sites, other proteins have also been targeted covalently in the past. Intriguingly, a cysteine on the opposite binding face of the regulator of G protein signaling (RGS) protein was modified by CCG-4986, leading to an allosteric change in protein conformation and completely inhibiting its protein interaction with the Gα subunit of the G protein[19]. Furthermore, covalent cysteine targeting of the transcription factor NFκB has been proposed to result in inhibition of DNA recognition and binding[20].

The therapeutic utility of covalent small molecules remains promising, as long as off-target effects can be prevented. This mode of small molecule inhibition has yet to be applied to the BCL-2 family of proteins, but the presence of physiologically important cysteines may allow for selective covalent targeting via a novel mechanism.

Results

Select small molecules irreversibly bind MCL-1's C286

Chapter 2 described the high-throughput screen we undertook to discover small molecules that selectively target MCL-1, and Chapter 3 then focused on the biochemical and cellular characterization of MIM1, a small molecule that binds MCL-1 specifically at its canonical BH3 binding pocket. Intriguingly, some small molecules that emerged from the initial high-throughput screen demonstrated *in vitro* activity consistent with irreversible, covalent small molecule modification. Based on the analysis of their structural scaffolds, a subset of molecules were predicted to be reactive and thus could potentially modify MCL-1 at specific residues by Michael addition or other covalent reaction. To examine whether small molecule hits bound reversibly or irreversibly to MCL-1, a rapid dilution assay was applied. For this assay, MCL-1 was incubated with compound for one hour to achieve equilibrium in a manner similar to the FP assay described in previous chapters. Next, the initial solution was diluted to 200 times the original binding volume, and the solution was then reconcentrated to the initial volume for binding analysis. Following the dilution and reconcentration procedure, the FITC-BID BH3/MCL-1 FP binding assay was repeated. If the small molecule was non-covalently bound and thus dialyzed away, FITC-BID BH3/MCL-1 would produce a binding curve similar to native unmodified MCL-1. If the molecule was covalently bound, inhibition of the FITC-BID BH3/MCL-1 interaction would persist after dilution (**Figure 4.1**).

Specific structural classes and compounds were found to bind MCL-1 irreversibly. Compounds that behaved as covalent interactors in the dilution assay were advanced to mass spectrometry-based analysis to confirm covalent modification and the affected amino acid site. First, compounds alone were examined by LC/MS to confirm stability and document exact mass.
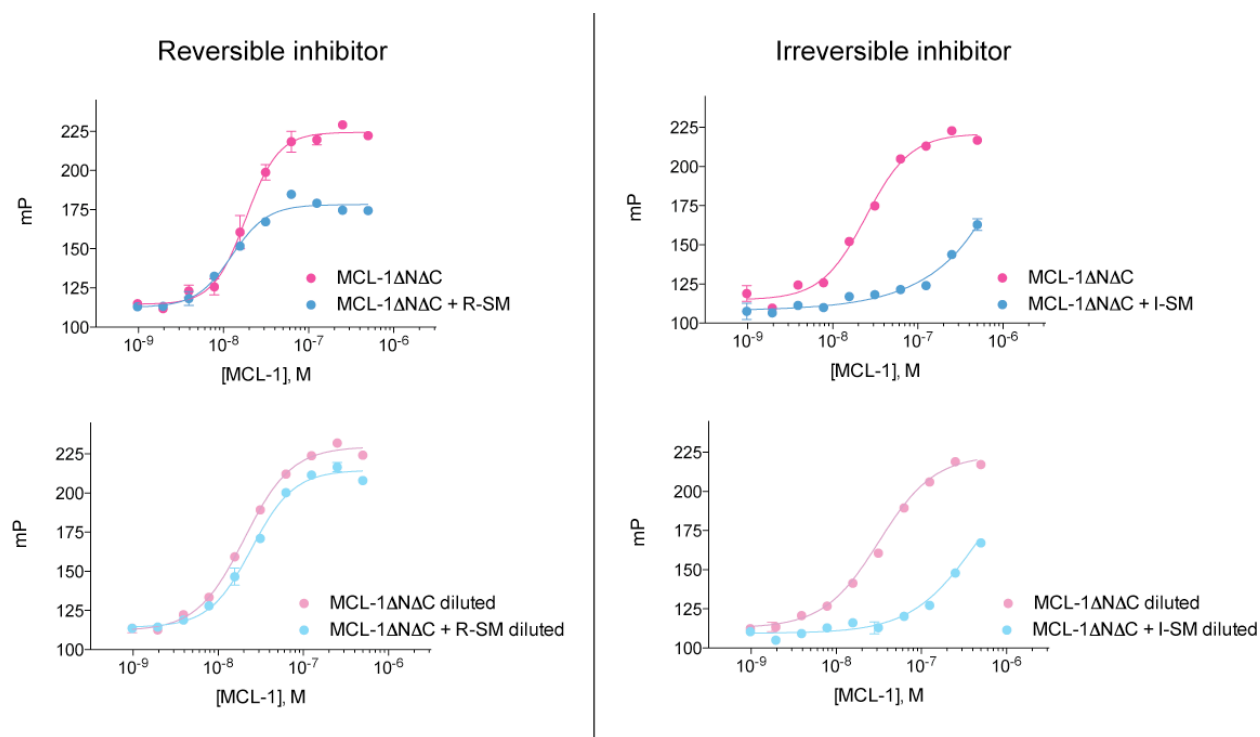
Figure 4.1. *A rapid dilution assay was used as a screening tool to determine whether compounds bind MCL-1 reversibly or irreversibly.* All molecules tested effectively inhibited FITC-BID BH3/MCL-1 binding prior to dilution. MCL-1 alone was used as a pre- and post-dilution control to ensure that protein concentration remained constant (curves shown in all panels in pink). Following dilution, a reversible inhibitor no longer inhibits FITC-BID BH3 binding, as the compound was effectively diluted to a concentration below its binding EC_{50} (left panel, SM-B1). Conversely, irreversible inhibitors remain bound to the protein regardless of dilution status and therefore continue to block FITC-BID BH3 binding to MCL-1 post-dilution (right panel, SM-A3).

Next, unmodified recombinant MCL-1 and compound-treated MCL-1 (following gel filtration to remove excess compound) were spotted and run using both MALDI and LC/ESI/MS to confirm covalent modification. If modification was confirmed, a peak equal to the mass of MCL-1 plus the specific compound was apparent. Unmodified and modified MCL-1 were then subjected to trypsin digestion, and the fragments were analyzed by nano-LC/ESI/MS using a vented column assembly as described[21]. The most abundant precursors in each MS scan were subjected to collisionally-activated dissociation. The specific residue modified was determined using a separate, targeted nano-LC/ESI/MS in which doubly and triply charged modified peptides were subjected to higher energy collisionally-activated dissociation. (**Figure 4.2**) This approach provided further evidence for cysteine residue modification; for example, b6 and y14 ions were detected in specific cases (mass errors ~3 ppm or less), leaving cysteine as the only possible modification site.

Applying the MS characterization described above, we determined that CSM-B2 (covalent small molecule-B2, see structural scaffold classification in Chapter 2) disrupted the FITC-BID BH3/MCL-1ΔNΔC interaction as a result of covalent modification of C286 (**Figure 4.2**). This unanticipated finding suggests that covalent cysteine modification could potentially regulate MCL-1 function *in vivo* and provides a novel approach to pharmacologic modulation of MCL-1's pro-survival functionality.

Covalent modification of C286 leads to BH3-only displacement from the canonical binding site

Synthetic or endogenous signaling molecules are capable of reacting with cysteine residues in proteins. Interestingly, MCL-1ΔNΔC's single cysteine is located on the face of the protein opposite to its canonical BH3 pocket (**Figure 4.2**), yet covalent binding of CSM-B2,

TINQES**C**IEPLAESITDVLVR

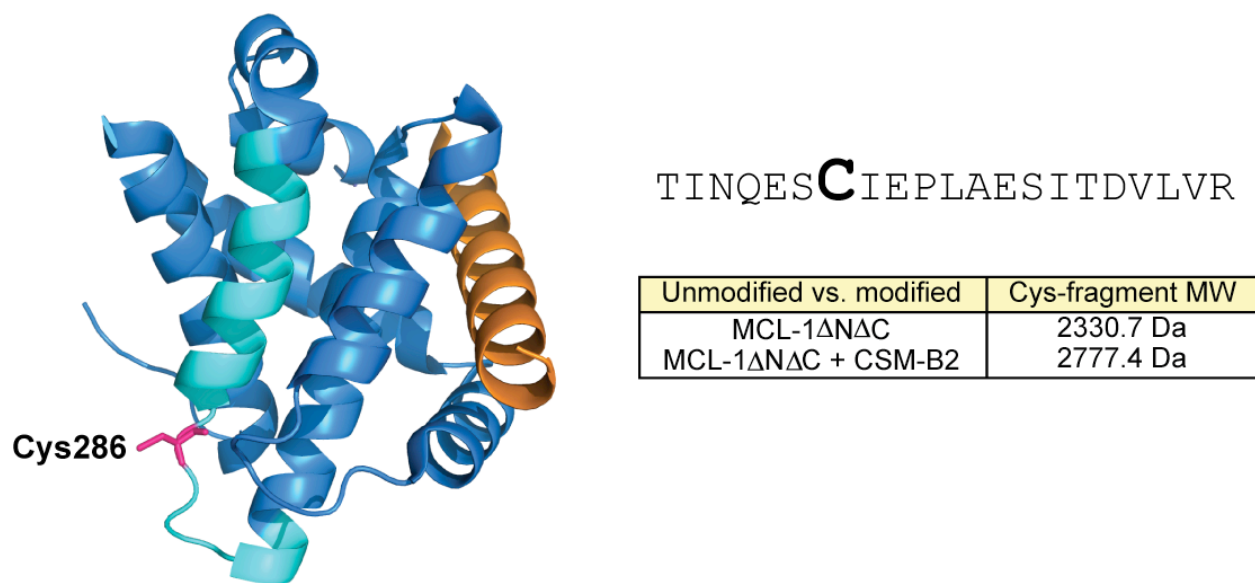| Unmodified vs. modified	Cys-fragment MW
MCL-1ΔNΔC	2330.7 Da
MCL-1ΔNΔC + CSM-B2	2777.4 Da

Figure 4.2. *Mass spectrometry uncovers covalent modification of MCL-1's C286 by select small molecules.* CSM-B2 covalently modifies MCL-1ΔNΔC on the cysteine-containing tryptic fragment; ESI-MS analysis revealed a mass increase of ~450 Da.

among other molecules, led to displacement of FITC-MCL-1 SAHB or FITC-BID BH3 from the canonical BH3 binding pocket. This suggests that through possible allosteric modulation, cysteine binding induced a structural change within MCL-1 that blocked peptide binding to the canonical BH3 groove.

As demonstrated in **Figure 4.2**, MS analysis documented that CSM-B2 disrupted MCL-1ΔNΔC/BH3 binding through covalent modification of C286. As C286 is not localized to the canonical BH3 binding pocket, I sought to determine whether the MCL-1 modulating effect was specific to the molecule's interaction at the C286 region or was explicitly dependent on C286 reactivity itself, supporting a more general role for cysteine modification in MCL-1 regulation. The effect of CSM-B2 treatment in a competitive FP assay was examined using FITC-BID BH3, MCL-1ΔNΔC, and MCL-1ΔNΔC C286S. Strikingly, CSM-B2 had no effect on MCL-1 binding activity in the absence of C286 (**Figure 4.3**). Additionally, the identical result was obtained when the reactive cysteine was alkylated with iodoacetamide (IAM) or when the molecule's reactive moiety was reduced with dithiothreitol (DTT). These data confirm that specific chemical modification of C286 impacts the BH3-binding activity of MCL-1ΔNΔC.

Furthermore, two analogs of CSM-B2 were analyzed for their ability to bind MCL-1 by competitive FP assay (**Figure 4.4A**). CSM-B2b still binds MCL-1, albeit with lower affinity (IC_{50} = 4.4 μM) due to its less reactive molecular structure. Binding still occurs, however, owing to preservation of the compound's fully conjugated resonance form at pH 8.0 (FP buffer), enabling covalent modification to proceed. In contrast, the diacetyl-modified analog of CSM-B2 (CSM-B2c) does not bind to MCL-1 (IC_{50} >50 μM), consistent with its resonance conjugation being irreversibly lost. With no electron acceptors on the molecule, covalent modification does not occur, and correspondingly, FITC-BID BH3 is not displaced from MCL-1. Based on these
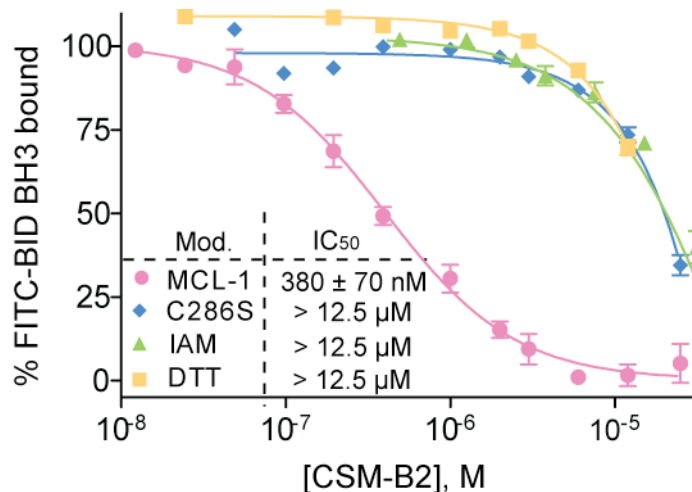
Figure 4.3. *The C286S mutation, IAM treatment, and DTT treatment block FITC-BID BH3 displacement from MCL-1 ΔNΔC by a cysteine-modifying small molecule.* CSM-B2 treatment impairs FITC-BID BH3 binding to MCL-1ΔNΔC but not to the C286S mutant, as assessed by competitive FPA. DTT and IAM also disrupt binding by reducing the reactive compound core and blocking the reactive cysteine, respectively.
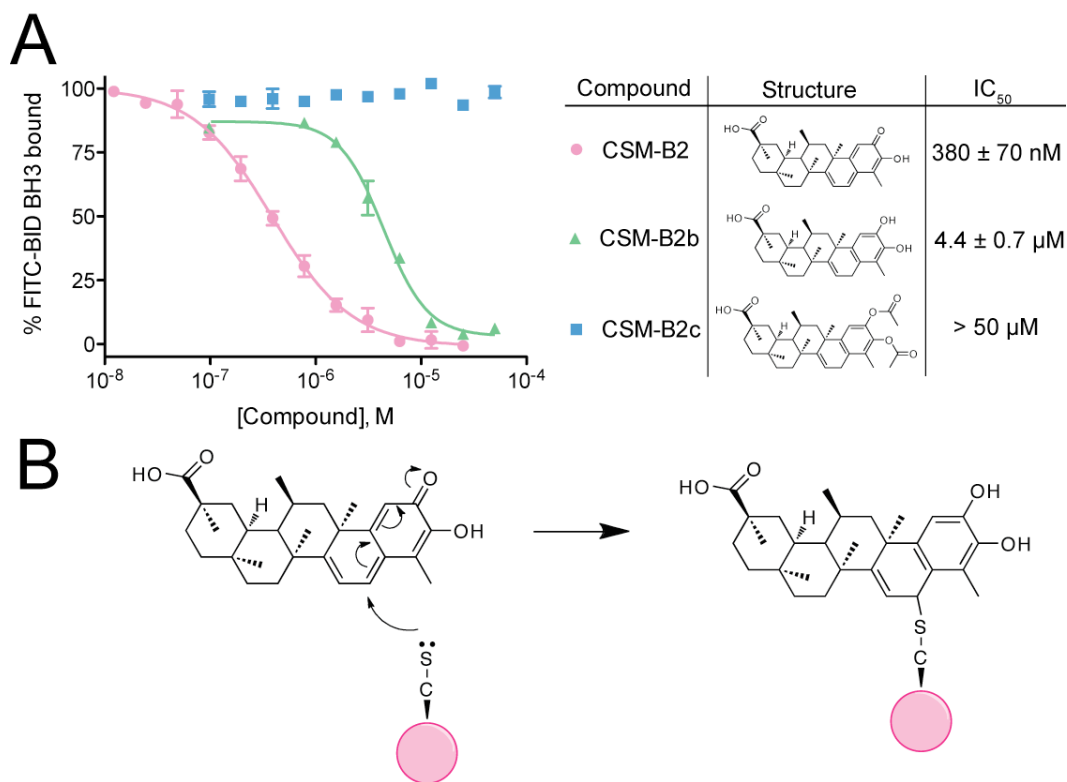
Figure 4.4. *The reactive core of CSM-B2 is predicted by SAR analysis*. (A) FP competition assay shows displacement of FITC-BID BH3 from MCL-1ΔNΔC in the presence of parental CSM-B2, but not upon exposure to an analog lacking the conjugated, reactive core. (B) A mechanism for cysteine modification of MCL-1ΔNΔC by CSM-B2 is proposed[22,23].

results and established cysteine derivatization reactions, a proposed mechanism for cysteine binding and modification is proposed (**Figure 4.4B**).

HSQC analysis reveals structural alteration upon covalent modification of C286

As previously accomplished for the interaction between MCL-1ΔNΔC and MIM1, we applied HSQC NMR in an effort to map the site of interaction for CSM-B2 on the MCL-1ΔNΔC surface. As the NMR structure of MCL-1 has been previously determined[24], we applied the amino acid assignments in HSQC experiments that employed ^{15}N-labeled MCL-1 and titrations of small molecules. The topographic confluence of chemical shift changes is highly suggestive of a ligand binding site, which can then be further validated by protein mutagenesis and SAR analysis. This approach successfully localized the binding site of MIM1 to the canonical BH3 binding groove of MCL-1ΔNΔC (Chapter 2). In this case, chemical shift changes were strictly localized to the topographic region of the BH3-binding groove, with the majority of MCL-1 ΔNΔC remaining unperturbed at a 1:2 ratio of protein:molecule. In marked contrast, upon CSM-B2 titration, global structural changes were observed, precluding assignment of a discrete region for the CSM-B2 interaction (**Figure 4.5**). This result suggests that an allosteric mechanism may exist, whereby cysteine modification by CSM-B2 causes disruptive structural changes in the BH3 pocket, preventing BH3 peptide interaction and potentially altering MCL-1 function in cells.

MCL-1ΔNΔC is S-nitrosylated in vitro

Among the physiologic mechanisms of cysteine modification, S-nitrosylation has previously been reported to impact the functional activity of several apoptotic regulators. Pilot
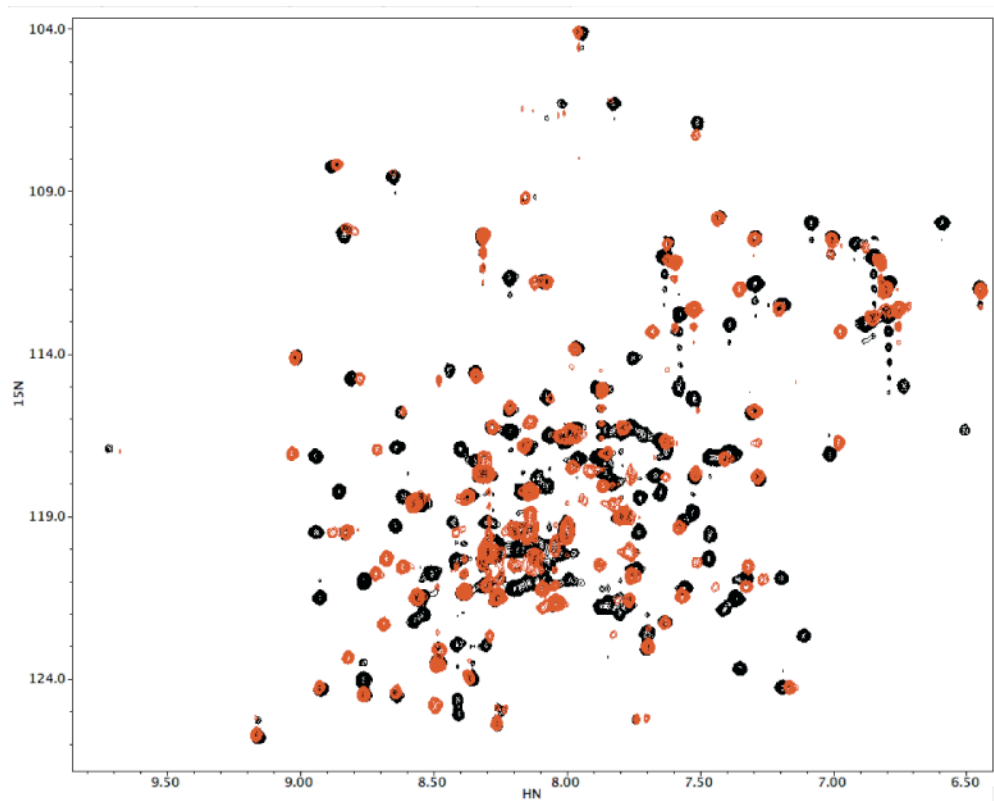
Figure 4.5. *Comparative HSQC spectra of MCL-1ΔNΔC alone and after CSM-B2 titration*

revealed a global structural alteration upon covalent modification. MCL-1ΔNΔC alone is shown

in black, and the 1:1 MCL-1ΔNΔC/CSM-B2 titration is shown in red.

nitrosylation reactions were conducted, exposing MCL-1ΔNΔC and its C286S mutant to the NO

donors S-nitroso-N-acetyl-D,L-penicillamine (SNAP) and S-nitrosoglutathione (GSNO) and the

control non-NO donor, N-acetyl-D,L-penicillamine (NAP). Note that the endogenous C16 is not

present in the truncated MCL-1ΔNΔC construct and was therefore not evaluated in this

experiment. Biotinylation of nitrosylated sites followed by electrophoresis and blotting with

streptavidin-HRP indeed revealed nitrosylation of MCL-1ΔNΔC, but not the C286S mutant, by

SNAP and GSNO (**Figure 4.6**). Importantly, the negative control agent NAP did not nitrosylate

MCL-1.

MCL-1 is S-nitrosylated in cells

　　　　To determine if cysteine modification of MCL-1 occurs in cells, a pilot

immunoprecipitation experiment was performed and indeed revealed basal MCL-1 nitrosylation

(**Figure 4.7**). MCL-1 was immunoprecipitated from OPM2 cells and probed with an anti-S-

nitrosylated cysteine (anti-SNO cys) antibody. Nitrosylation is detected at baseline conditions

and upon bortezomib treatment. Deciphering the physiologic relevance of this process, including

its regulation and phenotypic consequences, is an important next step to elucidating a potentially

novel mode of MCL-1 post-translational regulation and its impact on apoptosis.
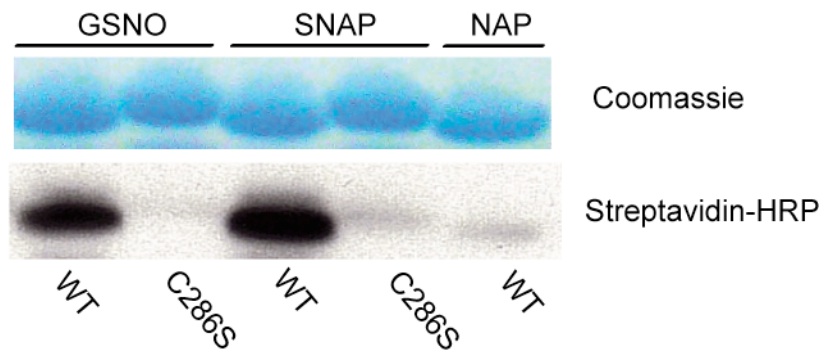
Figure 4.6. *MCL-1ΔNΔC is S-nitrosylated in vitro.* Wild-type MCL-1ΔNΔC, but not the C286S

mutant, is nitrosylated by GSNO (40 μM) and SNAP (40 μM), but not by NAP (40 μM), as

detected by the S-nitrosylated protein kit.
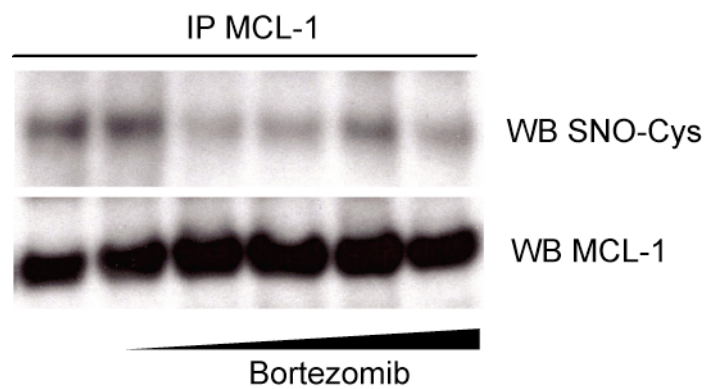
Figure 4.7. *MCL-1 is S-nitrosylated in cells*. MCL-1 was immunoprecipitated from OPM2 cells

and probed with anti-SNO cysteine antibody. Basal nitrosylation in the presence and absence of

the proteasome inhibitor, bortezomib, is shown.

Discussion

Anti-apoptotic MCL-1 is subject to extensive post-translational regulation, with such modifications affecting the protein's native interactions and cellular levels. Beyond MCL-1 phosphorylation and ubiquitination, little is known about protein modifications that derive from oxidative stress. Oxidative stress leads to ROS production, which affects the structure and function of a vast number of proteins, especially those residing at the mitochondria. ROS production promotes cysteine modification of proteins, including apoptotic proteins such as BCL-2, whose modification leads to functional alteration. Targeting post-translational modification in cells is a clinically viable approach to promoting or preventing apoptosis, either by targeting the enzymes responsible for post-translational modification (which can produce off-target effects) or by directly targeting the protein and preventing the modification. In the case of S-nitrosylation, covalent compounds that irreversibly bind cysteines could be used to block this modification and any functional downstream effects (e.g., altered degradation rates, increased apoptotic function, etc.).

Here, we discovered that select small molecules identified in our high-throughput screen disrupted BH3 peptide interactions with MCL-1 through cysteine modification. An allosteric mechanism is proposed, whereby covalent cysteine modification alters the structure and function of the canonical BH3 pocket, precluding FITC-BID BH3 interaction. This discovery could lead to novel approaches for modulating apoptotic function by targeting a discrete and previously unrecognized binding site on MCL-1. Selective therapeutic targeting of MCL-1 has remained a challenge due to structural similarity among anti-apoptotic proteins; however, targeting MCL-1's cysteine may provide a novel strategy for specific targeting, with important biological and therapeutic implications. Analogous to the insights derived from small molecule inhibition of

118

enzymes through cysteine modification, small molecule modulation of an anti-apoptotic target through cysteine-based covalent modification may not only serve as a therapeutic approach but also provide a powerful tool to dissect the functional impact of disrupting physiologic cysteine modification in cells.

Methods

BCL-2 family protein production

Recombinant MCL-1ΔNΔC was expressed and purified as previously reported[28,29]. Transformed *Escherichia coli* BL21 (DE3) were cultured in ampicillin-containing Luria Broth, and protein expression was induced with 0.5 mM isopropyl β-D-1-thiogalactopyranoside (IPTG). The bacterial pellets were resuspended in buffer (1% Triton X-100 in PBS, complete protease inhibitor tablet), sonicated, and after centrifugation at 45,000x*g* for 45 min, the supernatants were applied to glutathione-sepharose columns (GE Healthcare). On-bead digestion of GST-tagged protein was accomplished by overnight incubation at room temperature in the presence of thrombin (75 units) in PBS (3 mL). The tagless recombinant protein was purified by size exclusion chromatography (SEC) using a Superdex-75 column (GE Healthcare) with 150 mM NaCl, 50 mM Tris, pH 7.4 buffer conditions.

Fluorescence polarization binding assays

Fluorescence polarization assays (FPA) were performed as previously described[28,30]. Briefly, direct binding curves were first generated by incubating FITC-BID BH3 (15 nM) with serial dilutions of anti-apoptotic protein, and fluorescence polarization measured at 5 min on a SpectraMax M5 microplate reader (Molecular Devices). For competition assays, a serial dilution of small molecule or acetylated peptide was added to recombinant protein at ~EC_{75} concentration, as determined by the direct binding assay (MCL-1ΔNΔC, 45 nM. Fluorescence polarization was measured at equilibrium and IC_{50} values calculated by nonlinear regression analysis of competitive binding curves using Prism software (Graphpad).

Rapid dilution assay

Small molecule (excess) and MCL-1ΔNΔC (1 µM) were pre-incubated in 50 µL FPA buffer

(150 mM NaCl, 50 mM Tris, pH 8.0, 0.0625% CHAPS). These samples were then diluted into a

total volume of 10 mL and re-concentrated to their original volumes using Amicon Ultra-15

Centrifugal Filter Units (Millipore). MCL-1 protein samples (in the presence and absence of

small molecule, both pre- and post-dilution) were incubated with 15 nM FITC-BID BH3, and

binding activity was determined by direct FP analysis, as described above.

Mass spectrometry determination of covalent cysteine modification

Excess small molecule was removed by gel filtration (Microbiospin column; Bio-Rad), and the

protein was digested with trypsin overnight at 37ºC. Peptides were analyzed by nano-LC/ESI/MS

using a vented column assembly as described[21]. Briefly, peptides were injected using an

autosampler and HPLC (Waters NanoAcquity) onto a self-packed precolumn (4 cm, 100 µm

I.D., POROS10R2, Applied Biosystems) and gradient eluted (0-30% B in 20 min, A = 0.2 M

acetic acid in water, B = acetonitrile with 0.2 M acetic acid) to the resolving column (self-packed

30 µm I.D., 12 cm of 5 µm Monitor C18, Column Engineering), followed by introduction to the

mass spectrometer (Thermo Fisher LTQ-Orbitrap XL) via ESI (spray voltage = 2.2 kV). The top

8 most abundant precursors in each MS scan (image current detection, resolution = 30,000) were

subjected to CAD (electron multiplier detection, collision energy = 35%). A separate targeted

nano-LC/ESI/MS experiment was performed in which the doubly and triply charged compound-

modified peptide TINQES*CIEPLAESITVVLVR (*C= modified cysteine) was subjected to

HCD (higher energy collisionally-activated dissociation).

In vitro protein S-nitrosylation detection

To test the chemical reactivity of MCL-1 cysteine residues, recombinant MCL-1ΔNΔC protein

and its C286S mutant was expressed and purified as described previously[31]. MCL-1ΔNΔC

cDNA was cloned into the pGEX-4T1 vector, followed by site directed mutagenesis to produce

C286S (Stratgene's Quikchange Mutagenesis kit), which was confirmed by DNA sequencing. To

assess cysteine reactivity, the protein constructs were treated with serial dilutions of S-nitroso-N-

acetyl-D,L-penicillamine (SNAP) and S-nitrosoglutathione (GSNO), two effective nitric oxide

donors, and the negative control N-acetyl-D,L-penicillamine (NAP) that does not donate nitric

oxide. To monitor S-nitrosylation, the modified biotin switch method (Cayman S-nitrosylated

protein detection kit) was employed. Unreacted free thiols were first blocked, and then S-NO

bonds were reduced and labeled with biotin to capture the nitrosylated sites before NO loss[32].

Detection was readily achieved by electrophoresis and blotting with streptavidin-HRP. By

comparing the results from the various MCL-1ΔNΔC constructs, the reactivity of the cysteine

site was determined.

Detection of in situ MCL-1 cysteine derivatization

OPM2 cells were maintained in RPMI 1640 (ATCC) supplemented with 10% (v/v) FBS, 100

U/mL penicillin, 100 mg/mL streptomycin, 0.1 mM MEM non-essential amino acids, and 50

mM ß-mercaptoethanol. Cells (5×10^6) were incubated with vehicle or bortezomib (proteasome

inhibitor) in the above-indicated culture medium at 37ºC for 8 h. After cellular lysis in Buffer A

(50 mM Tris pH 7.4, 150 mM NaCl, 0.5% NP-40, complete protease inhibitor tablet), cellular

debris was pelleted at 14,000*g* for 10 min at 4ºC. The supernatant was exposed to pre-

equilibrated protein A/G sepharose beads and the pre-cleared supernatant subsequently incubated

with anti-MCL-1 antibody (anti-MCL-1 S-19, Santa Cruz Biotechnology) overnight at 4ºC, followed by the addition of protein A/G sepharose beads for 1 h. The beads were pelleted and washed with lysis buffer 3 times for 10 min at 4ºC. The washed beads were then pelleted, heated to 90ºC for 10 min in SDS loading buffer, analyzed by SDS/PAGE, and then immunoblotted for anti-S-nitrosylated cysteine (anti-SNO cys, Sigma); the blots were then stripped and reprobed with anti-MCL-1 (sc-819).

Contributions

N. Cohen performed all biochemical and cellular experiments (unless otherwise noted), with guidance from L. Walensky. E. Gavathiotis performed HSQC NMR analysis. S. Ficarro of J. Marto's laboratory identified the site of covalent modification by mass spectrometry. J. Tepper provided experimental support for rapid dilution assays. This chapter was written by N. Cohen and reviewed by L. Walensky.

References

1.   Ugarte, N., Petropulos, I. & Friguet, B. Oxidized mitochondrial protein degradation and repair in aging and oxidative stress. *Antioxidants and redox signalling* **13**, 539-549 (2010).

2.   Orrenius, S., Gogvadze, V. & Zhivotovsky, B. Mitochondrial oxidative stress: Implications for cell death. *Annu. Rev. Phamacol. Toxicol.* **47**, 143-183 (2007).

3.   Rudolph, T.K. & Freeman, B.A. Transduction of redox signalling by electrophile-protein interactions. *Science Signalling* **2**(2009).

4.   Li, Z., Yang, Y., Ming, M. & Liu, B. Mitochondrial ROS genetation for regulation of autophagic pathways in cancer. *Biochem Biophys Comm* **414**, 5-8 (2011).

5.   Hockenberry, D.M., Oltvai, Z.N., Yin, X.M., Milliman, C.L. & Korsmeyer, S.J. Bcl-2 functions in an antioxidant pathway to prevent apoptosis. *Cell* **75**, 241-251 (1993).

6.   Kane, D.J. et al. Bcl-2 inhibition of neural death: decreased generation of reactive oxygen species. *Science* **262**, 1274-1277 (1993).

7.   Hess, D.T., Matsumoto, A., Kim, S., Marshall, H.E. & Stamler, J.S. Protein S-Nitrosylation: Purview and parameters. *Nature Rev. Mol. Cell Biol.* **6**, 150-166 (2005).

8.   Stamler, J.S. et al. S-nitrosylation of proteins with nitric oxide: synthesis and characterization of biologically active compounds. *PNAS* **89**, 444-448 (1992).

9.   Azad, N. et al. S-Nitrosylation of BCL-2 inhibits its ubiquitin-proteasomal degradation: A novel antiapoptotic mechanism that suppresses apoptosis. *J Biol. Chem.* **281**, 34124-34134 (2006).

10.   Tsang, A.H. et al. S-nitrosylation of XIAP compromises neuronal survival in Parkinson's disease. *PNAS* **106**, 4900-4905 (2009).

11.   Guan, W. et al. S-nitrosylation of mitogen activated protein kinase phosphatase-1 suppresses apoptosis. *Cancer Lett.* **314**, 137-146 (2012).

12.   Lima, B., Forrester, M.T., Hess, D.T. & Stamler, J.S. S-nitrosylation in cardiovascular signaling. *Circulation Research* **106**(2010).

13.   Chung, K.K. Say NO to neurodegeneration: Role of S-nitrosylation in neurodegenerative disorders. *Neurosignals* **15**, 307-313 (2006).

14.   Brigelius, R., Lenzen, R. & Sies, H. Increase in hepatic mixed disulphide and glutathione disulphide levels elicited by paraquat. *Biochem Pharmacol* **31**, 1637-1641 (1982).

15.	Schwickart, M. et al. Deubiquitinase USP9X stabilizes MCL-1 and promotes tumour cell survival. *Nature* **463**, 103-108 (2010).

16.	Zhang, T. et al. Discovery of potent and selective covalent inhibitors of JNK. *Chemistry and Biology* **19**, 140-154 (2012).

17.	Hur, W. et al. Clinical stage EGFR inhibitors irreversibly alkylate Bmx kinase. *Bioorg. Med. Chem. Lett.* **18**, 5916-5919 (2008).

18.	Zhou, W. et al. A structure-guided approach to creating covalent FGFR Inhibitors. *Chemistry and Biology* **17**, 285-295 (2010).

19.	Roman, D.L., Blazer, L.L., Monroy, C.A. & Neubig, R.R. Allosteric inhibition of the regulator of G protein singaling-Galpha protein-protein interactions by CCG-4968. *Mol Pharmacol* **78**, 360-365 (2010).

20.	Pande, V., Sousa, S.F. & Ramos, M.J. Direct covalent modification as a strategy to inhibit NFKB *Curr Med Chem* **16**, 4261-73 (2009).

21.	Ficarro, S.B. et al. Improved electrospray ionization efficiency compensates for dimished chromatographic resolution and enables proteomics analysis fo tyrosine signalling in embryonic stem cells. *Anal Chem* **81**, 3440-3447 (2009).

22.	Sreeramulu, S., Gande, S.L., Gobel, M. & Schwalbe, H. Molecular mechanisms of inhbitiion of the human protein complex Hsp90-Cdc37, a kinome chaperone-cochapterone, by tripterine celastrol. *Agnew Chem Int Edit* **48**, 5853-5855 (2009).

23.	Salminen, A., Lehtonen, M., Paimela, T. & Kaarniranta, K. Celastrol: molecular targets of Thunder God Vine. *Biochem Biophys Res Commun* **394**, 439-442 (2010).

24.	Day, C.L. et al. Solution structure of prosurvival MCL-1 and characterization of its binding by proapoptotic BH3-only ligands. *J Biol. Chem.* **280**, 4738-4744 (2005).

25.	Bird, G.H., Bernal, F., Pitter, K. & Walensky, L.D. Chapter 22 Synthesis and Biophysical Characterization of Stabilized alpha-Helices of BCL-2 Domains. *Methods Enzymol* **446**, 369-86 (2008).

26.	Walensky, L.D. et al. Activation of apoptosis in vivo by a hydrocarbon-stapled BH3 helix. *Science* **305**, 1466-70 (2004).

27.	Walensky, L.D. et al. A stapled BID BH3 helix directly binds and activates BAX. *Mol Cell* **24**, 199-210 (2006).

28.	Pitter, K., Bernal, F., Labelle, J. & Walensky, L.D. Dissection of the BCL-2 family signaling network with stabilized alpha-helices of BCL-2 domains. *Methods Enzymol* **446**, 387-408 (2008).

29.   Gavathiotis, E. et al. BAX activation is initiated at a novel interaction site. *Nature* **455**, 1076-81 (2008).

30.   Bernal, F. et al. A stapled p53 helix overcomes HDMX-mediated suppression of p53. *Cancer Cell* **18**, 411-22 (2010).

31.   Stewart, M.L., Fire, E., Keating, A.E. & Walensky, L.D. The MCL-1 BH3 helix is an exclusive MCL-1 inhibitor and apoptosis sensitizer. *Nat Chem Biol* **6**, 595-601 (2010).

32.   Jaffrey, S.R. & Snyder, S.H. The biotin switch method for the detection of S-nitrosylated proteins. *Science STKE* **86**, pI1 (2001).

Chapter 5

Rationale and Discussion, Future Directions, and Conclusion

Rationale and Discussion

High-throughput screen for selective MCL-1 inhibitors

Chapter 2 described the FP-based high-throughput screen I undertook to discover selective small molecule inhibitors of MCL-1. The screen was based on displacement of FITC-MCL-1 SAHB from recombinant MCL-1 and was the first of its kind to utilize a stapled peptide as a screening ligand. A counter-screen examining displacement of FITC-BAD BH3 from BCL-X_L was concurrently performed, leading to the discovery of selective and potent small molecules for further studies. Small molecules were rigorously tested in secondary assays, including dose-response competitive FP assays and cellular toxicity screens. Molecular scaffolds that emerged from the screen allowed for categorization of compound subclasses that are capable of selectively binding MCL-1. From the screen, 28 potential small molecules were found to bind MCL-1 selectively, with varying efficacy in the functional assays.

High-throughput screens have long been utilized to discover novel small molecules with specific biological functions, with growing interest in recent years due to new technology development and increased diversity of compound libraries[1]. Specifically, manipulation of protein-protein interactions has become an important means of modulating cellular function. *In vitro* biochemical high-throughput screening is based on a reductionist approach that examines disruption of a specific protein-protein interaction with the hopes that this activity will be recapitulated in cells. While a drawback of biochemical high-throughput screening is that the small molecule hits may be cell-impermeable or manifest off-target effects, a series of rigorous assays can be developed to increase the chances of identifying compounds with on-target mechanism(s) of action. Indeed, this was the rationale for undertaking an *in vitro* biochemical screen rather than a chemical genetic screen[2]. In a chemical genetic screen, for example, small

molecule activity in MCL-1 overexpressing cancer cells versus normal cells could have been examined to identify compounds capable of selectively killing MCL-1-dependent cells. Although this type of screen would provide candidate therapeutic agents, the compound's mechanism of action would be unknown and require extensive investigation. Because MCL-1 is tightly regulated and is engaged by a variety of signaling pathways[3-8], total loss of MCL-1 function is also expected to have off-target effects. The motivation behind the design of our *in vitro* high-throughput screen was based on our discovery of a selective stapled peptide, which we reasoned may be deployed to effectively identify to potent and selective MCL-1-targeting small molecules for use as both research tools (e.g., to dissect the structural basis for differential molecular specificities among anti-apoptotic targets) and prototype therapeutics.

MIM1 selectively targets MCL-1 in vitro and in MCL-1-dependent leukemia cells

Chapter 3 described the application of our high throughput screen to identify a small molecule that directly binds and inhibits anti-apoptotic MCL-1 at its BH3-binding groove. MIM1 demonstrated exquisite selectivity in both *in vitro* binding and functional assays. Importantly, MIM1 triggered caspase 3/7 activation and apoptosis induction of a cancer cell line dependent on MCL-1 for survival, but had no effect on the corresponding BCL-X_L-dependent cell line, highlighting the molecule's specificity-of-action. Thus, we report the application of MCL-1 SAHB to identify a selective small molecule inhibitor of MCL-1 that exhibits anti-tumor activity in the specific context of MCL-1 dependence. We find that specific small molecule inhibition of MCL-1 is achievable, and further applications of this molecule could lead to next generation cancer therapeutics that, either alone or combined with ABT-737, could combat the apoptotic blockades of cancer.

Cancer cell dependence on MCL-1 is a prerequisite for successful single-agent MCL-1 small molecule targeting and would explain why MCL-1 inhibition does not induce apoptosis in normal cells, such as MEFs, or cancer cells driven by other survival factors (Chapter 3). Cells that express one or more anti-apoptotic proteins aside from MCL-1 will remain capable of suppressing apoptosis in the face of MCL-1 inhibition. By identifying cancer cells that are uniquely dependent on MCL-1, using techniques such as BH3 profiling, optimal therapeutic matches can be made between anti-apoptotic inhibitors and susceptible cell lines[9]. For example, cells dependent on MCL-1 are resistant to ABT-737, while those cells dependent on BCL-2 are highly sensitive to ABT-737[9]. The *p185+Arf-/-Mcl-1*-deleted cell lines applied in this study are ideal cellular models to probe specificity-of-action because upon *Mcl-1* deletion, the cells undergo apoptosis unless rescued by specific anti-apoptotic proteins, such as MCL-1 or BCL-X_L. Thus, selective targeting of individual anti-apoptotic proteins should induce apoptosis. Recently, acute myelogenous leukemia (AML) cell lines were reported to be sensitive to deletion of MCL-1 but not BCL-X_L[10]. MCL-1 was essential for sustained AML survival both in cultured cell lines and primary patient samples, and blockade of MCL-1 by an MCL-1-selective BIM mutant induced apoptosis in these cells[10]. The study again highlights the importance of MCL-1 in cancer pathogenesis and the need for selective agents (such as MIM1), applied singly or in combination, to reactivate apoptosis by overcoming MCL-1's barrier to cell death.

Irreversible cysteine modification of MCL-1

Chapter 4 described the discovery of irreversible small molecule hits derived from our initial high-throughput screen for selective MCL-1 inhibitors. Small molecules were screened in a rapid dilution assay coupled with FP to determine if they bound to MCL-1 reversibly or

irreversibly. Potential irreversible binders were then subjected to mass spectrometry analysis. First, covalent modification was confirmed, and next, the site of modification was identified. One such compound, CSM-B2, was found to covalently modify MCL-1 at position C286. This cysteine is unique to MCL-1 and is present at the opposite face of the protein from the canonical BH3-binding groove. Interestingly, covalent cysteine modification led to displacement of the FITC-BID BH3 peptide from MCL-1 in a competitive FP assay. Dramatic structural changes within the protein were observed upon cysteine modification of MCL-1, as demonstrated by HSQC NMR analysis. Thus, covalent cysteine modification of MCL-1 could possibly serve as an allosteric mechanism for modulating the protein's apoptotic function by altering access to the BH3-binding groove.

Because small molecules can modulate cysteine residues on MCL-1, we sought to determine whether these residues are biologically important. As a number of proteins including anti-apoptotic BCL-2 are subject to S-nitrosylation, with resultant impact on their apoptotic functions[11-13], we investigated whether MCL-1 could be S-nitrosylated *in vitro* and in cells. Interestingly, we found that MCL-1 is nitrosylated *in vitro* (upon incubation with nitric oxide donors) and in cells (basally), and mutation of the cysteine residue blocked nitrosylation, as expected. The rationale for examining covalent small molecules that inhibit BH3-binding to MCL-1 was to explore a potentially novel mechanism for MCL-1 inhibition. The Walensky laboratory's recent discovery of a new BAX interaction site that triggers its pro-apoptotic activity[14] suggests that functionally relevant, non-canonical binding surfaces could also be present on other apoptotic proteins. Given the importance of MCL-1 in cancer biology and organism homeostasis, uncovering novel modes of MCL-1 regulation may provide new insight

into a fundamental biological process, in addition to revealing new opportunities for modulating

MCL-1 for therapeutic benefit.

Future directions

MCL-1 lead optimization and the development of an MCL-1-selective therapeutic

Chapters 2 and 3 described our search for a highly selective and potent MCL-1 inhibitor and the discovery of MIM1. Using the structure of MIM1 as a lead point for MCL-1 targeting, next steps involve molecular derivatization and optimization in an effort to drive down its micromolar binding activity into the nanomolar or even subnanomolar range. In pursuing this medicinal chemistry effort, we hope to obtain novel constructs with increased affinity that will likewise retain MCL-1 specificity and cellular activity, as vetted by the series of rigorous assays developed for this thesis research. To further explore MIM1's cellular specificity for MCL-1, primary chronic lymphocytic leukemia (CLL) cells containing different levels of anti-apoptotic proteins will be examined. CLL cells manifest variable expression levels of distinct anti-apoptotic proteins; for example, CLL cells with high BCL-2 and low MCL-1 levels are especially sensitive to ABT-737, whereas patient samples containing high levels of MCL-1 are resistant[15]. MIM1 and its analogs would be predicted to manifest the opposite activity profile, further supporting their capacity to selectively target MCL-1 and thereby reactivating apoptosis in CLL cells with an MCL-1-specific anti-apoptotic expression profile.

Lead small molecules will undergo pharmacokinetic (PK) testing in mice, performed in conjunction with the DF/HCC Clinical Pharmacology Core. LC/MS-based analytical assays are developed in order to detect and quantify compound levels in plasma. For PK analysis, small molecules (e.g., 10, 50, 100 mg/kg) will be injected by tail vein or intraperitoneally into male C57/BL6 mice. Blood samples will be withdrawn by retro-orbital bleed at various time points and plasma isolated for compound quantification, followed by calculation of plasma half-life, peak plasma levels, total plasma clearance, and apparent volume of distribution. Small molecules

133

that exhibit selective MCL-1 targeting in cells and exhibit a favorable pharmacokinetic profile will be advanced to *in vivo* testing. In addition, the potential need for further medicinal chemistry-based optimization of the compounds will be determined by such PK analyses.

The most potent and selective compound bearing the best PK properties will be advanced in to *in vivo* efficacy testing. First, MCL-1- and BCL-X_L-dependent *p185$^+$Arf$^{/-}$Mcl-1*-deleted leukemia cells will be engrafted into SCID beige mice. Once peripheral leukemia is observed (e.g., white blood count > 20K), as monitored by weekly complete blood counts, mice will be intravenously injected once daily with MIM1 or its analogs. We would expect selective reduction of peripheral leukemia in the MCL-1-dependent model but not in the corresponding BCL-X_L-dependent mice. ABT-737 would serve as an effective control compound that should manifest the opposite activity profile *in vivo*. Such studies would also explore the potential toxicity of MCL-1 targeting *in vivo*, as assessed by necropsy, performed in collaboration with the Rodent Histopathology Core of HMS, and monitoring of complete blood counts, including FACS-based analysis of lymphocyte and granulocyte subsets given the central role of MCL-1 in lymphopoiesis and granulopoiesis[7,8]. Additional mouse genetic and xenograft models would also be employed to evaluate the scope of MIM1 or its analogs' activities in a variety of disease contexts.

Determining the crystal structure of MCL-1/small molecule complexes

MIM1 and any promising analogs will be examined in complex with MCL-1ΔNΔC in crystal-screening assays to achieve structural determination by X-ray crystallography, performed in collaboration with the Eck laboratory of the Dana-Farber Cancer Institute. The structures of small molecule/MCL-1 complexes may reveal key binding and selectivity determinants for

molecular engagement of the canonical BH3-binding pocket of MCL-1. 96-well crystal screens (Qiagen Protein Complex Suite, Qiagen Classics Suite, Hampton Research Index, and Eck1) have previously been performed using pure, recombinant MCL-1ΔNΔC (6.5 mg/mL) and small molecule incubated at a ratio ≥ 1:1 for one hour prior to plating. In pilot studies, needles, needle clusters, and rods were observed in discrete wells. As these wells contained similar conditions, 24-well scale-up screens were then performed, altering polyethylene glycol (PEG) molecular weight, pH, and PEG concentration. Thin needles were again found using these conditions, so additive screens were explored in an attempt to grow diffraction-quality crystals. Such follow-up crystallization studies are currently in progress. Favorable co-crystals of MCL-1 with the small molecule will be flash frozen and subjected to initial data collection using the Eck laboratory screening X-ray source, and if suitable crystals are obtained, definitive data collection will be accomplished at the National Synchotron Light Source (Argonne National Laboratory). Data will be processed using HLK2000[16], and molecular replacement will be performed using PHASER[17]. Data will then be analyzed and refined using PHENIX[18] and COOT[19] software.

In Chapter 4, I sought to determine the structural and biochemical consequences of cysteine modification of anti-apoptotic MCL-1. I advanced the covalent complex between CSM-B2 and MCL-1ΔNΔC to crystal-screening, including performing additive screens, streak seeding, and macroseeding to increase crystal size and three-dimensionality for X-ray analysis. Macroseeding crystal fragments and needles produced crystals with favorable appearance, but X-ray diffraction did not result. Optimization of protein, compound, and complex purity, in addition to broadening the crystal screens, are currently underway to advance this structural work. Indeed, the structure of cysteine-modified MCL-1 may reveal a new mode of BH3-binding pocket regulation with direct implications on anti-apoptotic activity.

Determining the functional consequences of MCL-1 cysteine modification

Future work will also interrogate the functional implications of cysteine modification on the pro-survival activity of MCL-1 in cells. HeLa cells were transfected with PCMV-10 vectors containing full-length MCL-1, or the C16S, C286S, C16S/C286S mutants. Initial optimization showed successful transfection (**Figure 5.1**) and FLAG immunoprecipitation to isolate both wild-type and mutant MCL-1 protein from cells (**Figure 5.2**). This system will be useful for future proteomic experiments that explore changes in MCL-1 binding partners upon cysteine mutagenesis, in addition to examining the *in situ* post-translational modifications of expressed MCL-1 isoforms.

To further to investigate the cellular consequences of cysteine modification in stable cell lines, *Mcl-1$^{-/-}$* MEFs will be reconstituted with wild-type MCL-1 and its cysteine mutants (C16S, C286S, and C16S/C286S). The full-length, wild-type *Mcl-1* sequence has been cloned into the MSCV-IRES-GFP (pMIG) vector and verified by DNA sequencing. The desired cysteine mutations have been obtained in this vector using the designed mutagenesis primers and the QuikChange Site Mutagenesis Kit. The vectors, now in hand, will be retrovirally transduced into *Mcl-1$^{-/-}$* MEFs so that the functional impact of cysteine modification on MCL-1's pro-survival activity at baseline and in response to cellular stress can be explored.
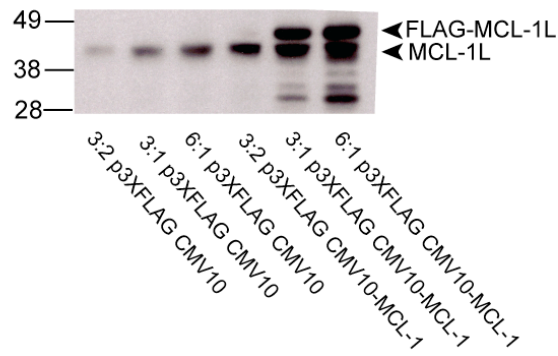
Figure 5.1. *FLAG-MCL-1 is successfully expressed in HeLa cells.* Both 3:1 and 6:1 ratios of

vector:FuGene produced the highest FLAG-MCL-1 expression levels by 24 hours post-

transfection (performed as per manufacturer's protocol), as demonstrated by anti-MCL-1
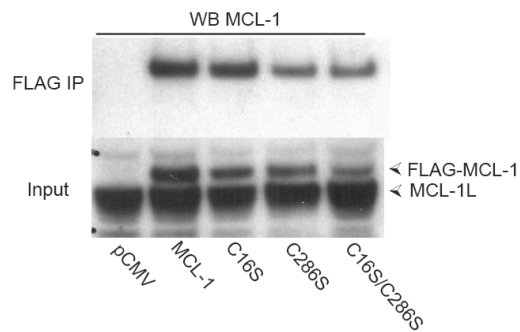
Western blot (sc-819).

Figure 5.2. *FLAG-MCL-1 is immunoprecipitated effectively from HeLa cells transfected with FLAG-MCL-1 and its cysteine mutants.* FLAG-MCL-1 protein was immunoprecipitated with anti-FLAG-agarose beads (Sigma) and probed with MCL-1 antibody (sc-819). Immunoprecipitation experimental methods are previously described in Chapters 3 and 4.

The potential cellular consequences of MCL-1 cysteine modification (either by nitrosylation or other chemical derivatization) include changes in ubiquitination status, degradation rates, and binding partners. I observed subtle changes in MCL-1 degradation and cleavage among the wild-type and cysteine mutant constructs upon HeLa cell transfection (**Figure 5.3**), a phenomenon that will be investigated further. Initial efforts will focus on documenting the presence or absence and type of cysteine modification on MCL-1. I previously used the S-nitrosylation kit to examine one possible mode of derivatization; however, a comprehensive approach will be undertaken to define which cysteines are modified and how using mass spectrometry. For example, cysteines can be labeled with cysteine-reactive probes, followed by LC/MS analysis to detect loss of labeling due to cellular cysteine modification, with further analyses applied to define the specific type of modification, as described[20]. Once specific cysteine locations and modifications are established, the reconstituted *Mcl-1*^{-/-} MEF system described above will be applied to examine the potential functional consequences of disrupting cysteine modification.
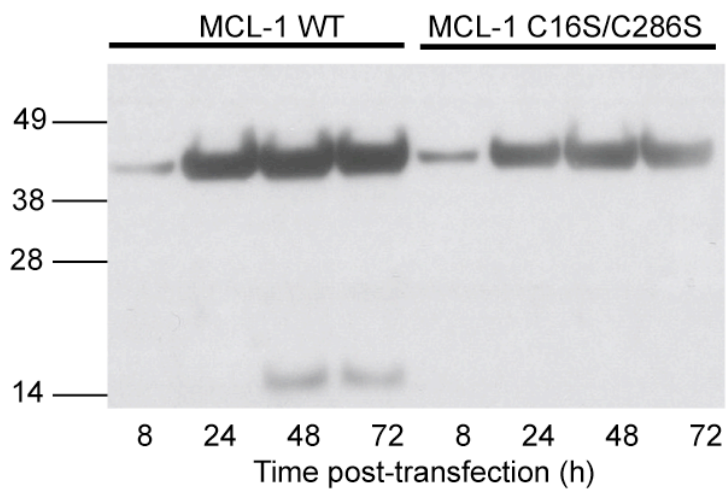
Figure 5.3. *Wild-type MCL-1 and the C16S/C286S double mutant display differential expression and cleavage levels post-transfection.* Both constructs were transfected into HeLa cells as previously described, and MCL-1 levels were monitored by anti-FLAG Western blot (Sigma). The short N-terminal cleavage form of MCL-1 is not seen when the double mutant is overexpressed.

Conclusion

Targeted inhibition of the BCL-2/BCL-X$_L$ subclass of anti-apoptotic proteins is a clinically validated approach to overcoming the survival advantage of select cancers driven by BCL-2-mediated apoptotic blockade. The emerging pathogenic role of MCL-1 in a remarkably broad range of human cancers has increased its importance as a high priority therapeutic target. Harnessing the potency and selectivity of a natural MCL-1 antagonist, the BH3 domain of MCL-1 itself, we conducted the first competitive small molecule screen against a high affinity stapled peptide/protein complex. Applying a series of rigorous biochemical and cellular assays designed to evaluate MCL-1 vs. BCL-X$_L$ anti-apoptotic subclass specificity, we validated MIM1 as a potent and selective MCL-1 antagonist capable of preferentially blocking MCL-1-mediated suppression of pro-apoptotic BAX *in vitro*, and inducing caspase 3/7 activation and cell death of an MCL-1-dependent leukemia cell line. Thus, we find that specific small molecule inhibition of MCL-1 is attainable, and further applications of a selective molecule could lead to next generation cancer therapeutics that, either alone or in combination with ABT-737, could reverse cancer's MCL-1-dependent apoptotic blockade.

References

1.   Spencer, R. High-Throughput Screening of Historic Collections: Observations on File Size, Biological Targets, and File Diversity. *Biotech and Bioeng* **61**, 61-68 (1998).

2.   Cong, F., Cheung, A.K. & Huang, S.M. Chemical genetics-based target identification in drug discovery. *Annu. Rev. Phamacol. Toxicol.* **52**, 57-78 (2012).

3.   Ding, Q. et al. Degradation of Mcl-1 by beta-TrCP mediates glycogen synthase kinase 3-induced tumor supporession and chemosensitization. *Mol. Cell Biol.* **27**, 4006-4017 (2007).

4.   Fujise, K., Zhang, D., Liu, J.-L. & Yeh, E.T.H. Regulation of Apoptosis and Cell Cycle Progression by MCL1. *J. Biol. Chem.* **50**, 39458-39465 (2000).

5.   Jamil, S., Mojtabavi, S., Hojabrpour, P., Cheah, S. & Duronio, V. An Essential Role for MCL-1 in ATR-mediated CHK1 Phosphorylation. *Mol. Biol. Cell* **19**, 3212-3220 (2008).

6.   Jamil, S. et al. A proteolytic fragment of Mcl-1 exhibits nuclear localization and regulates cell growth by interaction with Cdk1. *Biochem. J.* **387**, 659-667 (2005).

7.   Opferman, J.T. et al. Obligate Role of Anti-Apoptotic MCL-1 in the Survival of Hematopoetic Stem Cells. *Science* **307**, 1101-1104 (2005).

8.   Opferman, J.T. et al. Development and maintenance of B and T lymphocytes requires anti-apoptotic MCL-1. *Nature* **426**, 671-676 (2003).

9.   Certo, M. et al. Mitochondria primed by death signals determine cellular addiction to antiapoptotic BCL-2 family members. *Cancer Cell* **9**, 351-365 (2006).

10.   Glaser, S.P. et al. Anti-apoptotic Mcl-1 is essential for the development and sustained growth of acute myeloid leukemia. *Genes and Development* **26**(2012).

11.   Azad, N. et al. S-Nitrosylation of BCL-2 inhibits its ubiquitin-proteasomal degradation: A novel antiapoptotic mechanism that suppresses apoptosis. *J Biol. Chem.* **281**, 34124-34134 (2006).

12.   Guan, W. et al. S-nitrosylation of mitogen activated protein kinase phosphatase-1 suppresses apoptosis. *Cancer Lett.* **314**, 137-146 (2012).

13.   Tsang, A.H. et al. S-nitrosylation of XIAP compromises neuronal survival in Parkinson's disease. *PNAS* **106**, 4900-4905 (2009).

14.   Gavathiotis, E. et al. BAX activation is initiated at a novel interaction site. *Nature* **455**, 1076-81 (2008).

15.   Al-Harbi, S. et al. An antiapoptotic BCL-2 family expression index predicts the response of chronic lymphocytic leukemia to ABT-737. *Blood* **118**, 3579-3590 (2011).

16.   Otwinowski, Z. & Minor, W. Processing of x-ray diffraction data collected in oscillation mode. *Methods in Enzymology* **276**, 307-327 (2008).

17.   Storoni, L.C., McCoy, A.J. & Read, R.J. Likelihood-enhanced fast rotation functions. *Acta Crystallography D Biol Crystallography* **60**, 432-438 (2004).

18.   Adams, P.D. et al. PHENIX: building new software for automated crystallographic structure determination. *Acta Crystallography D Biol Crystallography* **58**, 1948-1954 (2002).

19.   Emsley, P. & Cowtan, K. COOT: model-building tools for molecular graphics. *Acta Crystallography D Biol Crystallography* **60**, 2126-2132 (2004).

20.   Chouchani, E.T., James, A.M., Fearnley, I.M., Lilley, K.S. & Murphy, M.P. Proteomic approaches to the characterization of protein thiol modification. *Curr Op Chem Biol* **15**, 120-128 (2011).